

MINISTRY OF EDUCATION AND RESEARCH

“VALAHIA” UNIVERSITY OF TARGOVIȘTE

**THE ANNALS
OF “VALAHIA” UNIVERSITY**

SECTION SCIENCES

**Nr. 15
2005**

Editorial Board

Editor in Chief

Prof. dr. Silviu Jipa - „Valahia” University of Târgoviște

Editors:

Conf. dr.Călin Oros – „Valahia” University of Târgoviște
Prof. dr. Ion V. Popescu - „Valahia” University of Târgoviște
Prof. dr. Marin Iordan - „Valahia” University of Târgoviște
Prof. dr. Radu Setnescu - „Valahia” University of Târgoviște
Prof. dr. Constantin Ghita - „Valahia” University of Târgoviște
Conf. dr. Cristinel Mortici - „Valahia” University of Târgoviște

SUMMARY

A. PHYSICS SECTION

SINGLE EXCIMER LASER PULSE ABLATION ON TiO₂ SURFACES CĂLIN OROS,
SILVIU JIPA, RADU SETNESCU, TRAIAN ZAHARESCU / PAG. 5

PIXE AND ICP METHODS APPLIED IN VEGETAL BIOLOGY
CLAUDIA STIHI, GABRIELA BUSUIOC, ION V. POPESCU, T. BADICA, CĂLIN OROS, GABRIEL DIMA, SERGIU DINU, SIMONA APOSTOL, OANA BUTE, V. STIHI, V. CIOBANU, D. STOIAN / PAG. 12

APPLICATION OF PIXE METHOD TO PHOSPHATASE ENZYME ANALYSIS
ION V. POPESCU, GABRIEL DIMA, CLAUDIA STIHI, LAUR MANEA / PAG. 18

EFFICIENCY INCREASE METHODS OF METALS HEATING BY LASER
CALIN OROS, DANA VLADESCU, MARIN IORDAN, MARIANA OLARIU / PAG. 22

PIXE ANALYSIS OF BASELLA ALBA L AND BASELLA RUBRA L LEAVERS
CLAUDIA STIHI, GABRIEL DIMA, GABRIELA BUSUIOC, ION V. POPESCU / PAG. 28

ON THE SENSITIVITY OF GRAVITATIONAL OSCILLATOR
MARIN IORDAN, CALIN OROS / PAG. 32

B. CHEMISTRY SECTION

**GREEN PIGMENTS DERIVATIVES FROM HETEROCYCLIC
DIQUINOXALINE-PIPERAZINE SYSTEMS**
CRISTIANA RĂDULESCU, ANA-MARIA HOSSU, IONICA IONIȚĂ / PAG. 37

**HPLC IN DETERMINATION OF D VITAMINS FROM PHARMACEUTICAL
PREPARATIONS**
DUMITRA HOSSU, ANA-MARIA HOSSU, MARIA TOMA BĂDEANU, CRISTIANA RADULESCU, IONICA IONITA / PAG. 44

**THE CHARACTERISTICS OF SYNTHESIZED CHROMOPHORES FOR
PHOTOCHROMIC MATERIALS**
IONICA IONIȚĂ, CRISTIANA RĂDULESCU, ANA-MARIA HOSSU / PAG. 48

C. MATHEMATICS SECTION

ITERATIVE SCHEME IN SOLVING THE PLAUSIBLE POINTS PROBLEM AIRISING IN PHASE TRANSITION

CONSTANTIN GHITA / PAG. 54

MODEL WITH NONLINEAR CRITERIA FOR HARDENING DEFORMATION

CONSTANTIN GHITA / PAG. 63

SOME REMARKS ON LIMIT LOADS FOR PERIODIC MATERIALS

GELU PASA /PAG. 79

A. PHYSICS SECTION

Single Excimer Laser Pulse Ablation on TiO₂ Surfaces

S. Dinu¹, C. Oros¹, G. Dima¹, C. Stihl¹, M. Iordan¹, M. Voicu¹

¹Physics Department, Faculty of Sciences and Arts,
Valahia University of Targoviste, 18 Unirii Blvd, Targoviste, Romania

Abstract

This paper presents both theoretical and experimental investigations of the surface temperatures of TiO₂ thin films under single nanoseconds excimer laser pulse irradiation. The target's temperatures were evaluated by solving the one-dimensional heat flow equation in the thin films approximation. From the measurements of the surface profile, the volume dilatation or depth of the ablation crater was obtained and, then, the surface's temperatures were determined in good correspondence with theoretical results.

Keywords: *excimer laser, titanium dioxide, surface temperature*

Introduction

Titanium dioxide (TiO₂) and TiO₂-based materials have been extensively studied [1,2]. This has been driven by their important applications in many fields such as heterogeneous catalysis, energy storage and transfer, photovoltaic cell production, sensor design, pigment production, corrosion protection, optical coating, ceramic manufacturing, electric device design, wastewater purification and selfcleaning coatings. TiO₂-based materials exhibit high photo-catalytic activity and they are good catalysts in solar cell development and the photo-assisted degradation of organic compounds. TiO₂ is non-toxic and plays a role in the biocompatibility of bone implants; Co-doped TiO₂ is an ideal candidate for spin-based electronic devices. In addition, nanostructured TiO₂ -based materials (e.g., nanoparticles [3], nanotubes [4], nanofibers [5], and nanoporous structures [6]) are currently receiving much attention because of their unique chemical, electronic and catalytic properties. In this context the study of laser interaction with TiO₂ thin films are of great both theoretical and experimental importance.

When a laser irradiates the surface of a solid, the energy may be absorbed. In metals the optical absorption is usually dominated by free carrier absorption, i.e. electrons in the conduction band absorb photons and gain higher energy. In semiconductors electrons are excited from the occupied valence bands to empty conduction band, provided that the photon energy exceeds the band gap. In dielectrics with band gap larger than the photon energy multiphoton transitions are necessary to promote electrons from valence band to the conduction band. In all these cases the timescale of the energy deposition is determined by the laser pulse duration. Following absorption the optical energy is transferred from electrons to phonons, that is, lattice heating occurs. In dielectric materials, the laser pulse initially excites electrons to the conduction band there they can be further excited by free-carrier absorption. During and after the excitation, electron-electron and electron-phonon scattering occur, resulting in the thermalization of the electron system and the electrons with the lattice, respectively. In semiconductors and dielectrics photoionization and electron-electron impact ionization can produce a free electron gas of comparable high density.

In thermal processing with laser radiation energy deposition and heating in a material are a consequence of the balance between the deposited energy, governed by optical material properties and characteristics of the laser radiation, and the heat diffusion, determined by thermo-physical material properties and the interaction time. Many studies made until now for different solid materials (metals, dielectrics) have shown that the laser intensity of $I \sim 10^5 \div 10^6 \text{ W/cm}^2$ produces only a heating of materials, the laser intensity of $I \sim 10^6 \div 10^7 \text{ W/cm}^2$ produces the evaporation of materials, and for the laser intensity of $I \sim 10^8 \div 10^9 \text{ W/cm}^2$ starts the laser-induced plasma regime.

Laser ablation of solids with nanosecond pulses of moderate intensity $I \sim 10^6 \div 10^7 \text{ W/cm}^2$ is widely used in modern technologies, such as thin film deposition, surface treatment, cluster formation etc. [7].

This study concerned with an investigation of the TiO_2 thin film surface temperature, solid heating and ablation induced by a nanosecond single excimer laser irradiation; to our knowledge there is not previous studies on this subject reported in the literature.

Experimental method

1. Laser

The experiments were performed with a COMpex 205 KrF excimer laser operating at 248-nm wavelength. The system is provided with a homogenizer. This laser delivers its energy, $E = 0.13 \text{ J}$, in a pulse duration of $\tau_p = 25 \text{ ns}$ (FWHM) with a nearly rectangular beam cross-section spatial profile. The laser radiation was focused onto the target's surface with a convergent lens to the desired spot size and was monitored by well-known methods of diagnostics by scanning the laser beam with a pinhole in combination with a suitable detector. In order to obtain differed laser intensities on the target the area of laser spot on the target was modified by changing the lens position in respect on the target's position, tab. 1. In these conditions the maximum value of laser intensity was above 10^7 W/cm^2 . The maximum rate of repetition for laser shots is 20 Hz. All experiments were performed by a single laser shot irradiation in air at normal conditions.

Table 1. The experimental laser intensities on the target's surface

| | | | | | |
|-------------------------------------|--------------------------|----------------------------|--------------------------|------------------------------|---------------------------------|
| Laser spot area (mm^2) | $S_1 = 7 \times 13 = 91$ | $S_2 = 6 \times 11.5 = 69$ | $S_3 = 5 \times 9 = 45$ | $S_4 = 3.25 \times 6 = 19.5$ | $S_5 = 2.25 \times 4.25 = 9.56$ |
| Laser intensity $I (\text{W/cm}^2)$ | $I_1 = 0.57 \times 10^7$ | $I_2 = 0.75 \times 10^7$ | $I_3 = 1.15 \times 10^7$ | $I_4 = 2.66 \times 10^7$ | $I_5 = 5.43 \times 10^7$ |

2. Targets

TiO_2 100-nm thickness was deposited on glass by magnetron sputtering deposition (MSD), which is known to produce films with nearly bulk-like refractive indices, low optical losses, and high laser breakdown thresholds [8]. The coating chamber is an industrial system (TSD 400-CD HEF&D) with various diagnostic facilities such as optical emission and mass spectrometers. The target is sputtered in DC mode with an ENI RPG 100 generator. A typical SEM image of TiO_2 is given in fig. 1.

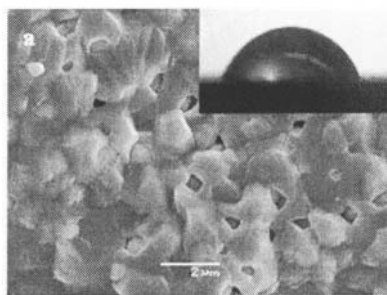


Fig.1. SEM image of TiO_2

Results and discussions

1. Theoretical results

The temperature rises in the target $T(z, t)$ is quantitatively assessed using well-known standard equation for the time-dependent heat flow in a solid [9]. The thermal effects during pulsed nanosecond laser irradiation can be explored by the solution of the one-dimensional heat flow equation with non-linear boundary conditions arising due to the formation and movement of the solid-liquid and vapor-liquid interface:

$$\rho c \frac{\partial T}{\partial t} = k_T \frac{\partial^2 T}{\partial z^2} + (1 - R) \cdot \alpha \cdot I e^{-\alpha z} \quad (1)$$

where z refers to the direction perpendicular to the plane of the target and t refers to the time. The terms $c(T)$, $R(T)$ and $\alpha(T)$ represent the temperature dependent specific heat capacity, reflectivity and absorption coefficient, respectively. $I(t)$ is the time dependent laser intensity striking on the surface. The one-dimensional nature of the problem is primarily due to the fact that the transverse dimensions of the laser beam are much larger than the thermal diffusion distance in nanosecond time scales. Assuming the applicability of a one-dimensional model for the short pulses used, and restricting consideration to single-pulse exposure, the temperature rise was calculated taking account of the finite optical absorption depth and pulse duration of the laser. If the absorption takes place in an infinitesimal thin layer (surface absorber), the temperature rise in the bulk $T(z, t)$ during the laser irradiation can be described by the solution of the heat flow equation (1) in the thin films

approximation, $h \ll l_{th}$, ($l_{th} = \frac{1}{2} \sqrt{\pi \chi_T \tau_p}$ is the thermal diffusivity length [9]):

$$T(z, t) = \frac{2(1-R)I}{k_T} \sqrt{\chi_T t} \sum_{n=-\infty}^{\infty} \left\{ \operatorname{ierfc} \frac{|z - 2nh|}{2\sqrt{\chi_T t}} - \operatorname{ierfc} \frac{[(z - 2nh)^2 + R_s^2]^{\frac{1}{2}}}{2\sqrt{\chi_T t}} \right\}, \quad (2)$$

where: $I = \frac{E}{S \tau_p}$ is the average laser intensity during the laser pulse (with E laser energy per pulse),

h is the film thickness, τ_p is the laser pulse duration, $\chi_T = \frac{k_T}{\rho c}$ is the thermal diffusivity, S is the target's laser spot area, and n is the number of iterations. In the approximate model the material parameters used are assumed to be constant, i.e. they have no temperature dependences.

The optical and thermo-physical parameters of TiO_2 used in calculations are [10,11]: the thermal conductivity $k_T = 6.52 \text{ Jm}^{-1} \text{ s}^{-1} \text{ K}^{-1}$, the thermal diffusion coefficient (thermal diffusivity) $\chi_T = 1.6 \cdot 10^{-6} \text{ m}^2 \text{ s}^{-1}$, thermal diffusion length $l_{th} \approx 180 \text{ nm}$, vaporization temperature $T_v = 2773 \div 3273 \text{ K}$, vaporization energy $E_{vap} = 6.6 \text{ eV}$. The reflectivity coefficient R was calculated by Fresnel formulas for $n = 2.37$ and $k = 1.29$: $R = 27\%$. The target surface temperature at the end of laser pulse was calculated with formula (2) which in our particular case could be written in the form:

$$T(0, \tau_p) = 1.6 \times \frac{E(J)}{S(\text{m}^2)}, \quad (3)$$

with T in Kelvins and τ_p in seconds. The resulting representative number of iterations in our calculations was $n=3$.

Accounting the electron interband transitions within the conduction and valence band under 248 nm photon action of energy $\varepsilon = 5 \text{ eV}$ in the optical absorption depth $\delta = 15 \text{ nm}$, with a TiO_2 band gap of $E_g = 3 \text{ eV}$, results an effective energy for heating the target's material: $Q = 0.4 \times E$, and the formula for temperature (3) become:

$$T(0, \tau_p) = 1.6 \times \frac{Q(J)}{S(\text{m}^2)} = 0.64 \times \frac{E(J)}{S(\text{m}^2)}. \quad (4)$$

The results are given in tab. 2 for five different conditions of laser irradiation, i.e., using the convergent lens we have modified the area of laser spot on the target (at laser energy and pulse duration constants).

For first three conditions of laser irradiation the target's surface calculated temperatures are smaller than TiO_2 vaporization temperature and one expect to have only heating of the material and a volume dilatation. For last two conditions of laser irradiation the calculated temperatures are greater than the vaporization temperature and in these cases are expected to have laser ablation and, eventually, laser-plasma ignition with a corresponding ablation crater.

Table 2. The target surface calculated temperatures

| Laser intensity I (see tab.1) | I_1 | I_2 | I_3 | I_4 | I_5 |
|------------------------------------|-------|-------|-------|-------|-------|
| Temperature T (K) | 915 | 1205 | 1850 | 3280 | 4360 |

In order to make quantitative predictions on whether plasma ignition takes place at a certain intensity I , one can make use of the well known plasma ignition condition [12]:

$$I\sqrt{\tau_p} \geq B, \quad (5)$$

with $B \approx 4 \times 10^4 \text{ W s}^{1/2} \text{ cm}^{-2}$. This rule was established for surface absorbing (metallic) targets with nanosecond or longer pulses, but may give a rough estimate also for other conditions. In our experiments $\tau_p = 25 \text{ ns}$ and the estimated laser intensity for plasma ignition is $I \approx 2.531 \cdot 10^8 \frac{\text{W}}{\text{cm}^2}$; this value is about ten times greater than our experimental intensities, so the plasma ignition does not take place.

2. Experimental results

The theoretical results can be correlated with the observations of the experimental profiles of the target's surface after single pulse laser irradiation. The measurements of the target's surface profile were made with a Dektak 3030 ST profilometer. The diagrams given in figs. 2-6 show the TiO_2 surface profiles induced after irradiation of different laser intensities (tab.1).

For the first three values of laser intensity the results are given in figs. 2-4. One can observe that we have no laser ablation; the laser pulse just heating the target and the thermal expansion of target's surface due to the laser heating induces a surface elevation in the spot. One can estimate the temperature in the area of interaction considering the thermo-deformation of the target's interaction area (a volume dilatation), and the temperatures are given in tab. 3.

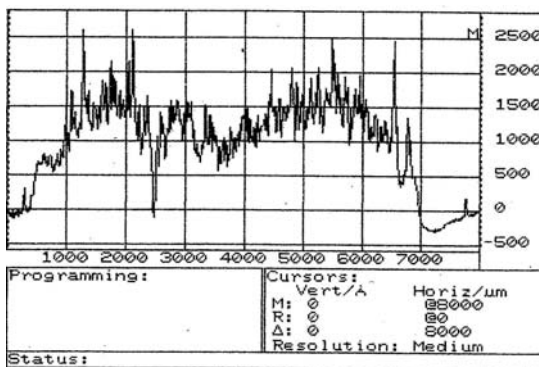


Fig. 2. $I = 0.57 \times 10^7 \text{ W/cm}^2$

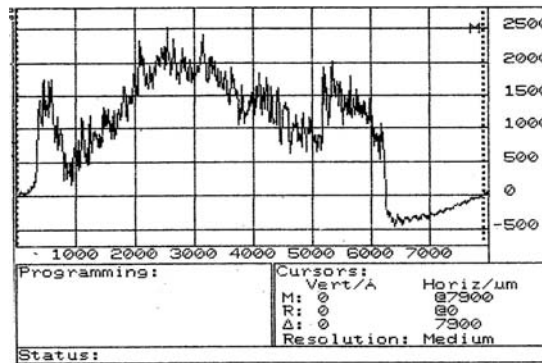


Fig. 3. $I = 0.75 \times 10^7 \text{ W/cm}^2$

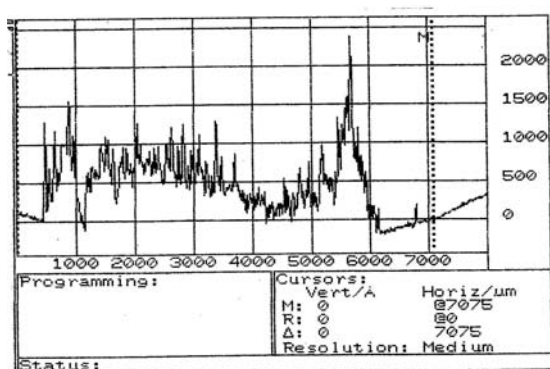


Fig.4. $I=1.15 \times 10^7 \text{ W/cm}^2$

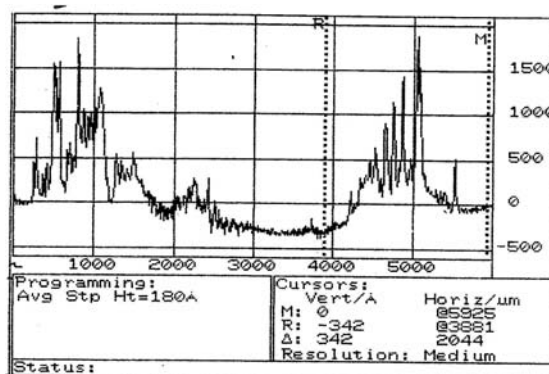


Fig. 5. $I=2.66 \times 10^7 \text{ W/cm}^2$

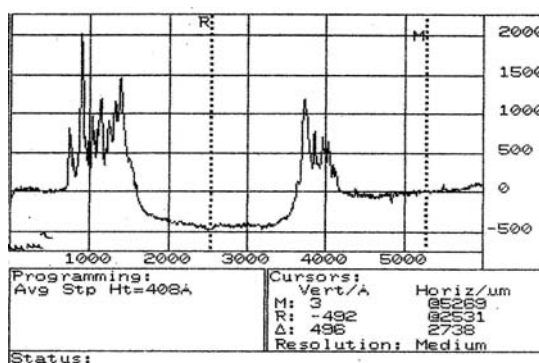


Fig. 6. $I=5.43 \times 10^7 \text{ W/cm}^2$

Figs. 2-6. TiO_2 target profile after laser irradiation

Experimental values of temperature are bigger than the theoretical ones because in our calculations we have no included the thermo-physical parameters dependence on temperature. Also, in our model we did not take account by the surface roughness before laser irradiation, but from tables 2 and 3 one can see that the results are in a relative good agreement.

Table 3: The estimated temperatures considering a volume dilatation

| Laser intensity I (see tab.1) | I_1 | I_2 | I_3 |
|------------------------------------|-------|-------|-------|
| Temperature T (K) | 1042 | 1375 | 2107 |

The starting point for laser evaporation of material can be seeing in fig. 4, where in distinction of figs. 2 and 3 a crater begins to arise. In figs. 5 and 6 a crater produced by laser ablation is observed. In these conditions the temperatures achieved on target's surface are greater than vaporization temperature of TiO_2 . Also, around the crater the melt material can not be observed; the surrounding surface is entirely devoid of any redeposited droplets, so is desirable to consider that the target material transforms direct from solid state in vapour state. Starting with evaporation time, the ablation rate per laser pulse can be estimated using the classical thermal rates equation [13]:

$$\nu = \nu_0 e^{-\frac{E_{vap}}{k_B T}} \quad (6)$$

where $\nu_0 = e^{23}$ molecular layers/ns (for TiO_2), k_B is Boltzmann constant, and E_{vap} is the vaporization energy. Because $E_{vap} = 6.6 \text{ eV}$ for normal pressure and vaporization temperature, $\nu = 1$ molecular layers/ns and from equation (6) results $\nu_0 = e^{23}$ molecular layers/ns (for TiO_2). Using this equation, the dimension of the crater induced by laser vaporization let us to estimate the ablation speed per pulse, ν , and target's surface temperature:

$$T(K) = \frac{76520}{\ln \frac{\nu_0}{\nu}} \quad (7)$$

The results are given in tab. 4 and they are also bigger than the theoretical ones, tab. 2. The explanation consists in the limit of the model. When dealing with processes such as vaporization, it is necessary to take account the fact it is a non-isothermal one, with a strong temperature dependence of evaporation rate constant and, in order to make a correct evaluation of temperature, it is necessary to know the values of the optical and thermal properties of the film and the substrate at high temperature. Unfortunately, these are not known at the highest temperatures involving in this work, and for this reason a theoretical evaluation of surface temperature is important in future applications regarding TiO_2 and TiO_2 -based materials interaction with laser radiations.

Table 4: Ablation rates and surface temperatures

| | | |
|---|----------------------------|-----------------------------|
| Laser spot area (mm^2) | $3.25 \times 6 = 19.5$ | $2.25 \times 4.25 = 9.56$ |
| Ablation rate ν (molecular layers/ns) | 7 (i.e. 35 nm/laser pulse) | 10 (i.e. 50 nm/laser pulse) |
| Temperature T (K) | 3635 | 3696 |

Also, at higher laser intensities we have observed that the film detached from the substrate. This can be explained in first approximation using the thermal model and supposing that the temperature film-glass substrate distribution is such that the interface stress is very high; but future work on this subject must be done.

Conclusions

We have investigated theoretically and experimentally the interaction of single nanosecond excimer single laser pulse with TiO_2 thin films deposited on glass by magnetron sputtering deposition. Theoretically, in the case of solid heating, from the one-dimensional equation of heat flow in the thin films approximation, the target's surface temperatures were estimated. In the case of laser ablation, the surface temperature is determined from classical thermal rates equation. A reasonable agreement with experimental data (surface temperatures and removal depths) was reached and the differences are explained by the limit of the theoretical model.

Acknowledgements: This work was partially supported by a Erasmus-Socrates Mobility Programm.

References

- [1]. U.Diebold, Surf.Sci.Rep. **48**, 53 (2003)
- [2]. P. Bonhote, E. Gogniat, M. Graetzel, P.V. Ashrit, Thin Solid Film **350**, 269 (1999)
- [3]. C.-Y. Wang, H. Groenzin, M.J. Shultz, J. Phys. Chem. B **108**, 265 (2004)
- [4]. Z.R.R.Tian, J.A.Voigt, J. Liu, B. Mckenzie, H.F. Xu, J. Am. Chem. Soc. **125**, 12384 (2003)
- [5]. S. Yoo, S.A. Akbar, K.H. Sandhage, Adv. Mater. **16**, 260 (2004)
- [6]. P.Yang, D. Zhao, D.I. Margolese, B.F. Chmelka, G.D. Stucky, Nature **396**, 152 (1998)
- [7]. D. Baurle, *Laser Processing and Chemistry* (Springer, Berlin 2000)
- [8]. D. Wei, Appl. Opt. **28**, 2813 (1989)
- [9]. I. Ursu, I.N.Mihailescu, A.M. Prokhorov, V.I. Konov, *Interactiunea radiatiei laser cu metalele (Interaction of Laser Radiation with Metals)*, Ed. Academiei Romaniei, 1986
- [10]. E. Palik ed., *Handbook of Optical Constants of Solids*, Academic Press, Orlando, 1985
- [11]. R.C. Weast ed, *CRC Handbook of Chemistry and Physics*, 67th edition, CRC Press, Boca Raton, 1986
- [12]. C.R.Phipps, Jr., T.P. Turner, R.F. Harrison, G.W. York, W.Z. Osborne, G.K. Anderson, X.F. Corlis, L.C. Haynes, H.S. Steele, K.C. Spicochi, T.R. King, J.Appl.Phys. **64**, 1083 (1988)
- [13]. M. Wautelet, E.D. Gehain, Semicond. Sci.Technol. **5**, 246 (1990)

PIXE and ICP methods applied in vegetal biology

C. Stihî^{*}, G. Busuioc^{}, I.V. Popescu^{*}, T. Badica^{***}, C. Oros^{*}, G. Dima^{*}, S. Dinu^{*},
S. Apostol^{*}, O. Bute^{*}, V. Stihî^{*}, V. Ciobanu^{****}, D. Stoian^{****}**

^{*}Valahia University of Targoviste, Physics Department, 2 Carol I street, 130024, Targoviste, Romania, E-mail: stihî@valahia.ro

^{**}Valahia University of Targoviste, Environmental Engineering Department, 2 Carol I street, 130024, Targoviste, Romania

^{***}IFIN-HH, Bucharest- Magurele, Romania

^{****}Transilvania University of Brasov, Faculty of Silviculture and Forest Engineering, Romania
Dimitrie Gusti High School, Bucharest, Romania

Abstract

High precision measurements of the physical-chemical environmental variables are essential but not sufficient to assess the response of ecosystems and humans to stress. A main goal of environmental monitoring is to monitor the state of whole ecosystems using bioindicators.

The article reports the basic data on elemental content of the vegetables leaves and soil from cropping areas. A correlation between elemental map of vegetables and elemental map of surface soil was made. The concentrations of elements in samples were determined by different methods: the Proton Induced X-ray Emission spectrometry (PIXE) and Atomic Emission spectrometry technique with Inductively Coupled Plasma (ICP-AES). The PIXE analysis was carried out at IFIN-HH in Bucharest using a 3 MeV proton beam which was supplied by the FN-tandem accelerator and the ICP analysis has been performed in Targoviste using a Baird ICP2070 - Sequential Plasma Spectrometer. The results obtained by the two methods were compared.

Introduction

Vegetal samples can be used in monitoring environmental pollution by heavy metals. Plants not only intercept pollutants from atmospheric deposition but also accumulate aerial metals from the soil. Aerial heavy metal deposit are taken up from the soil by plants via their root system and translocated to other regions of the plant. Particle deposition on leaf surfaces may be affected by a variety of factors, including particle size and mass, wind velocity, leaf orientation, size, moisture level and surface characteristics¹. The deposited particles may be washed by rain into the soil, resuspended or retained on plant foliage. The degree of retention is influenced by weather conditions, nature of pollutant, plant surface characteristics and particle size². Harrison and Chirgawi (1989) demonstrated experimentally the significance of foliar accumulation and translocation of air derived metal pollutants. The foliar route was found to be of similar importance to the soil-root pathway. Heavy metal absorption is governed by soil characteristics such as pH and organic matter content³. Thus, high levels of heavy metals in the soil do not always indicate similar high concentrations in plants. The extent of accumulation and toxic level will depend on the plant and heavy metal species under observation. In an investigation of Cd, Cu, Ni and Pb uptake from air and soil by *Achillea millefolium* (milfoil) and *Hordeum vulgare* (barley) in Denmark, Pilegaard and Johnsen (1984)⁴ concluded that Cu and Pb plant concentrations correlated with aerial deposition but not with soil concentrations. In contrast, Ni and Cd content in the plants correlated with deposition and soil content. The interpretation of analytical data is therefore complicated by

many factors. However, metal accumulation in plants can reflect the relative extent of the burden and its dispersal. The article reports the basic data on the heavy metal content in the vegetable leaves and soil from cropping areas obtained by Particle Induced X-ray Emission (PIXE) ⁵ method and Atomic Emission spectrometry technique with Inductively Coupled Plasma (ICP-AES) ⁶. Data collected indicated a direct influence of heavy metals concentrations in the chain soil-vegetables.

Experimental

Sampling

The sampling of vegetable, *Apium graveolens* (celery), *Brasica oleracea* (cabbage), leaves samples were made in phenological phase mature fruit of vegetables. The samples of fresh leaves were weighed, then were dried in drying stove at 105 °C for 1 hour.

The soil samples from vegetables cropping area were drew from different depths in soil: over surface, 10 cm in deep and 20 cm in deep. The soil samples were also dried in the same conditions as the biological samples.

PIXE experimental procedure

Sample preparation

A few tens of milligrams of vegetable leaves and soil were weighted and put in 50mL HDPE vials. For each sample an equal volume of 2-4mL HNO₃ and a few hundreds of microliters H₂O₂ and HF were added. In order to assure complete digestion the samples were heated 4 hours at 75°C. After digestion each sample was diluted with a convenient volume of deionized water followed by addition of internal standard (200µl solution of Y₂O₃ in HNO₃ medium, containing 160.8µg Y/ml). Volumes of 150µl were deposited and evaporated on Mylar foil (2,5µm thickness) fixed on aluminum frames.

Analysis

PIXE measurements of target elements were made using a 3 MeV proton beam extracted from the Tandem Accelerator FN-8 of the National Institute of Nuclear Physics – Horia Hulubei of Magurele, Bucharest. X-ray spectra were measured with a spectrometric chain with a CANBERRA Ge hyperpure detector with a 160 eV resolution at 6.4 KeV of Ka line of iron. The X-ray spectrum analyses were made off-line, at Valahia University of Targoviste, using LEONE fitting programs.

ICP-AES experimental procedure

Sample preparation

The dried leaves were grained and after powdering, 2.00 g powder leaves have been digested in 40 ml HNO₃. After a set aside in fume cupboard overnight the obtained liquid was gently boiled (without major loss of volume). For a good digestion 3 ml acid perchloric have been added and 2-3 ml water after cooling.

Analysis

The cooled sample solution was diluted with water at 250 ml solution and nebulized into plasma of spectrometer. ICP-AES measurements were made using the Baird ICP2070 -Sequential Plasma Spectrometer in Targoviste.

Results and discussions

PIXE analysis allowed determination of S, Cl, K, Ca, Ti, Mn, Fe, Ni, Cu, Zn, Sr in vegetable samples (table 1) and of K, Ca, Mn, Fe, Cu, Zn, Cr, Sr, Mo in soil samples (table 2) with the uncertainties of the data point of the order of 10%.

ICP analysis allowed determination of Na, Mg, Fe, Cu, and Zn in vegetables samples (table 3). The uncertainties are less then 6%.

We can observe the presence of toxic element Sr in soil and leaves of vegetables: the higher concentration of Sr is on the surface of soil and decrease inside the soil. Also the calcium, potassium and iron concentrations are higher at the surface soil and decrease inside the soil.

Table 1. Concentration (mg/100g fresh sample) of elements from vegetable leaves analysed with PIXE method

| Samples | S | Cl | K | Ca | Ti | Mn | Fe | Ni | Cu | Zn | Sr |
|---|-----------|------|-------|-------|-------|-------|-------|-------|-------|-------|-------|
| <i>Apium graveolens</i> (celery) leaves | 18 | 59 | 19.6 | 51 | 0.098 | 0.116 | 0.382 | 0.006 | 0.011 | 0.078 | 0.017 |
| <i>Apium graveolens</i> (celery) leaves | 14.3 | 51.5 | 15.78 | 66.6 | 0.111 | 0.172 | 0.346 | Nd* | 0.018 | 0.088 | 0.019 |
| <i>Brasica oleracea external</i> (cabbage) leaves | 45.6 | 89 | 12 | 7.84 | Nd* | 0.098 | 1.164 | 0.003 | 0.053 | 0.13 | 0.012 |
| <i>Brasica oleracea external</i> (cabbage) leaves | 49 | 88 | 10.7 | 6.7 | Nd* | 0.095 | 1.38 | Nd* | 0.061 | 0.138 | 0.014 |
| <i>Brasica oleracea inside</i> (cabbage) leaves | 21.8 4 | 5.99 | 36.3 | 11.9 | Nd* | 0.022 | 1.7 | 0.006 | 0.054 | 0.033 | 0.006 |
| <i>Brasica oleracea inside</i> (cabbage) leaves | 28.5 5 | 4.75 | 36 | 14.22 | 0.005 | 0.017 | 1.88 | Nd* | 0.045 | 0.031 | 0.008 |
| * not detected | | | | | | | | | | | |

Table 2. Concentration (mg/100g) of elements from soil samples analysed with PIXE method

| Samples | K | Ca | Mn | Fe | Cu | Zn | Cr | Sr | Mo |
|----------------------|------|------|------|------|-------|------|------|-----|------|
| Soil from surface | 37 | 12 | 0.07 | 46 | 0.005 | 0.13 | 0.04 | 3.6 | 0.13 |
| Soil from 10 cm deep | 27.2 | 8.12 | 0.77 | 35.6 | 0.007 | 0.02 | 0.06 | 2.6 | 0.1 |
| Soil from 20 cm deep | 23.6 | 7.80 | 1.33 | 31 | 0.008 | 0.01 | 0.16 | 1.2 | 0.05 |

Table 3. Concentration (mg/100g fresh samples) of elements from vegetable leaves analyzed with ICP-AES method

| Samples | Na | Mg | Fe | Cu | Zn |
|---|------|------|-------|-------|-------|
| <i>Apium graveolens</i> (celery) leaves | 5.24 | 0.92 | 0.374 | 0.017 | 0.07 |
| <i>Apium graveolens</i> (celery) leaves | 5.72 | 0.95 | 0.376 | 0.018 | 0.082 |
| <i>Brasica oleracea</i> external (cabbage) leaves | 12.2 | 1.25 | 1.17 | 0.05 | 0.131 |
| <i>Brasica oleracea</i> external (cabbage) leaves | 12.8 | 1.74 | 1.25 | 0.058 | 0.135 |
| <i>Brasica oleracea</i> inside (cabbage) leaves | 11.7 | 1.87 | 1.67 | 0.047 | 0.04 |
| <i>Brasica oleracea</i> inside (cabbage) leaves | 10.8 | 1.82 | 1.74 | 0.045 | 0.032 |

A correlation between elemental map of vegetables and elemental map of surface soil was made (figure 2). We found an order two polynomial dependence between the elemental maps of surface soil sample and celery leaves sample.

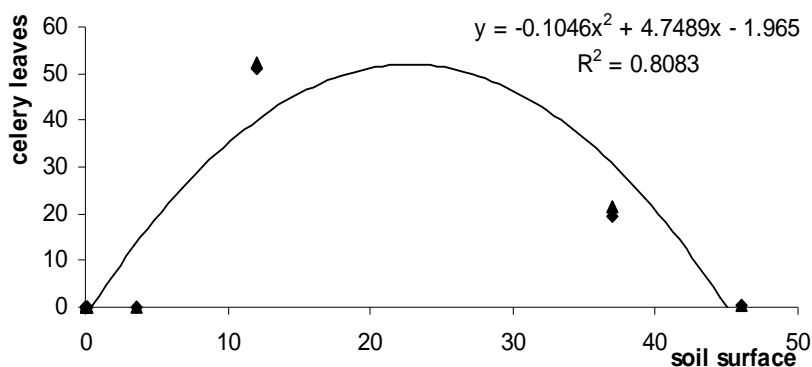


Figure 2 Correlation between elements concentrations of surface soil and celery leaves

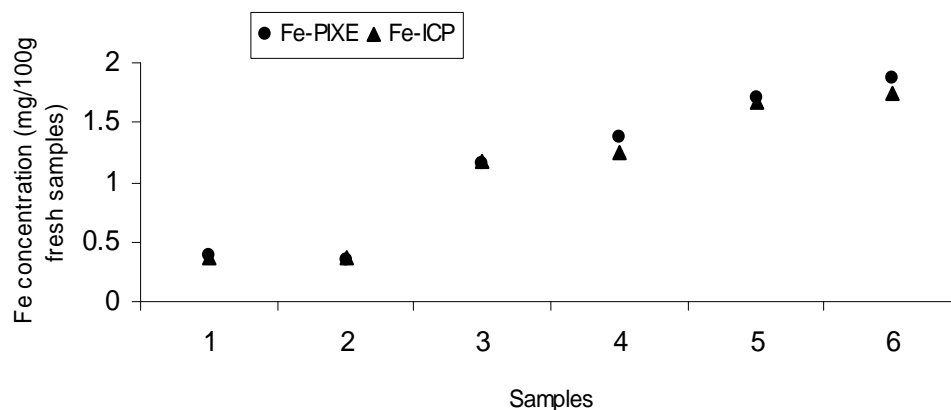


Figure 1a) Fe concentration in vegetables leaves obtained by PIXE and ICP methods

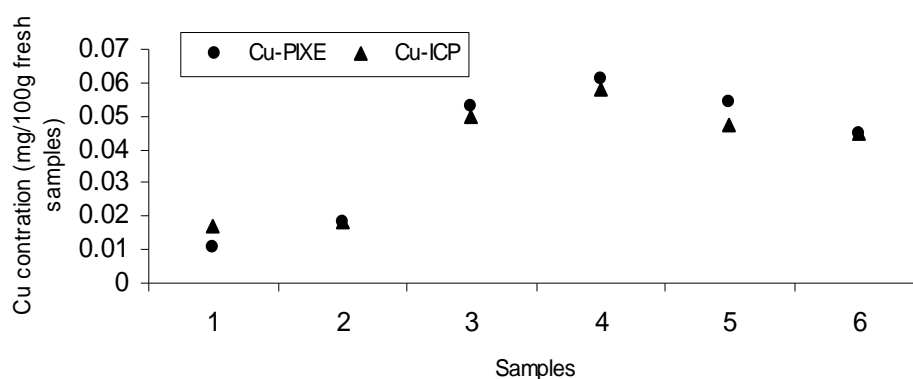


Figure 1 b) Cu concentration in vegetables leaves obtained by PIXE and ICP methods

Conclusions

The obtained elemental composition of soil can be use to establish the optimal distances to plant the vegetables used in agroalimentary domain. A good correlation between the elemental map of plants and the elemental map of soil samples can be made in the next work using the obtained basic data. For Fe Cu, elements which can be determine by both methods, the concentrations obtained by ICP method are in good concordance with the concentration obtained by PIXE method (figures 2 a, b). The obtained results demonstrate the complementarity of the two analytical methods PIXE and ICP, in determination of the whole elemental map of different samples.

References

1. Bache, C.A., Gutenmann, W.H., Rutzke, M., Chu, G., Elfving, D.C. and Lisk, D.J., Concentrations of metals in grasses in the vicinity of a municipal refuse incinerator, *Environmental Contamination and Toxicology*, **1991**, 20, 4, 538-542.
2. Harrison, R.M. and Chirgawi, M.B., The assessment of air and soil as contributors of some trace metals to vegetable plants, *Science of the Total Environment*, **1989**, 83, 1-2, 13-34
3. Csintalan, Z. and Tuba, Z., “The effect of pollution on the physiological processes in plants, Biological indicators in environmental protection”, Kovács, M. (ed.), Ellis Horwood, New York, 1992
4. Pilegaard, K. and Johnsen, I., Heavy metal uptake from air and soil by transplanted plants of *Achillea millefolium* and *Hordeum vulgare*. Rasmussen, L. (ed.), *Ecological Bulletins (NFR)*, **1984**, 36, 97-102
5. Johansson, S.A.E., Campbell, JPL., “PIXE: A Novel Technique for Elemental Analysis, Campbell’s First Book on PIXE”, John Wiley and Sons, New York, 1998
6. Bauman’s, R.W.J.M., “Inductively Coupled Plasma Emission Spectroscopy”, John Wiley and Sons, New York, 1987

APPLICATION OF PIXE METHOD TO PHOSPHATASE ENZYME ANALYSIS

Ion V. Popescu, Gabriel Dima, Claudia Stihl, Laur Manea

Abstract

The aim of this work is the microelemental analysis of blood serum samples by PIXE (Particle Induced X-Rays Emission) method in order to making correlation's with phosphatase alkaline enzyme activity. This enzyme is responsible of the bone formation and growth (Ca/P ratio) and the measurements are made on normal, rachitic, paretic and osteoporotic animals (cattle's). We used PIXE method in internal standard variant for systematically errors elimination's. The samples introduced into the reaction chamber are bombarded with 3.2 MeV proton beam. The characteristics X-rays spectra were detected by a Ge hyperpure detector with the energy resolution of 160 eV at the $K\alpha$ 6.4 keV X-ray iron line are recorded using an acquisition computer. As an internal standard element for spectrum's normalisation we used Yttrium. Using the calibration curve and the Leone software were making determinations on Ca, P, Fe and Mg content of analysed samples. We find a dependency of Ca/P ratio and Mg content of blood serum.

1. Introduction.

Phosphatase alkaline enzyme is implicated in bone growth process. In order to study their activity we have collected blood serum of some cattle's, interesting from medical reasons and make determinations of P, Ca and Mg content using the PIXE method.

For a normal organism, the ratio Ca/P is among 1 and 2, for rahitic organisms is grater then 3 and for osteoporoutic ones is less then 1. The Mg is an activator of the enzyme.

2. Samples preparations.

Blood serum samples are collected from jugular zone of cattle's selected by following criteria:

- the season of food alimentation (winter/summer);
- great milk productions;
- advanced pregnancy steady (last weeks);
- the weight of cattle's.

After the serum separation (24-36 hours), the target samples were doped with standard solution (1:1) of Yttrium for spectrum normalisation and deposited on mylar foils who are attached on aluminium supports in order to introduce them in irradiation chamber (a multitarget irradiation chamber). We have prepared 10 samples.

The cattle's having the experience number 4,5,6,7,8,9 are cattle's in the first days after born of the young's cattle's. The cattle's having the experience number 2,3,10 are cattle's in the last week of pregnancy.

3. The experimental set-up.

Measurements of mineral substances were made using a 3.2 MeV protons beam extracted from the TANDEM accelerator from IFIN-HH Magurele, Bucharest. X-ray's spectra were measured with a spectrometric chain, with a CANBERRA Ge hyperpure detector with a 160 eV resolution at 6.4 KeV of XK_{α} line of iron. Amplification, generation and analysis of electric signals were achieved by an adequate electronic device: a sensitive preamplifier with field effect cooled at the liquid nitrogen temperature, a linear amplifier and a multichannel analyser with 4096 channels having an acquisition computer for data output - PDP11. For each sample target were recorded the characteristic X-ray spectra. The X-ray spectrum's analyses were made off-line using a computer fitting programme -

LEONE. The calibrations of experimental set-up were made using standard targets witch are prepared by evaporating pure elements (Ni, Cu, Ge, Ag, Sn, Au, Pb) on mylar foil .

The determinations of phosphatase alkaline enzyme is analysed blood serum samples were made by spectrometric analysis using Bessey-Lowry method (the enzyme is a cathabolit for chemical reaction: $R-O-PO_3H_2+H_2O \rightarrow R-OH+H_3PO_4$).

4. Results and conclusions.

A typical X-ray spectrum of blood serum samples is shown in fig. 1.

The contents of Ca, P, Mg, alkaline enzyme of analysed samples and the normal values are shown in table 1. Analysing our data, we can see a good level of Ca. The samples number 1 is from a young cattle having a dismorexy's syndrome. We can see a great level of enzyme content. The sample number 10 have a great level of Ca and P than the normal one, and the result shows that in a young organism there are compensatory mechanisms for balancing the loses of Ca by a great milk production. The content of Mg in the same sample is grater than the normal value, because Mg is an activator of phosphatase alkaline enzyme.

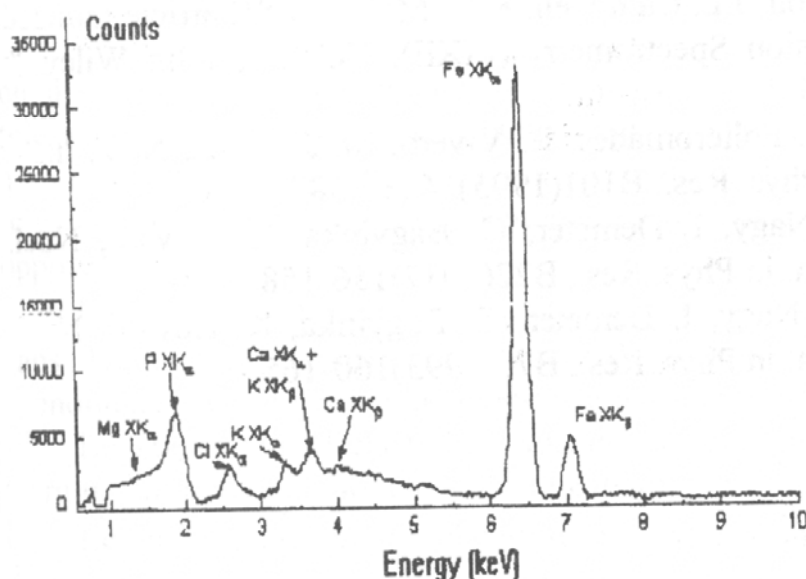


Figure 1.

Table 1.

| Sample | Ca (mg/dl) | P (mg/dl) | Mg (mg/dl) | Phosphatase alkaline (I.U./l) |
|--------------------|---------------|--------------|---------------|-------------------------------------|
| 1 | 9.7 | 6.5 | 2.3 | 40.42 |
| 2 | 12.2 | 5.9 | 3.1 | 15.19 |
| 3 | 9.8 | 7.5 | 2.3 | 17.15 |
| 4 | 9.1 | 6.6 | 2.5 | 9.55 |
| 5 | 9.2 | 7.0 | 2.3 | 11.27 |
| 6 | 10.8 | 5.5 | 2.6 | 13.23 |
| 7 | 10.1 | 7.0 | 2.7 | 9.55 |
| 8 | 9.3 | 6.5 | 2.9 | 8.57 |
| 9 | 9.5 | 7.0 | 2.7 | 9.55 |
| 10 | 12.3 | 8.1 | 3.5 | 29.75 |
| Reference value | 8-11 | 5-7.2 | 2.1-2.8 | 10-36 |

5. References

1. S.A.E. Johansson, J.L. Campbell, K.G. Malmqvist, Particle Induced X-Ray Emmission Spectrometry (PIXE), Vol.133, John Wiley & Sons Inc., 1995
2. M. Aspiazu, R. Policroniades, R. Vivero, M. Jimenez, Nucl. Instr. And Meth. in Phys. Res., B101(1995), 453-458
3. Z. Szokefalvi-Nagy, I. Demeter, C. Bagyinka, K. Kovacs, Nucl. Instr. And Meth. in Phys. Res., B22(1987)156-158
4. Z. Szokefalvi-Nagy, I. Demeter, C. Bagyinka, K. Kovacs, Nucl. Instr. And Meth. in Phys. Res., B75(1993)160-165

EFFICIENCY INCREASE METHODS OF METALS HEATING BY LASER

Calin Oros, Dana Vladescu, Marin Iordan, Marina Olariu
"Valahia" University of Târgaviste

Abstract

An efficient application of laser technology impose the choice of some irradiation conditions which permit metals heating until expected temperature with minimum irradiation duration and expanses.

This paper presents a review for some experimental data and theoretical observations regarding the influence efficiency increase metals heating by power laser, irradiation conditions, incidental angle and wave length.

1. The influence of irradiation conditions

*** Irradiation continuous regime**

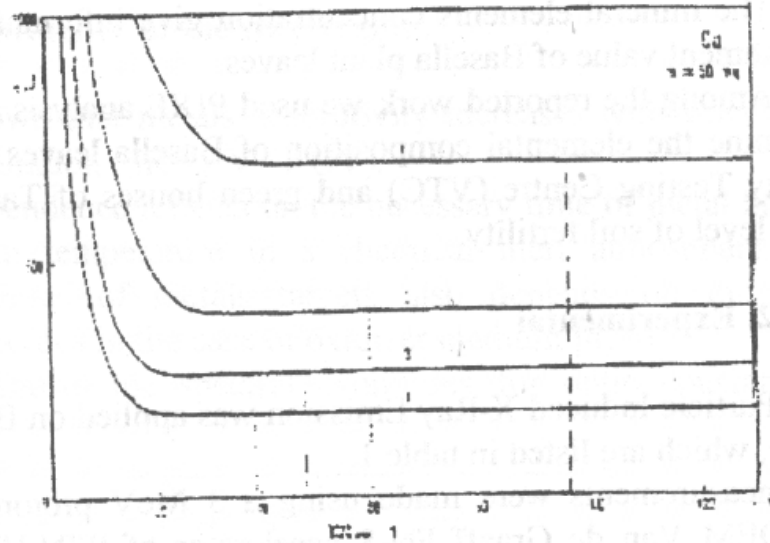
The consumption of energy for target heating under the action of a laser source with constant power P , until the melting temperature, T_m , is:

$$\epsilon_m = Pt_m$$

where t_m is the time of melting initiation.

Fig. 1 shows the dependences $\epsilon_m = \epsilon_m (P, A_0)$, (A_0 is the intrinsic absorptivity coefficient of the sample) for copper target irradiated with a CO_2 laser in continuous beam [1].

Fig. 1.

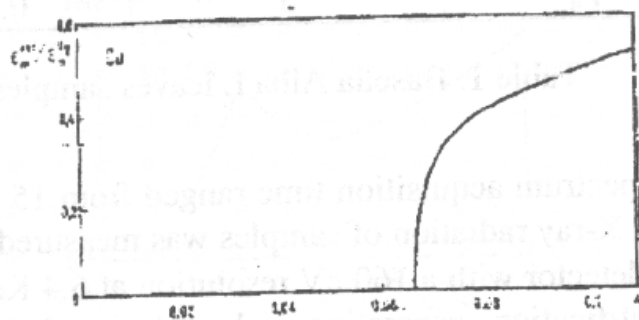


There is an optimum power laser which depends on the fact that in low values of the ratio $\frac{P}{S_s}$ (S_s is the irradiation spot area), the essential part of energy absorbed of metal is compensated for thermic damage.

* The irradiation medium

Fig. 2 shows the ratio $\epsilon_m^{\text{air}} / \epsilon_m^{\text{N}_2}$ between the necessary energies for heating until T_m in air and in nitrogen at P_{opt} , varying with the initial absorptivity of the copper target [2].

Fig. 2



The mineral elements concentration give information about the nourishment value of Basella plant leaves.

Among the reported work we used PIXE analysis method [1] to determine the elemental composition of Basella leaves. cultivated in Variety Testing Centre (VTC) and green houses of Targoviste for a given level of soil fertility.

2. Experimental

Particle Induced X-Ray Emission was applied on Basella Alba L leaves, which are listed in table 1.

The measurements were made using a 3 MeV protons beam of a TANDEM Van de Graaff FN-8 accelerator of IFIN-HH Bucharest. The target samples were placed into PIXE chamber, and the beam intensity was measured by means a Faraday cup. The beam diameter on the target was 4 mm and the targets were fixed at an angle of 45° to the beam direction and to the detector direction.

| Samples | Green mass [g] | Dried mass [g] |
|----------------|----------------|----------------|
| P ₁ | 5 | 0.2966 |
| P ₁ | 5 | 0.3080 |
| P ₂ | 5 | 0.4412 |
| P ₂ | 5 | 0.4133 |
| P ₃ | 5 | 0.4317 |
| P ₃ | 5 | 0.4174 |
| P ₄ | 5 | 0.4458 |
| P ₄ | 5 | 0.4511 |

Table 1. Basella Alba L leaves samples

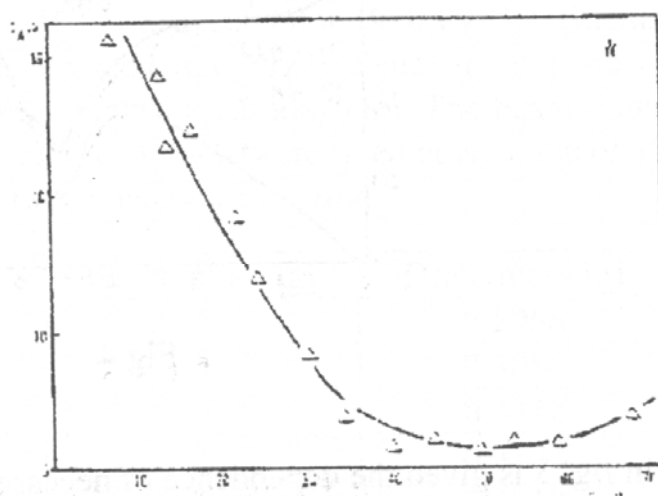
Usual spectrum acquisition time ranged from 15 to 30 min. The characteristic X-ray radiation of samples was measured by a Canberra Ge hiperpur detector with a 160 eV resolution at 6.4 KeV of XK_α line of iron. Amplification, generation and analysis of electrical signals were achieved by an adequate electronic device: a sensitive preamplifier, a linear amplificator and a multichannel analyser with

3. The influence of the incidental angle

The direction of laser radiation on target under an angle θ differed from 0° and the utilization of a polarized radiation involves a considerable diminution - in some cases with more orders of measure - of energy consumptions for laser heating of metals which oxidize.

Fig. 6. shows the evolution of firing time depending on the incidence angle of radiation $t_a (\Theta)$, at constant power $P \cong 700$ W. Wolfram targets with thickness $h = 200 \mu\text{m}$ were used [6]. The diameter of heating spot at $\Theta = 0^\circ$ was approximately 5 mm, much small than transversal dimensions of samples.

Fig. 6



On entire investigated domain of variation for Θ , the firing time value t_A is more low in the case of oblique incidency than in the case of normal incidency, even though the irradiation spot surface increases because of fascicle inclination.

4. The influence of the polarization of laser - radiation

The polarisation effect of laser radiation concerning metals heating was analysed by means of polarized CO_2 laser source, in periodical impulses [7].

The titan targets were used ($h = 50 \mu\text{m}$, $R_s = 3$ mm).

The radiation could be polarized both in incidence plane (\parallel) and in perpendicular plane (\perp) on this. The evolutions of activation relative times for titan targets oxidation both in the case $K_a = t_a(\Theta) / t_a(0^0)$ and in the case $k_a = t_a(\Theta) / t_a(0^0)$ are given in fig 7.

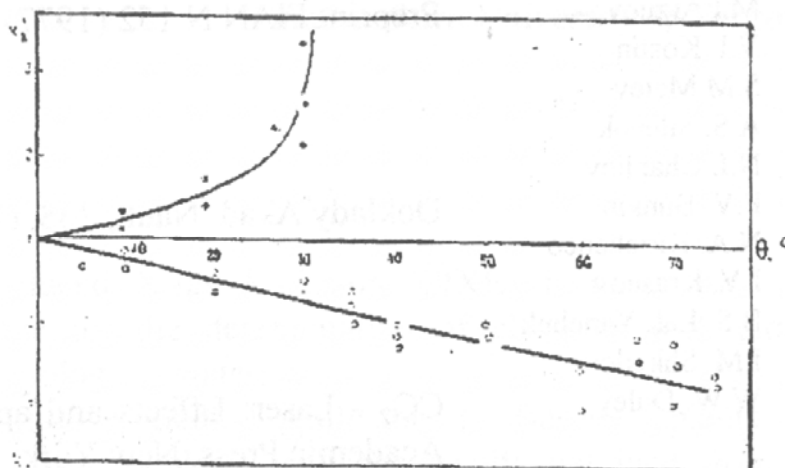


Fig. 7

The gain regarding energetically expenses obtained at inclination of laser beam is characterized of $1 / k_a$ and depends on choise for direction of polarisation.

The energetical gain which results through olique incidence of radiation is determined on angular dependence of metal - oxyde system absorbitivity and on great interdependence between oxidation process and heating process.

5. Conclusion

The consideration and correlation of analysed factors lead to maximalize the efficiency of laser metals heating trough reduction of energetical expenses.

6. References

1. M.I Arzuov Kratkiye Soobscheniya po Fizica N 11
F.V. Bunkin (1978), 43
N.A. Kirichenco
V.I. Konov
B.S. Luk Yanchuk
2. M.I Arzuov Preprint FIAN N 152 (1977)
V.I. Kostin
S.M. Metev
A.S. Silenok
N.I. Chapliev
3. F.V. Bunkin Doklady Akad. Nauk, 268, (1983), 598
N.A. Kirichenco
I.V. Krasnov
B.S. Luk Yanchuk
I.M. Shkedov
4. W.W. Duley CO₂ - Laser: Effects and application, Ed.
Academic Press, New York. 1976
5. J.F. Ready Effects of Higt - Power Laser Radiation,
Ed. Mir, Moscova, 1974
6. M.I Arzuov Kvant. Electron 6, (1979), 1432
A.I. Barchukov
F.V. Bunkin
N.A. Kirichenco
V.I. Konov
B.S. Luk Yanchuk
7. I.N. Goncharov Preprint FIAN N, 76, Moscova (1980)
A.A. Gorbunov
V.I. Konov
A.S. Silenok
Yu. A. Skvortsov
V.N. Tokarev
N.I. Chapliev

PIXE ANALYSIS OF BASELLA ALBA L AND BASELLA RUBRA L LEAVES

*Claudia Stihi, Gabriel Dima, Gabriela Busuioc, Ion V. Popescu
Valahia University of Targovite*

Abstract:

Particle Induced X-ray Emission (PIXE) is a sensitive and reliable technique for the determination of elements with atomic number > 13 in biological materials.

This quantitative method applicable to Basella plants, is described in this work, along with the results obtained from the elemental analysis of leaves from different Basella plants cultivated in Variety Testing Centre and in Green Houses of Targoviste. The target samples were bombarded with 3 MeV protons beam obtained at Tandem Accelerator of IFIN-HH Bucharest. The X-rays were detected with Ge hiperpur detector with 160 eV at 5.9 KeV energy resolution and the characteristic X-ray spectra were recorded using an acquisition system with a PC computer. The concentration obtained for the chemical elements who give a great nourishment value of Basella plants : P, Ca, Mg, K, Na, Fe, Mn, Zn, Cu, have an estimated precision of less than 12%.

1. Introduction

Basella plant belong to Basellaceae family is a tropical plant used as a vegetable.

One of the problems of actual foods department is the variety about the vegetables with a great nourishment value. Is the case of Basella plant like the native spinach (*Spinacea oleracea*).

The mineral elements concentration give information about the nourishment value of Basella plant leaves.

Among the reported work we used PIXE analysis method [1] to determine the elemental composition of Basella leaves. cultivated in Variety Testing Centre (VTC) and green houses of Targoviste for a given level of soil fertility.

2. Experimental

Particle Induced X-Ray Emission was applied on Basella Alba L leaves, which are listed in table 1.

The measurements were made using a 3 MeV protons beam of a TANDEM Van de Graaff FN-8 accelerator of IFIN-HH Bucharest. The target samples were placed into PIXE chamber, and the beam intensity was measured by means a Faraday cup. The beam diameter on the target was 4 mm and the targets were fixed at an angle of 45° to the beam direction and to the detector direction.

| Samples | Green mass [g] | Dried mass [g] |
|----------------|----------------|----------------|
| P ₁ | 5 | 0.2966 |
| P ₁ | 5 | 0.3080 |
| P ₂ | 5 | 0.4412 |
| P ₂ | 5 | 0.4133 |
| P ₃ | 5 | 0.4317 |
| P ₃ | 5 | 0.4174 |
| P ₄ | 5 | 0.4458 |
| P ₄ | 5 | 0.4511 |

Table 1. Basella Alba L leaves samples

Usual spectrum acquisition time ranged from 15 to 30 min. The characteristic X-ray radiation of samples was measured by a Canberra Ge hiperpur detector with a 160 eV resolution at 6.4 KeV of XK_{α} line of iron. Amplification, generation and analysis of electrical signals were achieved by an adequate electronic device: a sensitive preamplifier, a linear amplificator and a multichannel analyser with

4096 channels having an acquisition computer for data output-PDP11.

The X-ray spectrum's analysis were made off-line using an computer fitting programme - LEONE. Figure 1 show a graph of a typical X-ray spectrum (Basella Alba leaves sample) obtained with the experimental arrangement described.

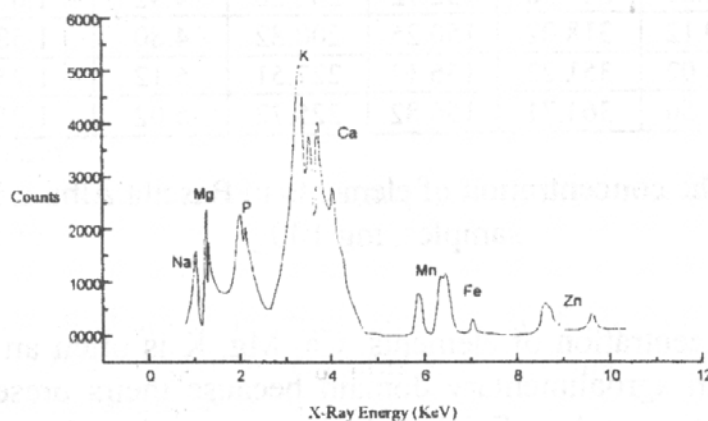


Fig. 1 A typical spectrum of Basella Alba leaves sample

In the experiment we used young Basella Alba Leaves [2] sorted in four groups: Basella Alba - green house (P_1 , P_1'); Basella Alba - VTC (P_2 , P_2'); Basella Alba - VTC cultivated in soil treated with an artificial fertiliser using N (P_3 , P_3'); Basella Alba - VTC cultivated in soil treated with natural fertiliser (P_4 , P_4').

The target sample have been prepared in the following manner: the washed leaves were simply air-dried at a temperature of 50^0 in a clean box preventing further contamination. The dried leaves were grained and after powdering a layer of the samples material were deposited on hostaphan foils.

3. Results and discussions

Using PIXE method we identified and we determined the amount of the following elements: P, Ca, Mg, K, Fe, Mn, Zn. In table 2 are presented the results of PIXE analysis on Basella Alba leaves samples with an instrumental error less than 12%.

| Samp-les | P | Ca | Mg | K | Fe | Mn | Zn |
|----------------|-------|--------|--------|--------|------|------|------|
| P ₁ | 67.40 | 294.31 | 147.02 | 230.04 | 4.80 | 1.50 | 1.32 |
| P ₁ | 67.54 | 293.27 | 146.81 | 231.82 | 4.72 | 1.37 | 1.25 |
| P ₂ | 82.40 | 381.37 | 158.20 | 228.32 | 5.20 | 1.72 | 1.24 |
| P ₂ | 82.78 | 389.33 | 161.25 | 225.20 | 4.98 | 1.80 | 1.33 |
| P ₃ | 88.20 | 316.38 | 152.72 | 202.20 | 4.92 | 1.62 | 0.98 |
| P ₃ | 89.12 | 318.02 | 150.25 | 200.82 | 4.80 | 1.58 | 0.87 |
| P ₄ | 94.02 | 351.22 | 156.12 | 227.51 | 5.12 | 1.25 | 1.12 |
| P ₄ | 94.50 | 364.71 | 156.82 | 225.72 | 5.02 | 1.25 | 1.02 |

Table 2. The concentration of elements in Basella Alba L leaves samples, mg/100g

The concentration of elements: Ca, Mg, K is often an essential requirement in agroalimentary domain because theirs presence in a big concentration is beneficial and give a remarkable nourishment value of Basella plants.

4. Conclusions

The use of PIXE technique give possibility to determine the elemental composition of plants with a great sensivity - the limit detection is 1 µg/g, that is genuine trace-element analysis capability [3]. A series of elements was put in evidence in Basella Alba leaves samples, elements which give a great nourishment value of Basella plant.

References:

1. S.A.E. Johansson, J.L. Campbell, K.G. Malmqvist, Particle Induced X-Ray Emission Spectrometry (PIXE), Volume 133, John Wiley&Sons, Inc., 1995;
2. W.E. Glassegen, J.W. Metzger, S. Heuer, Phytochemistry, Vol. 33, No.6, pp 1525-1527, 1993;
3. J. Aspiazu, R. Policroniades, R. Vivero, M. Jimenez, Nuclear Instruments and Methods in Physics Research B101 (1995) 453-458.

ON THE SENSITIVITY OF GRAVITATIONAL OSCILLATOR

Marin Iordan, Calin Oros

Valahia University of Targovite

Until year 1960, the very low energy of gravitational radiation has determined the deception of experimentators. In year 1960 J. Weber presents /1/ the theoretical and experimental principles of the direct observation of gravitational waves. The gravitational wave detector imagined as two masses m_0 united by an elastic spring has been studied of Einstein theory point of view of gravity.

We proposed /2/ a relativist - restricted linear theory of gravity that has an important advantage: the analogy with the electromagnetical field theory.

Considering the detector imagined by Weber from our theory point of view, we obtained for equation of motion of mass m_0 the equation

$$\frac{du_l}{ds} = G_{lk} u^k + \frac{1}{m_0 c^2} \mathcal{F}_l \quad (1)$$

where

$$G_{lk} = \frac{G_N}{(1 + G_N A_{mn} u^m u^n)} \left[u^i (A_{il,k} - A_{ik,l}) + u^i \left(u_k \frac{dA_{il}}{ds} - u_l \frac{dA_{ik}}{ds} \right) + 2 \frac{du^n}{ds} (u_k A_{ln} - u_l A_{kn}) \right]$$

$$\mathcal{F}_l = (1 + G_N A_{mn} u^m u^n)^{-1} * F_l$$

with G_N the Newton constant of universal attraction, A_{ik} stress potential of gravitational field, u^i velocity quadrivector. The first term from right part of equation (1) represents the contribution of gravitational field and the second term represents the un gravitational interaction between the two masses. Since each mass m_0 is moving on a univers line, let's consider a parameter with the propriety that for any univers line a value of α is corresponding.

derivating equation (1) in relation to the parameter α and using the notations

$$n^j = \frac{\partial x^j}{\partial \alpha}, \quad u^k G_k^l = E^l, \quad \frac{\partial \mathcal{F}}{\partial \alpha} = f^l \quad (2)$$

we obtain

$$\frac{d^2 n^1}{ds^2} = E^1_{,p} n^p + \frac{1}{m_0 c^2} f^1 \quad (3)$$

We choose for quadrivector n^p defined in (2) the expression

$$n^1 = r^1 + \xi^1 \quad (4)$$

where r^1 is the static component of the normal vector n^p at the univers lines and ξ^1 is the dynamic component. Certainly $A_{ik}=0$ and internal damping is very high $n^1 \rightarrow r^1$. If $r^1 \gg \xi^1$, taking into account (4), we obtain for the motion equation (3)

$$\frac{d^2 \xi^1}{ds^2} - \frac{1}{m_0 c^2} f^1 = E^1_{,k} r^k \quad (5)$$

We admit that f^1 consists of two terms, $-c D^1_k \frac{d\xi^k}{ds}$, corresponding to the damping force and the second term $-K^1_m \xi^m$ corresponding to the elastic force. By means of their, the equation (5) becomes

$$\frac{d^2 \xi^1}{ds^2} + \frac{1}{m_0 c} D^1_m \frac{d\xi^m}{ds} + \frac{1}{m_0 c^2} K^1_m \xi^m = E^1_{,k} r^k \quad (6)$$

In the proper reference system, with the origin in the center of the oscillator mass, the equation (6) becomes

$$\frac{d^2 \xi^1}{dt^2} + \frac{1}{m_0} D^1_m \frac{d\xi^m}{dt} + \frac{1}{m_0} K^1_m \xi^m = c^2 E^1_{,k} r^k \quad (7)$$

We consider the oscillator orientated to direction $x^1=x$, consequently $D^1_1=D$, $K^1_1=K$. In the hypothesis of a dynamic gravitational field described by

$$E^1_{,k}(x, t) = E^1_{,k}(x, \omega) e^{-i\omega t}$$

the solution $\xi^1(\omega, t) = \xi^1(\omega) e^{-i\omega t}$ of equation (7) offers us:

$$\xi^1(\omega) = \frac{m_0 c^2 (E^1_{,k}(\omega) r^k)}{-m_0 \omega^2 + i\delta_1^1 K + i\delta_1^1 \omega D} \quad (8)$$

We can observe from (8) that the deformation ξ^1 presents a maximum if the resonance condition $\omega^2 - \omega_0^2 = 0$ ($\omega_0^2 = K/m$) is fulfilled.

We assume that the total dissipation D takes the form of $D=D_{ex}+D_{in}$, where D_{ex} is characteristic for external dissipation and D_{in} is referred to the irreversible processes from the aerial. The mean power that may be returned to the external apparatus is .

$$\langle P_{ex} \rangle = \frac{1}{2} \omega^2 |\xi^1(\omega)|^2 D_{ex} \quad (9)$$

At resonance ,we obtain for (9), using the expression (8) of the deformation.

$$\langle P_{ex} \rangle = \frac{1}{2} m_0^2 c^4 \langle (E^1_{,k}(\omega) r^k)^2 \rangle / (D_{ex} + D_{in})^2, \quad (10)$$

that represent a maximum when $D_{ex}=D_{in}$, as

$$\langle P_{ex} \rangle_{\max} = \frac{1}{8} m_0^2 c^4 \langle (E^1_{,k}(\omega) r^k)^2 \rangle / D_{ex}^2 \quad (10')$$

The medium value $\langle (E^1_{,k}(\omega) r^k)^2 \rangle$ is obtained by the analogy with the electrodynamics as proceeded by Broginski /3/. Let be the gravitational analogue of the radiation vector Poynting then

$$\tau = \frac{c^3 \langle (F^a_{grav})^2 \rangle}{4\pi m_0^2 G_N \omega^2 |r|^2} \quad (11)$$

where it has been done the link between the electrical charge to the gravitational charge $m_0 \sqrt{G_N}$ and where

$$F^a_{grav} = m_0 c^2 E^a_{,m} r^m \quad (12)$$

By means of the equations (11) and (12) we obtain the requested mean value

$$\langle (E^a_{,m}(\omega) r^m)^2 \rangle = 4\pi \beta^2 G_N |r|^2 \tau / c^5$$

which introduced in (10) leads to

$$\langle P_{ex} \rangle_{\max} = \pi m_0^2 \beta^2 G_N \tau / (2c D_{in}) \quad (13)$$

Since the lost power by a quadrupolar oscillator is given by relation (4)

$$P = G_N \left(\ddot{I} \right)^2 / 60 c^5$$

from the expression of the total energy accumulated in the oscillator $W = \frac{1}{2} m_0 \omega^2 \xi^2$ and the definition of the oscillator quality factor

$$Q = \omega W / P = \frac{m_0 \omega}{D_{in}} \text{ we obtain for } D_{in} :$$

$$D_{in} = 2 G_N m_0 |r|^2 \omega^4 / 15 c^5$$

that introduced in (13) leads to the expression

$$\langle P_{ex} \rangle_{max} = \frac{15\lambda^2}{16\pi} \tau \quad (14)$$

expression that establishes for the efficient section of the oscillator the relation

$\sigma = 15\lambda^2/16\pi$
i.e. a efficient section proportional to the square of the wave length and independent of the gravitational constant . This is a consequence of our admitting ab initio that the internal damping is caused by the radiation , the condition not being fulfilled practically because other irreversible processes from the aerial are more important.

We assume that oscillator is orientated for a maximum reply , in this case the equality

$$\langle (E^1, k(\omega)r^k)^2 \rangle_{dir.} = \frac{4}{15} \langle (E^1, k(\omega)r^k)^2 \rangle_{reply. max.}$$

that leads to the expression for the absorbed power

$$P_a = \frac{15}{8} \pi G_N m_0 Q \beta^2 |r|^2 \tau / \omega c$$

that implicates the efficient section

$$S = \frac{15}{8} \pi G_N m_0 Q \beta^2 |r|^2 / \omega c \quad (15)$$

The result obtained by us, (15), is corresponding to that obtained by Weber. We appreciate that for evaluation of the gravitational waves of low intensity we may use the formalism of a linear theora. The theory proposed by us has the advantage of the analogy with the description of the electromagnetical field that leads to an easy development.

/1/Weber.J., Phys.Rev.,117,306(1960)

/2/Gottlieb.I.,Ionescu-Pallas N., Iordan,M.,Rev.Roum.Phys,
27, nr.2,115(1982)

/3/Braginski,V.B., U.F.N.,86,433,(1965)

/4/Ionescu-pallas, N., Relativitatea generala si cosmologie,
Ed.St. si Enciplopedica, Bucuresti,(1980).

B. CHEMISTRY SECTION

GREEN PIGMENTS DERIVATIVES FROM HETEROCYCLIC DIQUINOXALINE-PIPERAZINE SYSTEMS

C. Rădulescu¹, A.-M. Hossu¹, I. Ioniță¹, E. I. Moater¹

¹„Valahia” University of Târgoviște, Faculty of Science and Arts, 18-22 Unirii Blvd. 130082

Abstract: *In this paper, it was studied the alkylated compounds obtained by organic synthesis for first time, by spectral analysis, IR, UV-VIS and NMR. The alkylation reaction was realized with very good yields, if the process parameters were respected during the time of reaction. The alkylated diquinoxaline-piperazine-dicarboxylic acids were obtained by original synthesis and as thermorezistance green pigments can be used for paint as powder type.*

Key words: *pigment, diquinoxaline-piperazine-dicarboxylic acids, spectral analysis*

1. Introduction

Many traditional pigments and pigment preparations have difficulties to keep the pace with technological progress in processing equipment. In addition, recent toxicological findings put pressure on established dispersing additives, which formerly enjoyed broad application in the paint industry [1, 2]. In last temps were prepared, for example, some red pigment with very good properties which found suitable applications in automotive paints, high grade printing inks, plastics, high grade industrial and architectural paints and as electrophotographic toners [3]. Also, the literature [4] present another red pigments (1,4-diketo-3,6-diphenylpyrrolo[3,4-c]pyrrole) which have attracted attention as colorants for imaging areas as well as color filters of liquid crystal displays.

It is known [5, 6] that the light fastness benefit of pigments tends can be associated with a poorer, duller shade and has predisposed the two classes of colorant towards different applications. Of particular interest in recent years has been the development of inks for ink jet printing. Until recently almost all colour inks for use in Small Office/Home Office (SOHO) market have been based on dyes. The dominance of dyes is likely to continue in the developing “photographic” market, but for use on plain paper, pigment based inks, are becoming more prevalent [7-9].

This paper presents the syntheses and characteristics of new alkylated pigments derivatives from piperazine-quinoxaline systems. The experimental researches effected on these alkylated systems were demonstrated that due their ionic character can be utilized for paints of powder type under the thermorezistance green pigments.

2. Experimental

The condensation reaction, for the synthesis of diquinoxaline-piperazine dicarboxylic acids, was possible in DMF (Merck 99.9% and b.p. =153⁰C) either by the using the compounds **1** and **2** or the compounds **4** and **5**, or 2 equivalents compounds **4** (Figure 1). The results are the same: the obtaining of heterocycles systems **3**, respectively **6**, derivatives of fluorubin, yellow shadows with red fluorescence. A mixture of 0.01 moles 2,3-dicloroquinoxaline-6-carboxylic acid, 0.01 moles 2,3-diaminoquinoxaline-6-carboxylic acid and 500 mL DMF (or 0.01 moles 2-cloro-3-aminoquinoxaline-6-carboxylic acid, 0.01 moles 2-amino-3-cloroquinoxaline-6-carboxylic acid and 500 mL DMF) was refluxed in 12 hours, under stirring; then, 10 hours it was distilled the DMF.

The product was filtered and recrystallized from alcohol, yellow needles, separated and purified by TLC and HPLC methods; yield 74.8% [4, 5].

The heterocyclic systems **3** and **6** were methylated with dimethyl sulfate in excess acetic acid medium, the molar ratio was $(\text{CH}_3)_2\text{SO}_4$:system **3** or **6** = 3:1 at 60-70°C in 14 hours (until the chromatogram indicated total conversion) under stirring. The next step was the conditioning with NaCl time 15 minutes at 70°C where there were obtained needles yellow-green with yield 92.6% (figure 2) [7, 8].

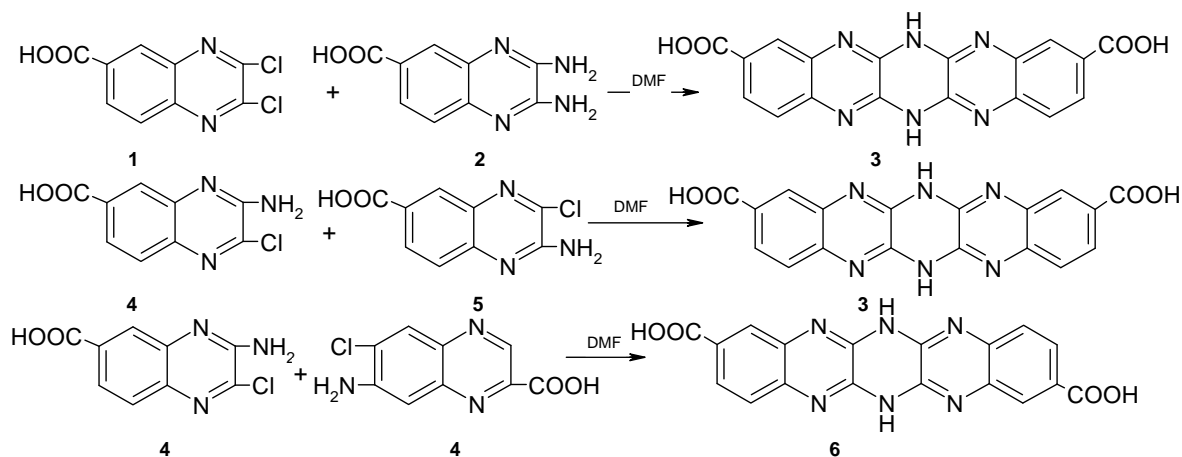


Fig. 1. The synthesis reactions of diquinoxaline[2,3-b][2,3-e]piperazine-6,6'-dicarboxylic acid, **3**, and diquinoxaline[2,3-b][2,3-e]piperazine-6,7'-dicarboxylic acid, **6**

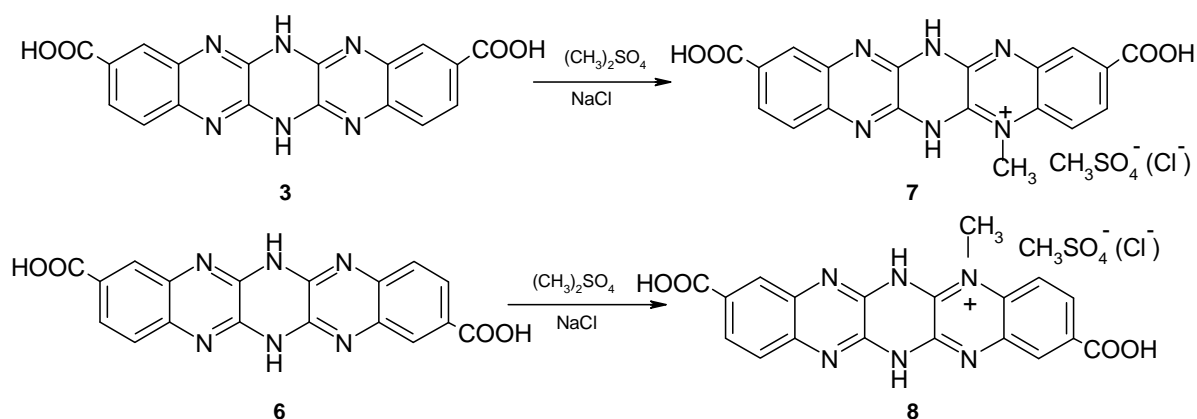


Fig. 2. The alkylation reactions of heterocyclic systems **3** and **6**

The results obtained from purification methods by TLC and HPLC, the melting points and the yields of synthesized compounds **3** and **6**, respectively **7** and **8** were presented in Table 1.

Table 1. The purification and separation by TLC and HPLC methods of compounds **3** and **6**, respectively **7** and **8**

| Compound | Thin-layer chromatography | HPLC chromatography | Melting point | Yields [%] |
|--|---|--|---------------|------------|
| <i>Diquinoxaline [2,3-b][2,3-e] piperazine dicarboxylic acids, 3 and 6</i> | <i>Substratum:</i> silica gel F ₂₅₄ (Merck) <i>Eluent:</i> n-butyl alcohol : DMF = 1:1 <i>R_f</i> ~ 0.92 and <i>R_f</i> ~ 0.76 yellow p | <i>Column:</i> Polygosil® 60-2540 C ₁₈ <i>Eluent:</i> 1.015 mM heptansulfonic acid in methyl alcohol solution 4% <i>Flow:</i> 0.8 mL/min. <i>Detection:</i> 307.5 nm | 357-358 | 74.8 |
| Alkylated diquinoxaline-piperazine-dicarboxylic acids, 7 and 8 | <i>Substratum:</i> silica gel F ₂₅₄ (Merck) <i>Eluent:</i> dioxane : formic acid : water = 10:1:1 <i>Solvent:</i> water, 0.01% solution <i>R_f</i> ~0.83 and <i>R_f</i> ~0.68 yellow-green shadow | <i>Column:</i> Nucleogen® 4000-7-DEAE <i>Eluent:</i> 5M urea, 20 mM phosphate buffer <i>Flow:</i> 1 mL/min. <i>Detection:</i> 348 nm for both compounds | 364-366 | 92.6 |

The HPLC results were obtained by using an apparatus *Jasco 800* with gel permeation columns Polygosil® 60-2540 C₁₈ and Nucleogen® 4000-7-DEAE. They were considered to be the most appropriate because they allow retention times long enough for an efficient separation and do not present the clogging phenomenon for the heterocyclic systems [9].

The TLC method was used: the absorbent layer silica gel, the plate material aluminum and the eluents which were chosen different for each compound.

The melting points were determined with a Boetius apparatus with microscope and heating plate, without correction and the results were presented in Table 1.

The spectral analysis

All organic compounds obtained by synthesis were studied employing chemical, *UV-VIS*, *NMR* and *IR* spectroscopy [12, 13] confirming the structures proposed.

The *UV-VIS* electronic spectra were performed with *Secoman S 750* apparatus in quartz cells (*l*=1cm) for DMF, respectively water of $c \sim 2 \times 10^{-5}$ M synthesized compounds solution. The characteristic absorbances were presented depending on the maximum wavelength.

The *IR* spectra were made including the synthesized compounds in KBr disk; the absorption has been measured with *FT-IR Jasco 620* spectrophotometer.

The heterocyclic systems, **3** and **6**, respectively **7** and **8** were analyzed by *NMR* spectroscopy using *Varian Gemini 300 BB* apparatus, the frequency of registration for proton spectrum, ¹*H-NMR*, is 300 MHz and for carbon spectrum, ¹³*C-NMR*, is 75 Hz. The purified prove was dissolved in deuterio-dimethylsulphoxide, DMSO-d₆, and the signals was reported at TMS.

3. Results and discussions

The alkylation of the pigments **3** and **6** was studied by chromatography during along time of reaction, on base of solubility difference in water for initial and final compounds. The reaction time can't be so long and the temperature so high, for not lead at partial decomposition of the pigment with the formation of the resin.

The alkylation reaction was effected by using dimethylsulfat in excess. In this case, finally, it was added hot water for the hydrolysis reaction of dimethylsulfat excess and then the next operations were: the adding of active carbon, the filtration, the reduction of acid character by neutralization and the precipitation of the pigments under chloride.

The problem which appearing was: where it was fixed by alkylation the –CH₃ group at heteroatoms of quinoxaline ring? The *NMR* spectroscopy was demonstrated the presence of only methyl group at nitrogen atom (example N¹ or N^{1'} for compound **3**, figure 3) at the biggest distant of the carboxyl group, a singlet at 3.58 ppm. In accordance with ¹*H-NMR* spectrum the polymethylations is not possible.

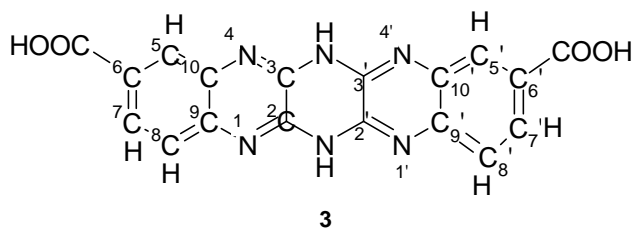
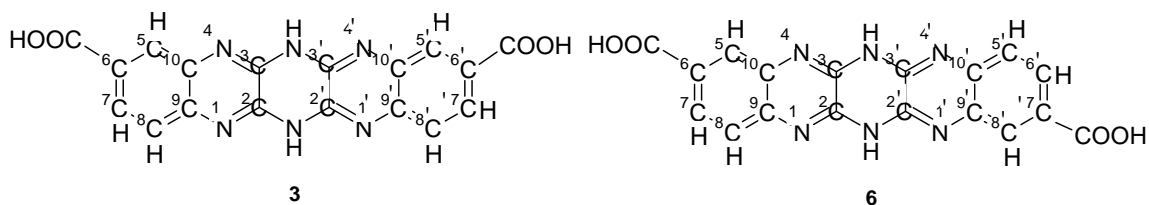


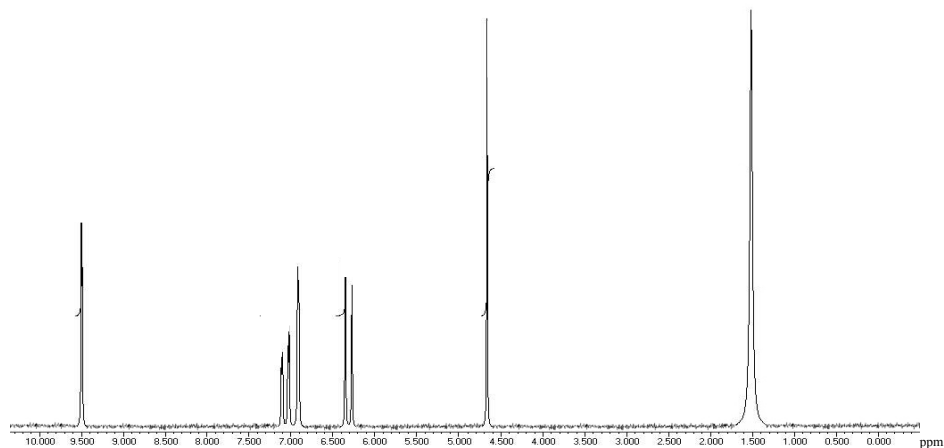
Fig. 3. The presence of methyl group at nitrogen atom of quinoxalinic ring, at compound **3**

The $^1\text{H-NMR}$ (DMSO-d_6) and $^{13}\text{C-NMR}$ (DMSO-d_6) results for each synthesized compounds were presented.

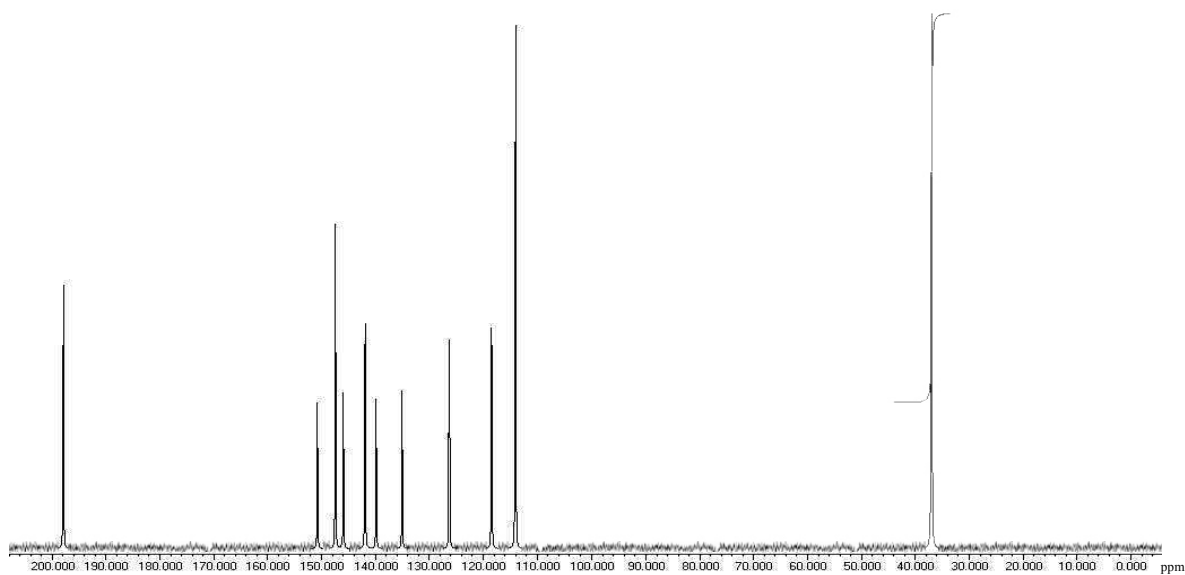
*Diquinoxaline[2,3-b][2,3-e]piperazine-6,6'-dicarboxylic acid, **3**, and diquinoxaline[2,3-b][2,3-e]piperazine-6,7'-dicarboxylic acid, **6***: δ_{H} (ppm): 6.92 (1H, s, C_6H_3); 7.07 (1H, d, C_6H_3); 6.32 (1H, d, C_6H_3); 9.50 (2H, s, 2COOH); 4.66 (2H, s, 2NH); δ_{C} : 114.2; 118.6; 114.2 ppm for C^5 , C^7 and C^8 ; 142.0; 142.0; 126.4; 140.0; 135.2 ppm for C^2 , C^3 , C^6 , C^9 and C^{10} ; 198.0 ppm (COOH).



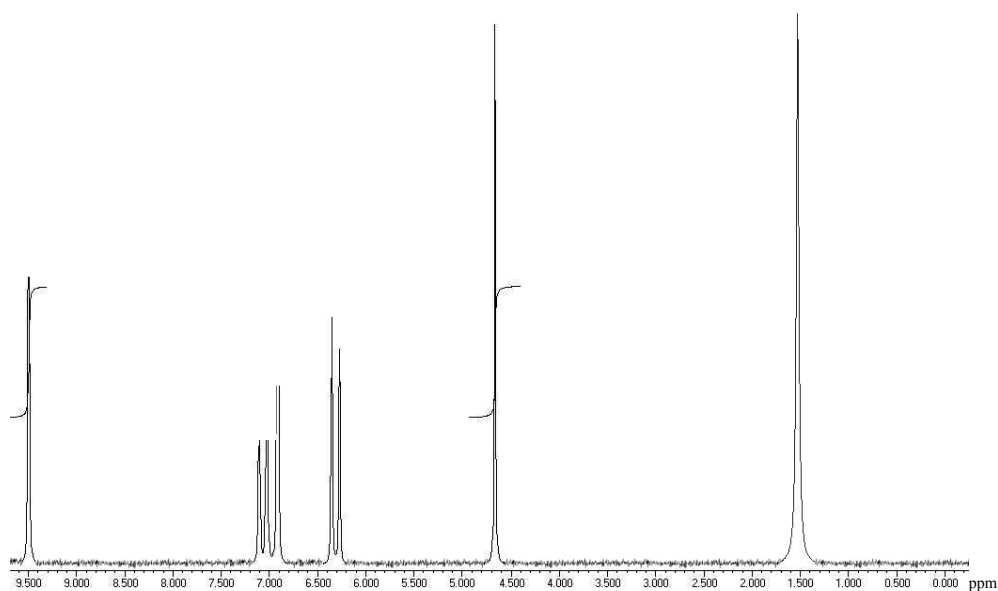
Diquinoxaline[2,3-b][2,3-e]piperazine-dicarboxylic acids, **3** and **6**



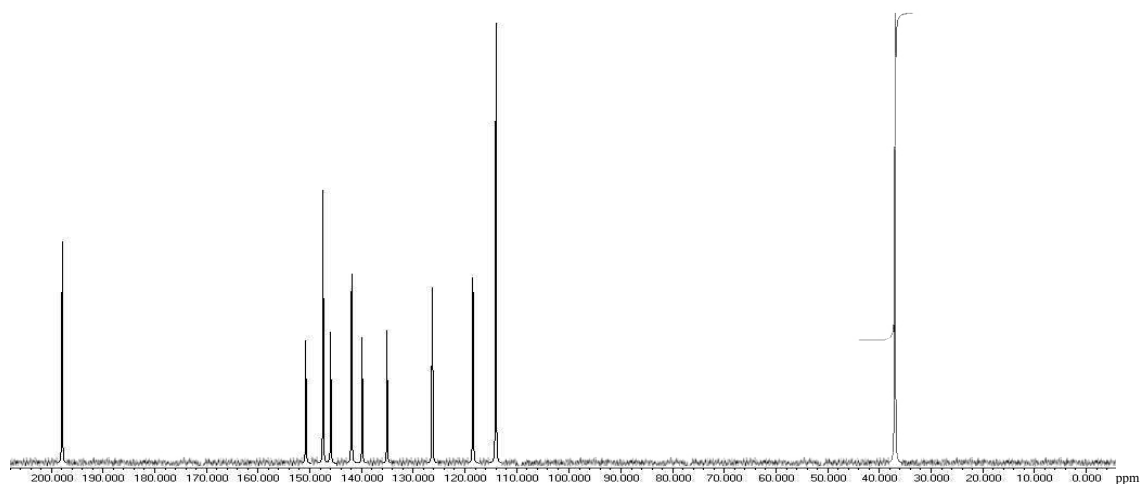
The $^1\text{H-NMR}$ spectrum for compound diquinoxaline[2,3-b][2,3-e]piperazine-6,6'-dicarboxylic acid



The ^{13}C -NMR spectrum for diquinoxaline[2,3-b][2,3-e]piperazine-6,6'-dicarboxylic acid

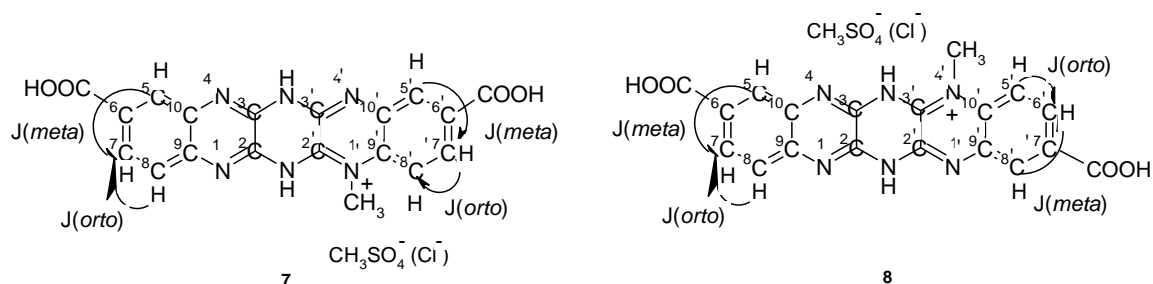


The ^1H -NMR spectrum for compound diquinoxaline[2,3-b][2,3-e]piperazine-6,7'-dicarboxylic acid

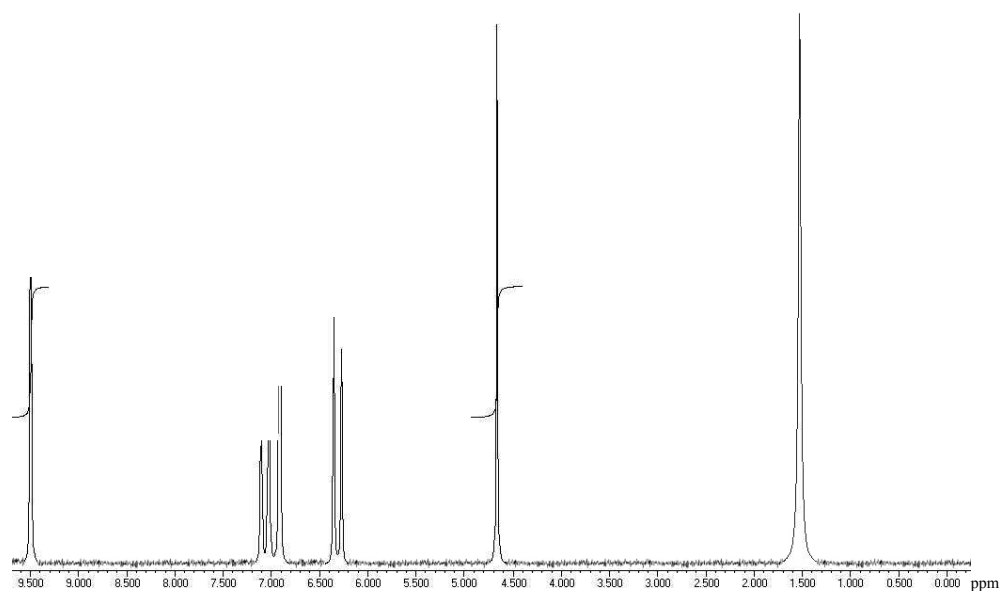


The ^{13}C -NMR spectrum for diquinoxaline[2,3-b][2,3-e]piperazine-6,7'-dicarboxylic acid

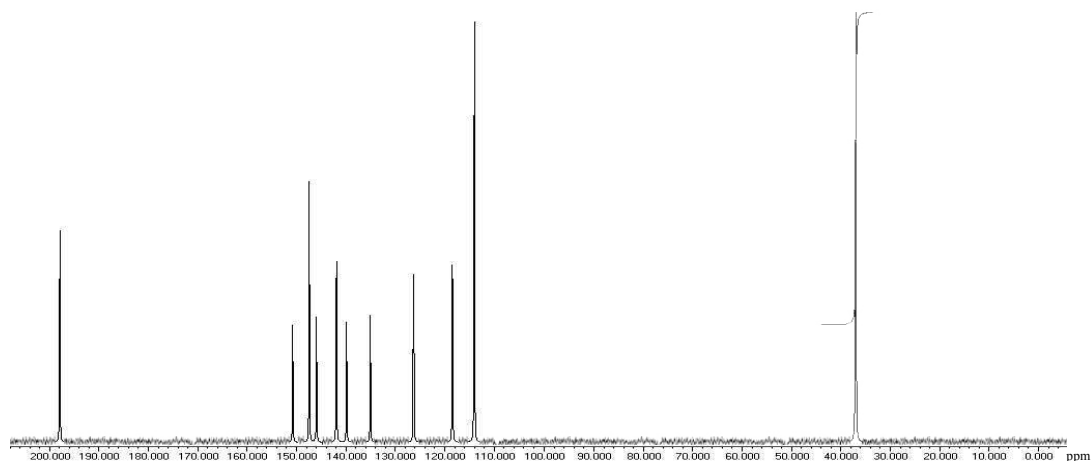
Alkylated diquinoxaline[2,3-b][2,3-e]piperazine-6,6'-dicarboxylic acid, **7**, and alkylated diquinoxaline[2,3-b][2,3-e]piperazine-6,7'-dicarboxylic acid, **8**: δ_H (ppm): 6.92 (1H, s, C₆H₃); 7.07 (1H, d, C₆H₃); 6.32 (1H, d, C₆H₃); 9.50 (2H, s, 2COOH); 4.66 (2H, s, 2NH); 3.58 (3H, s, CH₃) δ_C : 114.2; 118.6; 114.2 ppm for C⁵, C⁷ and C⁸; 142.0; 142.0; 126.4; 140.0; 135.2 ppm for C², C³, C⁶, C⁹ and C¹⁰; 198.0 ppm (COOH); 35.5 ppm for CH₃ resulted from alkylation reaction.



Alkylated diquinoxaline[2,3-b][2,3-e]piperazine-dicarboxylic acids, **7** and **8**



The ¹H-NMR spectrum for compound alkylated diquinoxaline[2,3-b][2,3-e]piperazine-6,6'-dicarboxylic acid



The ¹³C-NMR spectrum for alkylated diquinoxaline[2,3-b][2,3-e]piperazine-6,6'-dicarboxylic acid

The values of *IR* obtained spectra for unalkylated and alkylated compounds are in accordance with the emitted conclusions by the *NMR* spectrum.

- The -COOH group (Table 2) presents bands, approximately, at 1720 and 1410 cm^{-1} .
- The bands appeared at 1640, 1530-1570 cm^{-1} are proposed for the characterization of quinoxaline ring (depending by $\nu_{\text{C}=\text{N}}$ and $\nu_{\text{C}-\text{N}}$); these values are due to the conjugation with the aromatic ring (the bands are sharps) and lead at the values diminution $\nu_{\text{C}=\text{N}}$ and increase the intensity of valence vibration $\nu_{\text{C}-\text{N}}$.
- The C-NH- group, from piperazine ring, is characterized as faint absorptions as small intensity, at 1690 cm^{-1} and 1510 cm^{-1} .
- The large presented band at 2800 cm^{-1} was attributed of N^+-CH_3 group.
- The presence of alkylated nitrogen was identified at 1280, 1360 cm^{-1} .

Table 2. The IR spectra of compounds **3**, **6** and **7**, **8**

| Compound | ν_{COOH} | $\nu_{\text{N-CH}_3}$ | $\nu_{\text{N alkyl}}$ | $\nu_{\text{C}=\text{N}+}$ | $\nu_{\text{CH}=\text{N-}}$ | $\nu_{\text{C-NH-}}$ | ν_{Phenyl} |
|-----------------------|------------------------|-----------------------|------------------------|----------------------------|-----------------------------|----------------------|------------------------|
| 3 , 6 * | 1270; 1400; 1720; 1750 | - | - | - | 1640;1570 | 1690;1510 | 910; 850; 830; 1010 |
| 7 , 8 * | 1240; 1410; 1720; 1740 | 2800 | 1280; 1360 | 1690;1700 | 1630;1570 | 1695;1520 | 755; 845; 860; 890 |

*The IR spectrum for compounds **3** and **6** are identically, the same thing for products **7** and **8**.

By the study of *UV* spectra for alkylated compound was observed the apparition of a bathochromic shift with a great possibility of conjugation at chromophores system: from $\lambda_{\text{max}} = 307.5$ nm with maximum absorbance value 0.736 at $\lambda_{\text{max}} = 348$ nm with maximum absorbance 0.989 for $2 \cdot 10^{-5}$ mole/L solutions in DMF and water.

4. Conclusions

In this paper, it was studied the alkylated compounds obtained by organic synthesis for first time, by spectral analysis *NMR*, *IR* and *UV*. The alkylation reaction was realized with very good yields, if the process parameters were respected during the time of reaction. The alkylated diquinoxaline-piperazine-dicarboxylic acids were obtained by original synthesis and as thermorezistance green pigments can be used for paint as powder type. The pharmacological tests didn't proved toxicity and the lethal dose is insignificant for both alkylated compounds obtained by syntheses.

References

- [1] Schroder, J. *Prog. Org. Coat.*, 16, 3, 1988
- [2] Heys, B.G., *American Ink Marker*, 11, 28, 1990
- [3] Ed-Shahei, A., Hings, D., Freeman, H., *Acta Cryst.*, C59, o71-o73, 2003
- [4] Mizuguchi, J., Hao, Z., *U.S. Patent* 5,693,824, 1997
- [5] Le, H.P., *J. Imaging Science and Technology*, 42(1), 49, 1998
- [6] Foster, C.E., Leather, S., *Dyes and Pigments*, 48, 93, 2001
- [7] Haldnik, A., Muck, T., *Dyes and pigments*, 54, 254, 2002
- [8] Lewis, D.M., *J. Soc., Dyers, Col.*, 106, 270, 1990
- [9] Tanake, C.D., Hepworth, J.D., Heron, B.M., Partington, S.M., *Dyes and Pigments*, 47, 23, 2000
- [10] Atkinson, C.M., Simpson, J.C.E., Brown, C.W., *J. Chem. Soc.*, 26, 1956
- [11] Radulescu, C., *Rev. Chim.*, 56(2), 151, 2005
- [12] Radulescu, C., Tarabasanu-Mihaila C., Ionita, I., Irimescu, L., *Ovidius University Annals of Chemistry*, Constanta, 14, 113, 2003
- [13] Radulescu, C., Tarabasanu-Mihaila C., *Rev. Chim.*, 55(2), 102, 2004
- [14] Radulescu, C., Ionita, I., Hossu, A.M., *10th International Conference COLORCHEM'04, Proceedings*, Pardubice, Czech Republic, P25, 2004
- [15] Balaban, A.T., Banciu, M., Pogany, I., *Aplicatii ale metodelor fizice în chimia organica*, Ed. Stiintifica si Enciclopedica, Bucuresti , 1983

HPLC IN DETERMINATION OF D VITAMINS FROM PHARMACEUTICAL PREPARATIONS

D. Hossu¹, A.-M. Hossu², M. Toma Bădeanu³, C. Rădulescu², I. Ioniță²

¹ School „Coresi”, 2 Aleea Trandafirilor, Târgoviște, România

² University “Valahia” from Târgoviste, Faculty of Sciences and Arts, Chemistry Department, Blvd. Unirii 18-22, Târgoviste, România

³ National College „Constantin Carabela”, 58 Lct. Pârvan Popescu Street, Târgoviste, România

Abstract: *The determination of vitamin D has gained increased significance in several areas of analytical chemistry such as pharmaceutical, clinical and food application.*

A large number of methods have been developed for quantifying vitamin D contents in pharmaceutical. The present paper presents research results regarding the establishing of the optimal working conditions for the determination of vitamin D from pharmaceuticals by HPLC.

Keywords: *vitamin D, pharmaceuticals, high performance liquid chromatography.*

1. Introduction

Vitamins D₂ and D₃ are very important fat soluble vitamins for human and animal diets. For this reason, they take part in many pharmaceutical preparations, foods and feed formulation. Due to the biochemical activity of the vitamins, their concentrations in the preparation are always very low. For this reason, a specific and sensitive method was essential for determination of vitamins D₂ and D₃.

The first physico-chemical technique for quantification of vitamins D and their principals isomers was the measurement of their absorption in UV. Vitamins D, also the principals isomers and their degradation products present absorption in a spectral domain beetwen 250 and 300 nm [1-5]. Other quantification methods were elaborate such as: colorimetry [6,7], spectrofluorimetry [8-10], voltametry [11], spectroscopy IR [12-16], mass spectrometry coupled with chromatographic technics (HPLC or GC) [17-19] and NMR spectroscopy [20].

The quantification of vitamins D in pharmaceutical preparations for human usage is realised in the most of cases by HPLC method coupled with UV spectrophotometrically detection [21-23]. Because of the simplicity and fastness of these methods, they represente the advantage of their utilisation in current mode. The analytical procedure is realising by absorption HPLC [24], or by inverse phase HPLC.

In this study, we described a rapid and straightforward method for the determination of vitamin D in their commercial pharmaceutical preparation without purification. The described method could also be applied for determination of other vitamin D derivatives, fat soluble vitamins, and sterols, after extraction from their samples.

2. Experimental part

A liquid chromatograph equipped with a pump P 4000 Spectra-Physics Analytical, with detector UV 2000 Spectra-Physics Analytical was used. It was coupled to a computer Pentium III 800MHz, soft Chromquest.

For the first determination, the parameters were:

- chromatographic column type Zorbax-SIL [4,6mm × 25cm];
- mobile phase: 2,5% isopropanol in hexane;

- wavelength for detection $\lambda = 254$ nm.
For the second determination, the work parameters were:
- chromatographic column type Zorbax-SIL [4,6mm \times 25cm, 6 μ m];
- mobile phase: isopropanol:hexane = 90:10 (v/v);
- wavelength for detection $\lambda = 254$ nm.
In the third determination, the column and the mobile phase were changed:
- chromatographic column type Zorbax-SIL [2,1mm \times 25cm];
- mobile phase: mixture from 0,02% methanol in dicloromethan (v/v) enriched in methanol to 6%;
- wavelength for detection $\lambda = 254$ nm.

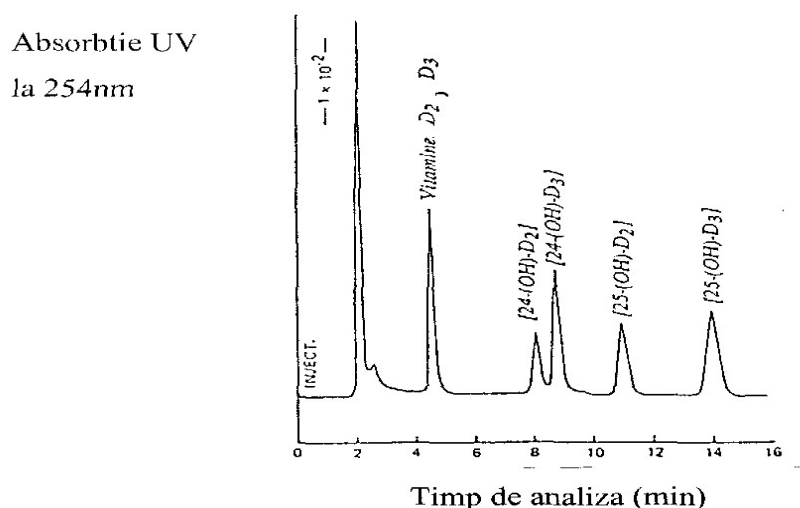


Figure 1. The separation of vitamins D₂ and D₃ from their metabolites by absorption HPLC

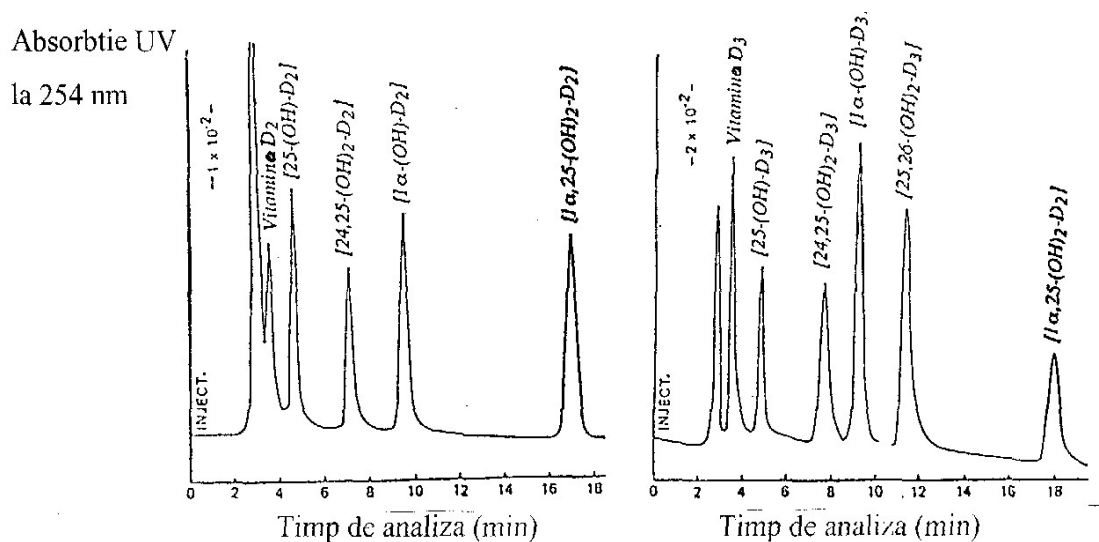


Figure 2. The separation by absorption HPLC of vitamin D₂ from its hydroxylated metabolites and vitamin D₃ from its hydroxylated metabolites

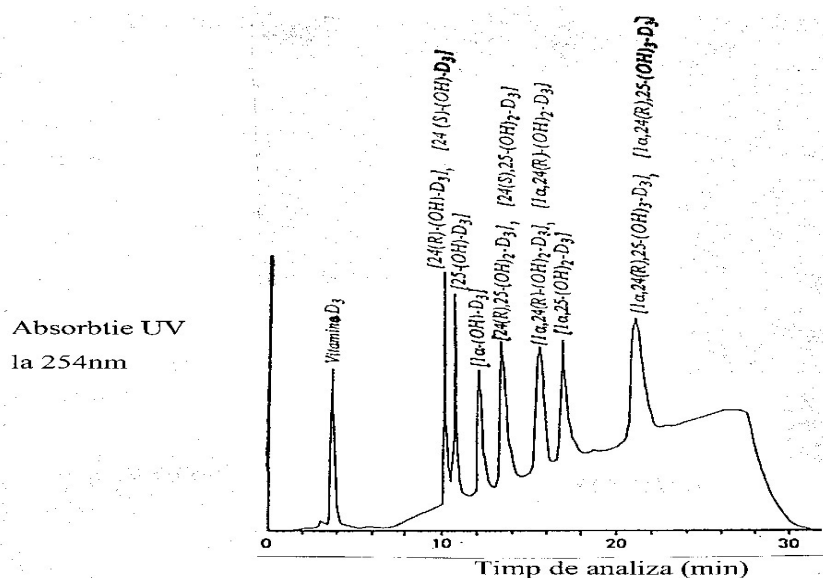


Figure 3. The separation by absorption HPLC of dihydroxylated metabolites of vitamin D₃

3. Results and discussions

The absorption chromatography is applied well on separation of metabolites and isomers of vitamins D. It starts from stationary phases with absorbant properties, porous silicagels and alumine, which are perfect for the separation of this kind of compounds a little polar and soluble in organic solvents.

The mobile phases used in vitamins D and their related molecules analysis by absorption HPLC are mixtures from hexane and a weak percent of isopropanol, these compounds are perfect soluble in them. Vitamins D₂ and D₃ can be separated on silice in izocratic mode with a mobile phase from 2,5% isopropanol in hexane, from their monohydroxylated metabolites: [24-(OH)-D₂], [24-(OH)-D₃], [25-(OH)-D₂], [25-(OH)-D₃]

(Figure 1). If the isopropanol percent is increased (90/10 v/v), each vitamin can be separated in the most part from their hidroxylyated metabolites (Figure 2). The using of ternar mixtures hexane/isopropanol/methanol permit the minimization of the phenomenon observed in particulary at the level of peak corresponding to [24,25-(OH)₂-D₃] [10].

A new gradient can be used at the basis of a mixture from 0,02% methanol in dicloromethan, enriched in methanol to 6%, for the separation of a mixture with dihidroxylated metabolites of vitamin D₃ (Figure 3). In the same conditions, this gradient permits the research with a superior height of teoretical peak comparative with that obtained for a ternar mixture hexane/isopropanol/methanol. The using of mixtures based on dicloromethan and methanol often induce the forming of bules. This kind of problem can be avoided by using of a ternar mixture hexane/dicloromethan/methanol (80/10/10 v/v/v), problem which will be studied in other paper.

4. Conclusions

After all bibliographic informations, this method: HPLC coupled to UV absorption spectrophotometry detection represents an interesting potential and can be the most compatible technique with quantification of vitamins D in pharmaceutical preparations. Other detection methods could be compatible, but there are many problems with the practical part.

Bibliografie

1. W.C.H. SHAW, J.P. JEFFERIES, T.E. HOLTS, *Analyst* **82**, 1957, p. 2.
2. W.C.H. SHAW, J.P. JEFFERIES, *Ibid.* **82**, 1957, p. 8.
3. (a) A. MAYER, C.W. PICARD, F. WOKES, *Pharm. Acta Helv.* **33**, 1958, p. 603.
(b) J.C. STERNBERG, H.S. STILLO, R.H. SCHWENDEMAN, *Anal. Chem.* **32**, 1960, p. 84.
4. A. VERLOOP, A.L. KOEVOET, E. HAVINGA, *Ibid.* **74**, 1955, p. 1125.
5. E.B. DECHENE, *J. Pharm. Pharmacol.* **16**, 1964, p. 158.
6. E.T. EWING, G.V. KINGSLEY, R.A. BROWN, A.D. HEMMET, *Ang. Eng. Chem. Anal. Ed.* **15**, 1943, p. 301.
7. C.H. NIELD, W.C. RUSSEL, A. ZIMMERLI, *J. Biol. Chem.* **136**, 1940, p. 73.
8. P.S. CHEN, H.B. BOSMAN, *J. Nutr. Res.* **83**, 1964, p. 133.
9. P.S. CHEN, A.R. TEREPKA, K. LANE, *Anal. Biochem.* **8**, 1964, p. 34.
10. A.J. PASSANANTE, L.V. AVIOLI, *Ibid.* **15**, 1966, p. 287.
11. R. TAKAHASHI, *Agr. Biol. Chem.* **27**, 1963, p. 8.
12. G. PIRLOT, *Anal. Chim. Acta* **2**, 1949, p. 744.
13. H. ROSENKRANTZ, in *Methods of Biochemical Analysis* (D. Glick ed., Wiley Interscience, New York) 1957, p. 416.
14. J.L.J. VAN DE VLIERVOET, P. WESTERHOF, J.A. KEVERLING BUISMAN, A. HAVINGA, *Rec. Trav. Chim.* **75**, 1956, p. 1179.
15. A. VERLOOP, A.L. KOEVOET, E. HAVINGA, *Ibid.* **76**, 1957, p. 689.
16. W.W. MORRIS, J.B. WILKIE, S.W. JONES, L. FRIEDMAN, *Anal. Chem.* **34**, 1962, p. 381.
17. W.H. ELLIOT, G.R. WELLER, in *Biochemical Applications of Mass Spectrometry* (G.R. Weller ed., Wiley Interscience, J. Wiley and Sons, Inc., New York, London) 1972.
18. Z.V.I. ZARETSKII, R. LAUBER, U.P. SCHLUNEGGER, *Org. Mass Spectrom.* **18**, 1983, p. 315.
19. K. TSUKIDA, K. SAIKI, *Int. J. Vitamins Nutr. Res.* **42**, 1972, p. 242.
20. R.M. WING, W.H. HOKAMURA, A. REGO, M.R. PIRIO, A.W. NORMAN, *J. Am. Chem. Soc.* **97**, 1975, p. 4980.
21. G. JONES, H.F. DE LUCA, *J. Lipid Res.* **16**, 1975, p. 448.
22. G. JONES, *J. Chromatogr. Biomed Applic.* **221**, 1980, p. 27.
23. N. IKEKAWA, N. KOIZUMI, *J. Chromatogr.* **119**, 1976, p. 227.
24. E.J. DE VRIES, F.J. MULDER, B. BORSJE, *J. Assoc. Off. Anal. Chem.* **64**, 1981, p. 61.

THE CHARACTERISTICS OF SYNTHESIZED CHROMOPHORES FOR PHOTOCHROMIC MATERIALS

I. Ioniță¹, C. Rădulescu¹, A.-M. Hossu¹

¹Valahia University Târgoviște, Faculty of Science, Department of Chemistry,
18-22 Unirii Bdv., Târgoviște, Romania

Abstract

Photochromic compounds are able to change their absorption spectra when exposed to light or dark condition. This process is reversible when the photochromic moieties exist, as usually occurs, in two different forms, whose relative concentration depends on the wavelength of incident light. Polymers with side-chain photochromic groups have recently attracted a great deal of interest because the photoisomerisation of the chromophores can induce reversible variation of the macromolecular structure and hence their physical properties.

Keywords: photochromic, polymeric materials.

Introduction

The problem of “intrinsic colouring” of macromolecular compounds represents a subject that continuously preserves its actuality. Multiple practical applications (predictable or in current use) could be taken into consideration; their physico-chemical properties being, of course the direct consequence of an appropriate structural architecture.

Obviously, the main feature of colored polymers is their capacity (as such, or as a mixture with other polymers) to exhibit colour; chemical bonding of chromophore groups would eliminate expensive dyeing techniques, but on the other hand would prevent dye losses (the undesired phenomenon called migration). However, another interesting feature of such structures is their potential to form liquid crystals; this fact allows applications in numerous fields of high technology. Not in the least, we have to mention another set of uses, known in general as non-linear optics (NLO).

Polymers have a number of desirable properties which taken together should make them materials of choice for optical devices: may be tailored by conventional synthesis methods to meet specific device requirements (transparency at particular wavelengths and stability at particular temperatures); offer many processing options toward desired device formats which should reduce the cost of active device.

In general all criteria are satisfied by the model where electron donating (D) and electron accepting (A) groups are separated by an electronic bridge such as π -electron conjugated group (see figure 1).

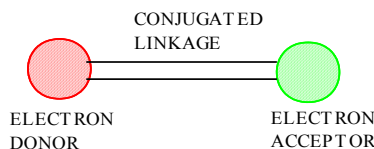


Figure 1: Structural Model for Chromophores

Procedures to fabricate NLO polymeric materials from a chromophore are schematically shown in figure 2.

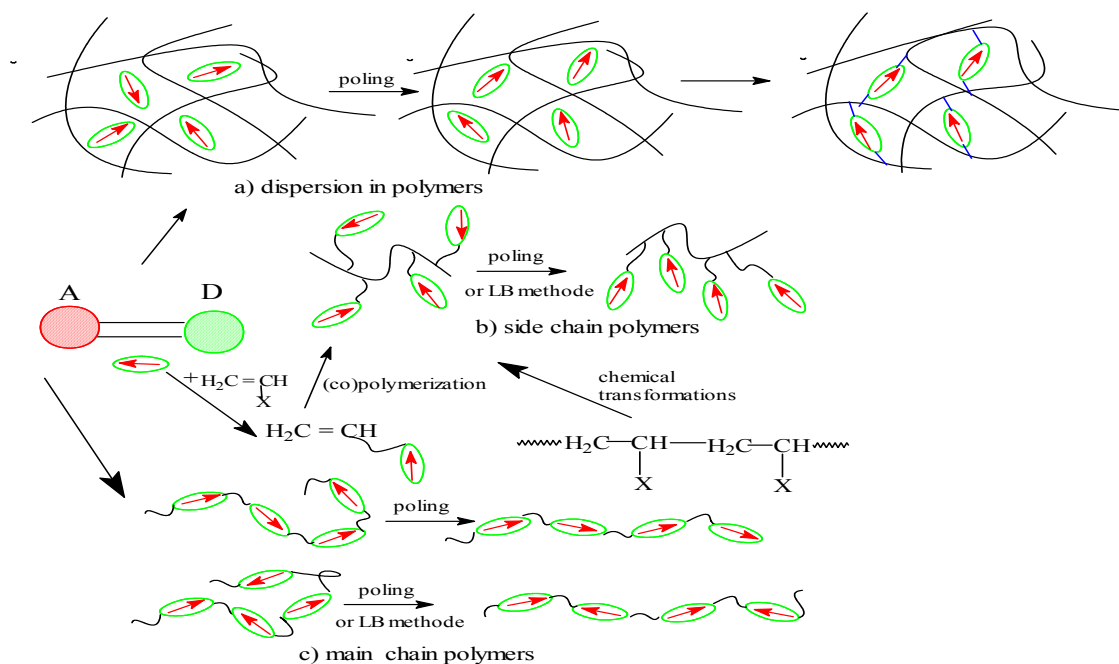


Figure 2: Fabrication of Polymeric NLO Materials from a Chromophore

From the point of view of the chromophore content, the polymers with covalent bonded chromophores are advantageous because, in general cases of chromophore dispersion, the chromophore content cannot increase more 20% due to phase separation of chromophores in polymers to produce crystals. Basically, these types of polymeric materials can be obtained, according to the final application, in two distinct ways:

Synthesis of monomers containing chromogen groups (CM); in turn, they would generate colored polymers, either by step polymerisation or through chain (co)polymerisation.

A polymer-analogous procedure: in the first step, a high-molecular polymer, containing reactive functions, has been obtained; subsequently, the reactive function is modified, either by a condensative coupling, or by a series of reactions involving a substituent of the initial polymer.

Comparing (co)polymerisation of colored monomers with the method of polymer-analogous transformations, it becomes apparent that the latter method present the advantage of working with a chain having a definite size, suitable for a certain application; on the other hand, polymer-analogous reactions, as any other chemical transformation has a given conversion, so that an accurate control of the included chromophore (as well as its distribution along the chain) is not feasible. Furthermore, this technique implies subsequent purification, to remove the un-reacted chromogen.

Attachment of a chromogen on a given polymer support may be performed by two distinct ways illustrated in the figure 3.

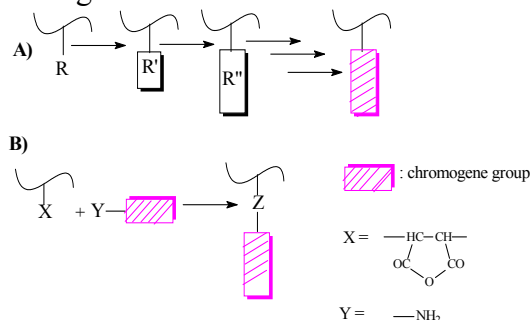


Figure 3: Modification of Polymeric Materials: A) by the Succession of Chemical Modification; B) by a Condensativ Coupling Reaction on the Chromogene

Using the technique B (unique coupling reaction) we have investigated the possibility to modify the copolymer's maleic anhydride–styrene (MA-S); maleic anhydride- dicyclopentadiene (MA-DCPD), butyl-vinyl ether–maleic anhydride–dicyclopentadiene (BVE-MA-DCPD), obtained by classical methods (radical polymerisation in bulk, solution or solution-suspension); all experiments were carried out under nitrogen, 2,2'-azo-iso-butyro-dinitrile being the initiator preferred in reactions with chromophore structures, prepared in our laboratories [9].

The UV-Vis characteristics of synthesized chromophores are summarized in the table 1.

Table 1: UV-Vis characteristics absorption for synthesized chromophores

| Dye | $\lambda_{\max 1}$ [nm] | $\epsilon_{\max 1}$ [l/mol.cm] | $\lambda_{\max 2}$ [nm] | $\epsilon_{\max 2}$ [l/mol.cm] |
|-----|----------------------------|-----------------------------------|----------------------------|-----------------------------------|
| | 266 | 6690 | 416 | 7460 |
| | 266 | 2780 | 417 | 13513.51 |
| | 266 | 16157 | 415 | 27626 |
| | 267 | 14046 | - | - |
| | 266 | 12163 | 437 | 3791.4 |
| | 267 | 9481 | 300 | 10107 |

Copolymers based on MA have been modified based on a nucleophilic reaction of chromogen (by its functional group) to the anhydride ring; obviously, for each type of chromophore coupled, we have chosen the appropriate reaction conditions.

The main conclusions regarding syntheses and are the following:

The initial colour of the low-molecular dye has been conserved; this represents a first proof for its bonding to the polymer chain.

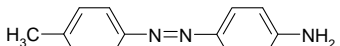
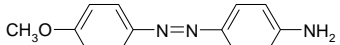
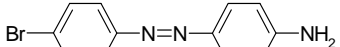
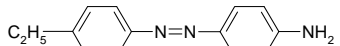
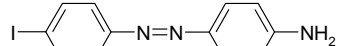
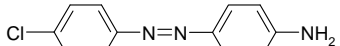
Subsequent IR spectra have confirmed the attenuation (even the total absence) of the corresponding anhydride peak (1860 cm^{-1}), as well as the apparition of new specific peaks indicating new functions such as amide (1668 cm^{-1} –first amide peak; $1590\text{-}1600\text{ cm}^{-1}$ - second amide peak), carboxyl (1780 cm^{-1} and 3330 cm^{-1} respectively), or even imide; the last group may be explained either by a high reaction temperature, or a too long reaction time.

High dye concentrations and/or elevated reaction temperatures favour obtaining gel fractions, thus confirming the formation of cross-linked structures.

UV-Vis spectra have shown for transformed polymers powerful absorptions at $340\div 450\text{ nm}$, due to the azoic function.

The absorption peak in UV domain is determined by nature of polymeric support and chromophore structure: in principal the nature of R substituent. Irradiant the chromophor solution with UV radiation for a short time, we observe a change in the spectral absorption domain (see table 2).

Table 2: Absorption characteristics for irradiated chromophores solution

| Substance | t _{ir} (min) | Conc. | λ ₁ (nm) | A ₁ | λ ₂ (nm) | A ₂ |
|---|-----------------------|------------------------|---------------------|----------------|---------------------|----------------|
|  | - | 4.74·10 ⁻⁴ | 263 | 0.960 | 405 | 1.99 |
| | 4.5 | | 263 | 0.995 | 405 | 1.972 |
|  | - | 6.61·10 ⁻⁴ | 287 | 1.122 | 426 | 0.225 |
| | 4.5 | | 287 | 1.148 | 426 | 0.215 |
|  | - | 1.993·10 ⁻⁴ | 263 | 1.147 | 422 | 1.974 |
| | 4.5 | | 263 | 1.175 | 422 | 1.902 |
|  | - | 5.93·10 ⁻⁴ | 263 | 1.327 | 409 | 1.615 |
| | 4.5 | | 263 | 1.329 | 409 | 1.619 |
|  | - | 1.77·10 ⁻⁴ | 293 | 1.293 | 415 | 0.491 |
| | 4.5 | | 293 | 1.295 | 415 | 0.500 |
|  | - | 1.73·10 ⁻⁴ | 263 | 1.181 | 408 | 1.312 |
| | 1.5 | | 263 | 1.179 | 412 | 1.069 |
| | 4.5 | | | 1.167 | 410 | 1.138 |

In recent years we have witnessed the extension in the applications of photochromic materials due, of course, to their distinctive optical properties. Such materials may be obtained either by using photochromic pigments, or starting from photochromic polymers. The first alternative implies a major disadvantage, namely the so-called wipeout phenomena; they are due to homo- or hetero-molecular aggregations, or emission is essentially an attribute of isolated molecules. Accordingly, there is an increased tendency to produce this type of materials starting from polymer substrates on which fluorescent chromogens are coupled.

Even if the method has been proved to be very efficient for SMA, however, for this substrate we have preferred the direct condensation of chromogen on the anhydride ring; without doubt, the later method is far easier to control, as we have already previously explained.

Spectroscopic analysis (IR, UV-Vis) has put into evidence on one hand the keeping of the peaks characteristic to the initial materials (substrate and chromogen respectively), and on the other additional lines, showing the new polymer-chromogen links.

Unfortunately not all the new materials prepared have been already tested to find out their possible applications.

In present we continue the work of characterization for these new types polymer materials.

Conclusions

The procedure by polymer analogues reactions, applied to the high polymers, with reactive functions, are characterized to the peculiar determined by the steric influence of chromogen fraction and the reaction conditions.

The physical characterization of the materials from future applications take theme to the limited of specifically values referring in the scientifically reference materials.

References

- [1]. Durr, H.; Bous-Laurent, H.; eds "*Photochromism Molecules and Systems*", Elsevier, Amsterdam;
- [2]. Natansohn, A., Rochon, P.; Pezolet M; Audet, P. Brown, D.; To, S.; *Macromolecules*, **1994**, 27(9), 2580-2585;
- [3]. Rochon, P.; Gosselin, J.; *Appl. Phys. Lett.*; **1992**, 60(1), 4-5;
- [4]. Natansohn, A., Rochon, P.; *Can. J. Chem.*, 2001, 79, 1093-1100;
- [5]. Hore, D.; Natansohn, A., Rochon, P.; *Can. J. Chem.*, **1998**, 76, 1648-1653;

- [6]. Meng, X.; Natansohn, A., Rochon, P.; Barrett, C.; *Macromolecules*, **1994**, 29(3), 946-952;
- [7]. Meng, X.; Natansohn, A., Rochon, P.; Ho, M.-S.; Barrett, C.; *Macromolecules*, **1995**, 28(12), 4179-4183;
- [8]. Delaire, J.A. Nakatani, K.; *Chem. Rev.*, **2000**, 100, 1817-1845;
- [9]. Ioniță, I., Albu, A.-M., Tărbășanu-Mihăilă, C., Bădulescu, R., Rădulescu, C., International Conference Polymeric Materials **2004**, 29 septembrie-1 octombrie 2004, Halle/Saale, Germany, PI40

C. MATHEMATICS SECTION

ITERATIVE SCHEME IN SOLVING THE PLAUSIBLE POINTS PROBLEM ARISING IN PHASE TRANSITION

Constantin Ghita

Abstract

We define the so-called plausible points whose coordinates are state variables characterizing the liquid phase gap and the nuclei germination region in a body submitted to the phase change. We introduce an algorithm concerning with the aspects of approach calculus of the plausible points of the stable state of the liquid gaps.

Introduction.

This paper deals with an algorithm of Newton type for determination of the so called plausible points of invariant regions in a two-dimensional space arising from phase transitions. Apart from a standard Stefan problem, a new model of a free boundary in phase transition, which emphasize that supercooling (the melt is present below its freezing point) is an equilibrium phenomenon based on a finite size interface between the solid and liquid phase was introduced in [1], [3], [5]. The behaviour of a system submitted to solidification with supercooling is characterize by phase transition state parameters: the reduced temperature u and the phase field function ϕ , a measure of the interaction of an atom with a mean field created by the other atoms (*Landau - Ginzburg* theory of phase transitions). The treatment of the stability of the governing equations of the phase change with supercooling in (ϕ, u) - plane have needed an investigation of the invariant sets for a local solution of a *Chauchy* problem. They provide a unifying criterion for determining the interfacial region and indicate values of some intimate parameters for which various values of phase field function ϕ generate stable points.

The formulating of the evolution problem as a flow in (φ, u) -space have permitted the finding of three invariant regions [1], [2], let us designate by $\Sigma_0, \Sigma_1, \Sigma_2$, each of them is specified as a parallelepiped having a boundary consisting of vertical lines and lines of slope q in (φ, u) - space. Recall that $q = \frac{\xi^2/2}{(\xi^2/\tau) - K}$ is a nonpositive parameter in view of the stability inequality $\frac{\xi^2}{\tau} < K$, where $\frac{\xi^2}{\tau}, K$ are the two eigenvalues of an operator of evolution equation of the problem and where K is the thermal conductivity of the body, l latent heat of fusion (per unit mass) ξ the thickness of interfacial region, τ a relaxation time (the time in which change occurs on the thickness of interface).

Remark that the invariant regions depend on the ratio $\frac{\xi^2}{\tau}$ through q , but not on ξ and τ independently. If the point (φ, u) determine the state variables and lies in Σ_0 , it characterize that part of the body at the interface level where both phases are present in equilibrium. The set Σ_0 contains the local extremum $M_1\left(\frac{1}{\sqrt{3}}\frac{1}{g}, -\frac{1}{6g\sqrt{3}}\right), M_2\left(-\frac{1}{\sqrt{3}}\frac{1}{g}, \frac{1}{6g\sqrt{3}}\right)$ of the function $f(\varphi, u) = \frac{1}{2}(\varphi - g^2\varphi^3) + 2u$ in the (φ, u) - plane. The set Σ_1 which lies itself in the half-plane $\varphi > \frac{1}{\sqrt{3}g}$ suggests a definition for the liquid phase gap: the set of points of the body for which the state variables (φ, u) remain in Σ_1 . The set Σ_2 lying in half-plane $\varphi < -\frac{1}{\sqrt{3}}\frac{1}{g}$ define the nucleation region, that part of the body where occurs the nuclei germination of solid phase. In this way, the mushy region take place to sharp interface and the thickness of that region is given by the distance between points for which $\varphi = -\frac{1}{\sqrt{3}}\frac{1}{g}$, and those for which $\varphi = \frac{1}{\sqrt{3}}\frac{1}{g}$. Note that g is associated with the values $\varphi = \pm\frac{1}{\sqrt{3}}\frac{1}{g}$ for which the free energy of the system is lower.

Consider a sufficiently large invariant region Σ_0 with boundary consisting of the curves:

$$C_1 : \varphi = \alpha, \alpha > \frac{1}{g}; A\left(\alpha, \frac{\alpha}{4}(g^2\alpha^2 - 1)\right),$$

$$C_2 : u = q(\varphi - \alpha) + \frac{\alpha}{4}(g^2\alpha^2 - 1); B\left(-\alpha, -2\alpha q + \frac{\alpha}{4}(g^2\alpha^2 - 1)\right),$$

$$C_3 : \varphi = -\alpha; A'\left(-\alpha, -\frac{\alpha}{4}(g^2\alpha^2 - 1)\right),$$

$$C_4 : u = q(\varphi + \alpha) - \frac{\alpha}{4}(g^2\alpha^2 - 1); B'\left(\alpha, 2\alpha q - \frac{\alpha}{4}(g^2\alpha^2 - 1)\right),$$

where $2\alpha q < \frac{\alpha}{4}(g^2\alpha^2 - 1)$ (figure 1). In the same way the minimal region of the liquid phase gap Σ_1 may be limited by the curves:

The formulating of the evolution problem as a flow in (φ, u) -space have permitted the finding of three invariant regions [1], [2], let us designate by $\Sigma_0, \Sigma_1, \Sigma_2$, each of them is specified as a parallelipiped having a boundary consisting of vertical lines and lines of slope q in (φ, u) -space. Recall that $q = \frac{\xi^2/2}{(\xi^2/\tau) - K}$ is a nonpositive parameter in view of the stability inequality $\frac{\xi^2}{\tau} < K$, where $\frac{\xi^2}{\tau}, K$ are the two eigenvalues of an operator of evolution equation of the problem and where K is the thermal conductivity of the body, l latent heat of fusion (per unit mass) ξ the thickness of interfacial region, τ a relaxation time (the time in which change occurs on the thickness of interface).

Remark that the invariant regions depend on the ratio $\frac{\xi^2}{\tau}$ through q , but not on ξ and τ independently. If the point (φ, u) determine the state variables and lies in Σ_0 , it characterize that part of the body at the interface level where both phases are present in equilibrium. The set Σ_0 contains the local extremum $M_1\left(\frac{1}{\sqrt{3}}\frac{1}{g}, -\frac{1}{6g\sqrt{3}}\right), M_2\left(-\frac{1}{\sqrt{3}}\frac{1}{g}, \frac{1}{6g\sqrt{3}}\right)$ of the function $f(\varphi, u) = \frac{1}{2}(\varphi - g^2\varphi^3) + 2u$ in the (φ, u) -plane. The set Σ_1 which lies itself in the half-plane $\varphi > \frac{1}{\sqrt{3}g}$ suggests a definition for the liquid phase gap: the set of points of the body for which the state variables (φ, u) remain in Σ_1 . The set Σ_2 lying in half-plane $\varphi < -\frac{1}{\sqrt{3}}\frac{1}{g}$ define the nucleation region, that part of the body where occurs the nuclei germination of solid phase. In this way, the mushy region take place to sharp interface and the thickness of that region is given by the distance between points for which $\varphi = -\frac{1}{\sqrt{3}}\frac{1}{g}$, and those for which $\varphi = \frac{1}{\sqrt{3}}\frac{1}{g}$. Note that g is associated with the values $\varphi = \pm\frac{1}{\sqrt{3}}\frac{1}{g}$ for which the free energy of the system is lower.

Consider a sufficiently large invariant region Σ_0 with boundary consisting of the curves:

$$C_1 : \varphi = \alpha, \alpha > \frac{1}{g}; A\left(\alpha, \frac{\alpha}{4}(g^2\alpha^2 - 1)\right),$$

$$C_2 : u = q(\varphi - \alpha) + \frac{\alpha}{4}(g^2\alpha^2 - 1); B\left(-\alpha, -2\alpha q + \frac{\alpha}{4}(g^2\alpha^2 - 1)\right),$$

$$C_3 : \varphi = -\alpha; A'\left(-\alpha, -\frac{\alpha}{4}(g^2\alpha^2 - 1)\right),$$

$$C_4 : u = q(\varphi + \alpha) - \frac{\alpha}{4}(g^2\alpha^2 - 1); B'\left(\alpha, 2\alpha q - \frac{\alpha}{4}(g^2\alpha^2 - 1)\right),$$

where $2\alpha q < \frac{\alpha}{4}(g^2\alpha^2 - 1)$ (figure 1). In the same way the minimal region of the liquid phase gap Σ_1 may be limited by the curves:

perpendicular, enters in our analysis. We perform a rotation of the coordinate sustem $X \oslash Y$ by angle $\nu = \pi - \mu \in \left(0, \frac{\pi}{2}\right)$, where $\mu = \text{Arctg } q \in \left(\frac{\pi}{2}, \pi\right)$, its boundary intersects the curve $f(\varphi, u) = 0$ and we state that the plausible points are obtained. We write the ellipse equation

$$(1.1) \quad \frac{\varphi^2}{\alpha^2(1+q^2)} + \frac{u^2}{\left(\frac{\alpha}{4}(g^2\alpha^2-1)-q\alpha\right)^2(1+q^2)} = 1.$$

At this stage we still have to made a backward rotation by $-\nu$, described by the equations

$$(1.2) \quad \varphi = \varphi' \cos \nu + u' \sin \nu, \quad u = -\varphi' \sin \nu + u' \cos \nu,$$

such that $\cos \nu = \frac{1}{\sqrt{1+q^2}}$, $\sin \nu = \frac{q}{\sqrt{1+q^2}}$ and consequently we obtain the above mentioned domain E .

It is only in this last step that the inverse transform: $\varphi' = \varphi \cos \nu - u \sin \nu$, $u' = \varphi \sin \nu + u \cos \nu$, after some elementary calculations leads to the equation

$$(1.3) \quad M\varphi^2 + Nu^2 + 2P\varphi u = Q,$$

here and in what follows M, N, P, Q are given by the expressions:

$$M = \left(\frac{\alpha}{4}(g^2\alpha^2-1)-q\alpha\right)^2 + \alpha^2 q^2(1+q^2) > 0,$$

$$N = q^2 \left(\frac{\alpha}{4}(g^2\alpha^2-1)-q\alpha\right)^2 + \alpha^2(1+q^2) > 0,$$

$$P = q \left[\alpha^2(1+q^2)^2 - \left(\frac{\alpha}{4}(g^2\alpha^2-1)-q\alpha\right)^2 \right],$$

$$Q = \alpha^2(1+q^2)^2 \left(\frac{\alpha}{4}(g^2\alpha^2-1)-q\alpha\right)^2 > 0.$$

The point V lying in the first quadrant of Cartesian coordinates will be reffered to as a *plausible point* of the liquid gap. The part of the body having the state characterised by the coordonates of the point V will be considered as a liquid gap, and we are only interested to obtain numerical approach states of the point V . In this way we formulate

Problem 1.1: Find $(\varphi, u) \in R^2$, such that $\varphi, u > 0$, and $\frac{1}{2}(\varphi - g^2\varphi^3) + 2u = 0$, $M\varphi^2 + Nu^2 + 2P\varphi u = Q$, where $g \in R, g > 0$.

2. Some considerations about an algorithm for solving a system of equations. Let X be a bidimensional *Banach* space, whose elements are denoted by x and $f \in C^1(X)$; consider the equation

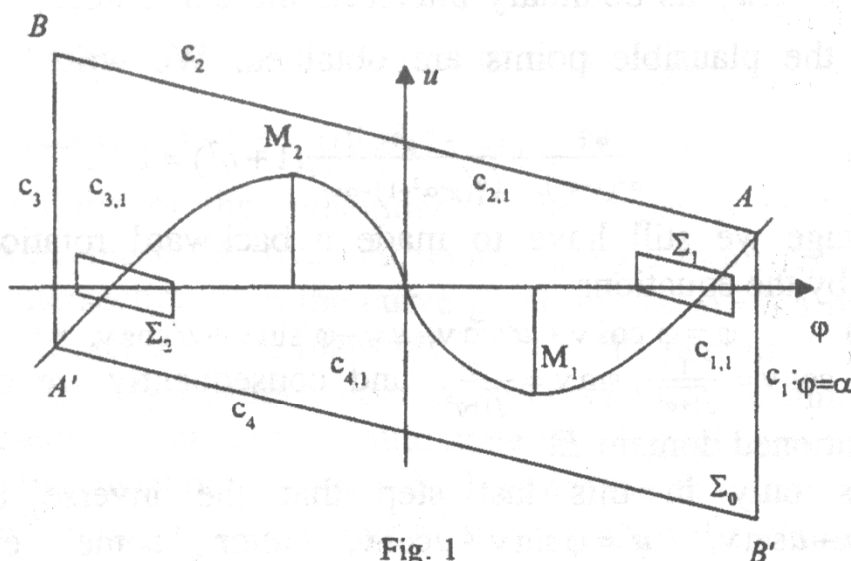


Fig. 1

$$(2.1) \quad f(x) = 0.$$

Without any assumption on f , suppose that (2.1) have an unique solution x^* . We now propose an algorithm of *Newton* type, having as goal to determine the solution x^* , i.e.

$$(2.2) \quad x_{n+1} = x_n + (f'(x_n))^{-1} f(x_n),$$

where x_0 is an arbitrary point in a neighbourhood of x^* ; we take it as an initial data such there exists $(f'(x_0))^{-1} \in L(X)$.

Remark that the choice of the initial data x_0 is essential for the rapidity of the convergence of (2.2) to x^* . Indeed, we emphasize a mapping on X which satisfy the *Picard-Banach* fixed point theorem ([4]), more precisely we set

Theorem 2.1: Assume that f fulfils the previous conditions of regularity and suppose in addition that there exists a positive number r , the smallest root of the equation $r^2 - ar + b = 0$, such that f' is Lipschitz continuous on $B(x_0, r)$, i. e.

$$(2.3) \quad \|f'(x) - f'(y)\| \leq L\|x - y\|, \text{ for some } L \in \mathbb{R}_+;$$

here $a = \frac{1}{\|f'(x_0)^{-1}\|L}$, $b = \frac{\|f'(x_0)^{-1} f(x_0)\|}{\|f'(x_0)^{-1}\|L}$, and suppose $\Delta = a^2 - 4b > 0$. Then there exists a unique solution $x^* \in B(x_0, r)$ of (2.1) and the algorithm (2.2) converge strongly to x^* .

Proof. Consider $B(x_0, r)$ endowed with the euclidian norm induced by X and $g: B(x_0, r) \rightarrow X$, defined by

$$(2.4) \quad g(x) = x - (f'(x_0))^{-1} f(x).$$

The mapping g verifies some expected properties: it is continuous differentiable on $B(x_0, r)$, having

$$g'(x) = I - (f'(x_0))^{-1} f'(x) = f'(x_0)^{-1} (f'(x_0) - f'(x)),$$

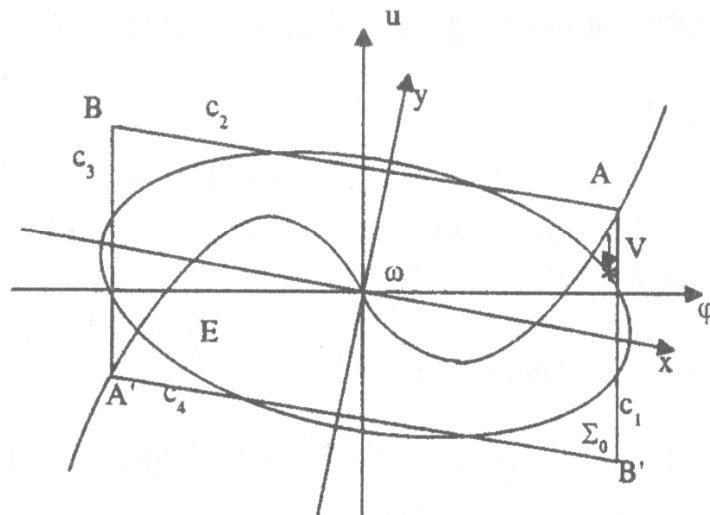


Fig. 2

where I is identity on X and $g'(x_0) = 0$; it applies $B(x_0, r)$ into itself; indeed, using (2.3) we get

$$\begin{aligned} \|g(x) - x_0\| &= \|(f'(x_0))^{-1} [f'(x_0)(x - x_0) - f(x) + f(x_0)] - (f'(x_0))^{-1} f(x_0)\| \leq \\ &\leq \|(f'(x_0))^{-1}\| \|f'(x_0)(x - x_0) - f(x) + f(x_0)\| + \|(f'(x_0))^{-1} f(x_0)\|. \end{aligned}$$

We set $F(x) = f(x) - f(x_0) - f'(x_0)(x - x_0)$, and apply the *Lagrange* theorem on $B(x_0, r)$:

$$\|F(x)\| = \|F(x) - F(x_0)\| = \|F'(\xi)\| \|x - x_0\| < Lr^2,$$

$\xi = x_0 + t(x - x_0)$, $t \in (0, 1)$, since $\|F'(\xi)\| = \|f'(\xi) - f'(x_0)\| \leq L\|\xi - x_0\| < Lr$. Finally, we have $\|g(x - x_0)\| \leq \|(f'(x_0))^{-1}\| Lr^2 + \|(f'(x_0))^{-1} f(x_0)\| = r$, in virtue of equation satisfied by r . We notice that we have $\|g'(x)\| = \|g'(x) - g'(x_0)\| = \|(f'(x_0))^{-1} (f'(x) - f'(x_0))\| \leq \|(f'(x_0))^{-1}\| L\|x - x_0\| \leq Lr \|(f'(x_0))^{-1}\| < .5$, therefore, g is a contraction on $B(x_0, r)$.

The existence of a unique solution x^* of the equation $x = g(x)$ is an immediate consequence of the *Picard-Banach* theorem. Moreover, x^* is the strongly limit of the sequence $\{x_n\}_{n \in \mathbb{N}}$, given by the algorithm (2.2); hence x^* verify (2.1). Also the error estimate can be obtained in view of this theorem, i.e.

$$(2.5) \quad \varepsilon_n = \|x_n - x^*\| \leq \frac{C}{2^{n-1}}, \text{ for some } C \text{ positive value.}$$

Remark 2.1: The assumptions of *Theorem 2.1* are not sufficiently, that is only a good choice of the initial data assure a rapidly convergence of the algorithm (2.2), but one may choose an arbitrary x_0 not satisfying that assumptions and the algorithm (2.2) converge to x^* .

3. Iterative scheme for solving the plausible point problem of the liquid gap. Here we shall return to the *Problem 2.1* for finding a numerical scheme. according to what has been shown abstractly above.

Let us take

$$X := \mathbb{R}^2 \cap \Sigma_0, \quad x_0 = \left(\frac{1}{g}, 0\right), \quad f(\varphi, u) = \left(\frac{1}{2}(\varphi - g^2\varphi^3) + 2u, M\varphi^2 + Nu^2 + 2P\varphi u\right)$$

and we preserve the notations of the sections 1 and 2. After some usual calculations we have:

$$Jf(\varphi, u) = \begin{pmatrix} \frac{1}{2}(1 - 3g^2\varphi^2) & 2 \\ 2M\varphi + 2Pu & 2Nu + 2P\varphi \end{pmatrix}, \quad f\left(\frac{1}{g}, 0\right) = \begin{pmatrix} 0 \\ \frac{M}{g^2} \end{pmatrix}, \quad Jf\left(\frac{1}{g}, 0\right) = \begin{pmatrix} -1 & 2 \\ \frac{2M}{g} & \frac{2P}{g} \end{pmatrix},$$

$$Jf\left(\frac{1}{g}, 0\right)^{-1} = \begin{pmatrix} -\frac{P}{P+2M} & \frac{M}{P+2M} \\ \frac{g}{P+2M} & \frac{g}{2(P+2M)} \end{pmatrix}, \quad Jf\left(\frac{1}{g}, 0\right)^{-1} f\left(\frac{1}{g}, 0\right) = \frac{M}{g(P+2M)} \begin{pmatrix} \frac{M}{g} \\ \frac{1}{2} \end{pmatrix}.$$

We adopt the maximum of all the sums of absolute values on line of a matrix as a norm of an element of the space $L(X)$, hence

$$M := \left\| Jf\left(\frac{1}{g}, 0\right)^{-1} \right\|_{0,1} = \frac{1}{10} \max \left\{ \frac{|P+M|}{|P+2M|}, \frac{3g}{2|P+2M|} \right\}.$$

In the same way a norm of a column vector is the maximum of absolute values of its components, therefore

$$C := \left\| \left(Jf\left(\frac{1}{g}, 0\right)^{-1} f\left(\frac{1}{g}, 0\right) \right) \right\|_{0,1} = \frac{1}{10} \max \left\{ \frac{M^2}{g^2|P+2M|}, \frac{M}{2g|P+2M|} \right\}.$$

The constant of *Lipschitz* for f is retrieved from the matrix of *Hess* of the function f

$$L := \left\| Hf\left(\frac{1}{g}, 0\right) \right\|_{0,1} = \frac{1}{10} \max \left\{ \left\| \begin{pmatrix} -3g & 0 \\ 0 & 0 \end{pmatrix} \right\|, \left\| \begin{pmatrix} 2M & 2P \\ 2P & 2N \end{pmatrix} \right\| \right\} =$$

$$= \frac{1}{10} \max \{ 3g, 2 \max \{ M + |P|, N + |P| \} \}.$$

Taking into account algorithm (2.2) and in view of particular definition of the function f we get the nonlinear iterative scheme

$$\varphi_{n+1} = \frac{1}{P+2M} \left(-\frac{g^2P}{2}\varphi_n^3 - M^2\varphi_n^2 - MNu_n^2 - 2PM\varphi_n u_n + \frac{1}{2}(4M+3P)\varphi_n + 2Pu_n \right) \quad (3.1)$$

$$u_{n+1} = \frac{g}{P+2M} \left(\frac{g^2}{2}\varphi_n^3 - \frac{M}{2}\varphi_n^2 - \frac{N}{2}u_n^2 - Pu_n\varphi_n + \frac{1}{g}(P+2M-2g)u_n - \frac{1}{2}\varphi_n \right),$$

with $\varphi_0 = \frac{1}{g}$, $u_0 = 0$.

Let us remark that the scheme (3.1) can be used in order to obtain an approximate point of the plausible point V of the liquid gap. In opposition with this iterative scheme, apart from the point $(-\frac{1}{g}, 0)$ with essential modifications of the iterative scheme (3.1), incorporating new M, N, P , a similar procedure can be implemented for the plausible nucleation point. The necessary number of iterations in order to obtain an error estimate ε , can be computed via formula (2.5),

$$n^* = \left\lceil \frac{1}{\ln 2} \ln \frac{C}{\varepsilon} \right\rceil + 1,$$

where $\lceil M \rceil$ designe the greatest integer less than M .

The use of iterative scheme allow us to replace a plausible point with a family of aproximate points $\{(\varphi_n, u_n)\}_{n \in \mathbb{N}}$, characterizing the stable state of liquid gaps at the interface level. The results supply by the iterative procedure concerning state parameters of the two phase are usefull in the topography of the boundary layer.

Let us apply the previous considerations to the system having the following characteristics:

$g = 1$, $\alpha = 1.9$, $l = 65 \text{ cal/g}$, $c = 0.17 \text{ cal/g}^\circ\text{C}$, $\rho = 7.8 \text{ g/cm}^3$, $\xi = 0.01 \text{ cm}$, $\tau = 0.1 \text{ s}$; substituting these values into expression of M, N, P, Q we get: $K = 0.136 \text{ cm}^2/\text{s}$, $q = -0.024$, $M = 1.654$, $N = 0.003$, $P = -4.708$, $Q = 5.791$. From the foregoing it follows that $M = 0.05$, $C = 0.0837$, $L = 1.27$; observe that $MCL = 0.005$, and we can apply *Teorem 2.1* and the algoritm (3.1).

REFERENCES

- [1] G. Caginalp, *An Analysis of a Phase Field Model of a Free Boundary*, Arch. Rat. Mec. Anal., nr.3, vol 92, 1986, 317-351
- [2]. G. Caginalp & J. T. Liu, *A numerical Analysis of an Anisotropic Phase Field Model*, IMA Journ. of Appl. Math., vol. 39, 51-66
- [3]. N. Goldenfeld, *Introduction to pattern selection in dendritic solidification*, in "Metastability and Incompletely Posed Problems", IMA, Springer-Verlag, 1987
- [4]. S. Sburlan, *Finite-dimensional Mathematical Analysis* (course in roumanian), Constana, 1986
- [5]. B. E. E. Stoth, *The Cahn-Hilliard equation as degenerate limit of the phase field equations*, Quart. of Appl. Math., nr. 4, vol. LIII, 1995, 695-700

Department of Mathematics
Electrical Engineering Faculty
University VALACHIA of Targoviste

*Schéma itératif pour la résolution du problème des points plausibles
apparaissant dans la transition des phases*

Resumé

On définit les points plausibles dont les coordonnées sont des variables d'état de la zone lacunaire liquide ou de la zone de germination dans un système soumis au changement de phase. On introduit un algorithme en ce qui concerne le calcul approximatif des coordonnées des points plausibles comme des paramètres des états stables des lacunes liquides au niveau de l'interface.

MODEL WITH NONLINEAR CRITERIA FOR HARDENING DEFORMATION

CONSTANTIN GHITA

ABSTRACT

The quasi-static equilibrium of a system subject by hardening deformation under time depending pressure was studied theoretically. The mechanical considerations show that the hardening deformation problem, defined here as a variational problem, can be splitted into a sweeping process problem for elastic and hardening components and a selection problem for a strain rate. It was found an existence result and the uniqueness was derived by means of approximation of a quasi-static process with dynamical ones, which causes neglected inertial forces and small velocity. Many of the results of this paper are motivated by the technical implications of required hypotheses.

INTRODUCTION

In recent years, much effort has been devoted to the study of the quasi-static and dynamic equilibrium of a system involving nonlinear constitutive laws, by means of variational methods (G. Duvant & J. L. Lions, 1972), dual methods (J. J. Moreau, 1974; B. Nayroles, 1974). In order to formulate the dual framework of the treatment for the equilibrium equations of a system governed by constitutive law of Prendtl-Reuss type, we obviously impose some hypotheses which seem to have much greater generality then the ones previously defined. It is the purpose of this paper to give an equivalence between an original variational problem and a sweeping process problem for elastic and hardening components of the deformation, adding a selection problem for plastic one.

The motivation for this study stems from introduction of a Hilbert space of admissible process of deformations with hardening and a few significant sufficient conditions leading to the ideas of admissibility and selection. The great difficulty in applying the general theory of dissipative mappings (V. Barbu, 1976) lies in the fact that one has to establish appriori bounds for the solution of a Cauchy problem, that is an evolution equation associated with an accretif operator. Consequently, we apply the regularization tool and approximated method.

The development of the study is done in such a way that we evaluate an abstract condition of hardening. done firstly in this paper, we employ the plastic work factor in order to extend, in a natural way, the dual framework exposed by J. J. Moreau, 1974, 1975. To do this, it is an easy task to write the restrictions of configuration and constraints as static laws and resistance laws, respectively. The transposition of the thermoplastic flow equation in dual energetic spaces has to be done

in such a way that as much information as possible about the behaviour of material system is carried over to the abstract setting.

By means of directional deformation we introduce also an anisotropic factor (satisfying the Bauschinger effect) counted as a translation in the same direction as the development of the load surface.

In the remainder of this paper the formulation of an evolution problem for dynamic equilibrium of a system has been made in order to obtain a uniqueness in displacements for a cvasi-static process. In this way, the cvasi-static deformation can be seen as a limit process of dynamical process which involve the small velocity. It is also possible to extend many of the previous results (J. J. Moreau, 1974, 1975) to the actual situation of hardening deformation.

PRELIMINARIES

The definitions, notations and elementary results of this section are basic for the whole paper. They will be used, usually without further mentions, throughout this paper.

Let $[0, T]$ be a finite nonempty interval of real line, U , E and Q real Hilbert spaces, having particular meanings in mechanics. Supposing that the injection $i: U \rightarrow U^*$ is compact, where U^* is the dual space of U , we denote the interpolation space of inertial terms by $H = [U, U^*]_{1/2}$. Of course the injection $H \subset U$ is also compact. Consider now $C([0, T]; U)$ the Banach space of all continuous vectorial-valued functions and $L^2([0, T]; U)$ the Hilbert space of all (equivalence class of) measurable vectorial valued functions, whose second powers are integrable on the interval $[0, T]$. Analogous, we define the same spaces for E and Q , respectively.

Let $H^1([0, T]; U)$ be the hilbert subspace of all vectorial-valued functions of $L^2([0, T]; U)$ such that the derivative (by means of distributions) $\dot{u} \in L^2([0, T]; U)$, with the norm

$$\|u\|_{H^1([0, T]; U)} = (\|u\|_{L^2([0, T]; U)}^2 + \|\dot{u}\|_{L^2([0, T]; U)}^2)^{1/2} \quad (1.1)$$

Each element $u \in H^1([0, T]; U)$ is called the process associated with mechanical system, roughly speaking u is a displacement process.

We consider the well known mappings of the theory of plasticity which characterize the geometry and the behaviour of the system. Let $K: U \rightarrow E$ be the operator of the theory of deformation, whose adjoined operator K^* is defined from E to U ; suppose the operator K satisfies the following condition

$$\|Ku\| \geq k \|u\|, \text{ for every } u \in U \text{ and some } k > 0. \quad (1.2)$$

In order to obtain a more precise information about elastic behaviour of the system and to introduce a technical energetical norm, we define $A: E \rightarrow E$, a linear bounded self adjoined operator of elasticity. We are interested in special case where A satisfies a positive defined condition, i.e. there exists $\alpha \in \mathbb{R}$, such that

$$(Ae, e) \geq \alpha \|e\|^2, \text{ for every } e \in E. \quad (1.3)$$

It should be noted that the plastic properties are usually presupposed given by a proper convex l.s.c. functional (B. Nayroles, 1974).

Next we discuss some developed approaches which are tested, but which are based on new ideas that hardening occurs. The same procedure is based on the technical properties obtained in section 3. Consequently, there are several possibilities for generalizing the previous results of J. J. Moreau (1974, 1975), replacing the plastic potential by a proper convex l.s.c. functional β on $E \times Q$.

Consider the equilibrium problems for an elasto-plastic system subject to the quasi-static and dynamic deformations, governed by a constitutive law of Prendtl-Reuss type:

Problem 1.1 Suppose that $e^0 \in H^2([0,T]; E)$, $c \in H^1([0,T]; U^*)$, $u_0 \in U$, $\sigma_0 \in E$, $q_0 \in Q$, satisfy

$$K^* \sigma_0 = c(0) \in U^*, (\sigma_0, q_0) \in \mathcal{D}(\beta), \beta(\sigma_0, q_0) < +\infty, \quad (1.4)$$

$$p_0 = Ku_0 + e^0(0) - A^{-1}\sigma_0$$

($\mathcal{D}(\cdot)$ denote the definition domain). Prove the existence of

$$Ku(t) + e^0(t) = \varepsilon(t), \varepsilon(t) = A^{-1}\sigma(t) + p(t) \quad (1.5)$$

$$K^* \sigma(t) = c(t) \quad (1.6)$$

$$(\dot{p}(t), -\dot{q}(t)) \in \partial\beta(\sigma, q)(t) \quad (1.7)$$

$$(u, \sigma, p, q)(0) = (u_0, \sigma_0, p_0, 0) \quad (1.8)$$

Problem 1.2 Suppose (1.4) satisfied. Find $(u, \dot{u}, \sigma, p, q) \in H^1([0,T]; U \times H \times E^2 \times Q)$ which verifies the conditions (1.5) and (1.7) of the Problem 1.1 and

$$\dot{u}(t) + K^* \sigma(t) = c(t) \quad (1.9)$$

$$(u, \dot{u}, \sigma, p, q)(0) = (u_0, v_0, \sigma_0, p_0, q_0) \quad (1.10)$$

THE MAIN EXISTENCE RESULT

Let K be a Hilbert space, (J, Q) and $(\mathcal{L}, \mathcal{V})$ two pairs of dual subspaces of K such that $J \cap \mathcal{L} = \emptyset$ and $Q \cap \mathcal{V} = \emptyset$. Motivated by our necessity, it is to be expected that the two subspaces $\mathcal{L} \times J$ and $\mathcal{V} \times Q$ are supposed orthogonal subspaces and K splits into $\mathcal{L} \times J$ and $\mathcal{V} \times Q$. In order to obtain the reduced sweeping process problem derived from the hardening problem, we impose hypotheses which do not seem to be very restrictive. As we shall show, these hypotheses are always met in term of Hausdorff topology on the Hilbert space K . Indeed, for every pair of subsets A and B of K we denote

$$e(A, B) = \sup_{a \in A} d(a, B) = \sup_{a \in A} \inf_{b \in B} d(a, b),$$

where $d(\cdot, \cdot)$ is the distance defined by the norm of K .

In this way consider the topology given by the so called Hausdorff distance

$$d(A, B) = \sup \{e(A, B), e(B, A)\} \quad (2.1)$$

We note by $[\cdot, \cdot]$ the inner product of K .

Problem 2.1 Find the absolutely continuous functions $t \rightarrow v(t)$, $t \rightarrow y(t)$, defined on the interval $[0, T]$, such that $(v, y) \in C([0, T]; \mathcal{L} \times \mathcal{V})$, $(v, y) \in L^1(0, T; \mathcal{L} \times \mathcal{V})$ and verify a Cauchy problem for an evolution equation, i.e.

$$(\dot{v}(t), -\dot{q}(t)) \in \partial \Psi_{S(t)+a(t)}(-y(t)-c(t)-e^0(t), q(t)) \quad (2.2)$$

$$-y(0) = -y_0 \in (S(0)+a(0)+c(0)+e^0(0)) \cap \mathcal{V}, q(0) = 0,$$

where $t \rightarrow a(t)$, $t \rightarrow c(t)$, $t \rightarrow e^0(t)$ are absolutely continuous functions and $t \rightarrow S(t)$ is a bounded map, having an absolutely continuous variation with respect to the Hausdorff topology previously defined.

We call Problem 2.1 the anisotropic hardening problem.

Problem 2.2 The regularity hypotheses on the functions a , c , e are the same as in the problem 2.1, then determine $(-y, q) \in C([0, T]; K)$ such that $y \in L^1([0, T]; \mathcal{V})$ and the following evolution equation

$$(-\dot{y}(t), -\dot{q}(t)) \in \Psi_{(S(t)+a(t)+c(t)+e^0(t)) \cap \mathcal{V} \times Q}(-y(t), q(t)) \quad (2.3)$$

with initial condition

$$q(0) = 0, -y(0) = -y_0 \in (S(0)+a(0)+c(0)+e^0(0)) \cap \mathcal{V} \times Q, \text{ is verified.}$$

We call this problem the general sweeping problem associated with the convex subset $\bar{S}(t) := (S(t)+a(t)+c(y)+e(t))$

The following theorem gives sufficiently conditions for the equivalence between the above defined problems.

Theorem 2.1 The following statements are satisfied:

1. a , c , e are absolutely continuous functions on $[0, T]$ with values in K , moreover there are $a, c, e^0 \in L^1([0, T]; K)$, $c(t) \in \mathcal{L}$, $e(t) \in \mathcal{V}$, for all $t \in [0, T]$;
2. $\text{Int}(\bar{S}(t) \cap \mathcal{V} \times Q) \neq \emptyset$, for every $t \in [0, T]$ (it is called the admissible load condition of the system), then the Problems 2.1 and 2.2 are equivalent.

Proof. Sufficiency: Due to the fact that $(-y, q) \in W^{1,1}([0, T]; \mathcal{V} \times Q)$ is a solution of generalized sweeping problem with initial condition $(-y_0, q_0) \in S(0) \cap \mathcal{V} \times Q$, it follows that

$$\partial \Psi_{\mathcal{V} \times Q}(-y(t), q(t)) = \begin{cases} \mathcal{L}J, & \text{if } (-y(t), q(t)) \in \mathcal{V} \times Q \\ +\infty, & \text{otherwise} \end{cases} \quad (2.4)$$

Consequently, for $(-y, q) \in W^{1,1}([0, T]; \mathcal{L} \times Q)$ there exists an element of $\mathcal{L} \times J$, it suffices to take $(\dot{v}(t), -\dot{q}(t)) \in \mathcal{L} \times J$, for almost everywhere $t \in [0, T]$, such that

$$(\dot{v}(t), -\dot{q}(t)) \in \partial \Psi_{\mathcal{V} \times Q}(-y(t), q(t)) \quad (2.5)$$

At this stage we don't give more information about the regularity of the function $t \rightarrow v(t)$ on $[0, T]$. We shall show latter that $(\dot{v}, -\dot{q}) \in L^1([0, T]; K)$. However, by condition 2 follows that the mapping $t \rightarrow \text{Int}(\bar{S}(t) \cap \mathcal{V} \times Q)$ define a nonempty variety whose variation (with respect to Hausdorff topology) is absolutely continuous.

In the case when (2.5) holds, the two elements $(\dot{V}(t)-\dot{Y}(t), -\dot{Q}(t))$, $(-y(t)-c(t)-e^0(t), q(t))$ consist of a dual pair for the two polar functionals $\psi_{S(t)+a(t)}$, $\psi^*_{S(t)+a(t)}$. Then, it follows from the transversality conditions (Fenchel equality), using the fact that $(-y, q)$ is a solution for the Problem 2.2:

$$\psi^*_{S(t)+a(t)}(\dot{V}(t)-\dot{Y}(t), -\dot{Q}(t)) + [(-\dot{V}(t)+\dot{Y}(t), -\dot{Q}(t)), (-y(t)-c(t)-e^0(t), q(t))]=0 \quad (2.6)$$

By a straightforward calculation we obtain an equivalent form :

$$\psi^*_{S(t)}(\dot{V}(t)-\dot{Y}(t), -\dot{Q}(t)) + [(-\dot{V}(t)+\dot{Y}(t), -\dot{Q}(t)), (-y(t)-a(t)-c(t)-e^0(t), q(t))]=0 \quad (2.7)$$

which represents an image of an affine variety at point $(-y(t)-a(t)-c(t)-e^0(t), q(t))$. This define an exactly support at the convex variety $S(t)$.

Consider now the map $t \rightarrow \psi(t)$, defined by

$$\psi(t) = \{z \in K / \psi^*_{S(t)}(z) - [z, (-y(t)-a(t)-c(t)-e^0(t), q(t))]=0\} \quad (2.8)$$

which range contains the point $(\dot{V}(t)-\dot{Y}(t), -\dot{Q}(t)) \in \mathcal{L}XJ - \{(\dot{Y}(t), -\dot{Q}(t))\}$. Then, we claim that in the case of condition 2 of the Theorem the two varieties $\psi(t)$ and $\mathcal{L}XJ - \{(\dot{Y}(t), -\dot{Q}(t))\}$ have nonempty intersection.

On the other hand, because the subset $S(t)$ has an absolutely continuous variation and $\psi^*_{S(t)}$ is the support function of $S(t)$, it is obvious that $t \rightarrow \psi^*_{S(t)}$ is a measurable absolutely continuous map and $t \rightarrow -y(t)-a(t)-c(t)-e^0(t)$ is an absolutely continuous function. Since $(-y, q) \in W^{1,1}([0, T]; K)$, it should be noted that

$$t \rightarrow \psi(t) \cap (\mathcal{L}XJ - \{(\dot{Y}(t), -\dot{Q}(t))\}) \quad (2.9)$$

is a nonempty measurable mapping with absolutely continuous variation. In this case, by means of condition 2, it may be possible to get an absolutely continuous function $\gamma: [0, T] \rightarrow K$ and a small parameter $\rho > 0$ (see also J. J. Moreau, 1974), such that

$$\gamma(t) \in S(t) \cap \mathcal{V}XQ \quad (2.10)_1$$

$$B_\rho(\gamma(t)) \subset S(t) \cap \mathcal{V}XQ \quad (2.10)_2$$

By the definition of the support function $\psi_{S(t)}$ and inclusion (2.10)₂ it follows

$$\psi^*_{S(t)}(z) \geq [\gamma(t) - (a(t)+c(t), q(t)), z] + \rho \|z\|^2, \text{ for all } z \in K \quad (2.11)$$

We shall evaluate now the support function of the variety $S(t)$ at the point $(-y(t)-a(t)-c(t)-e^0(t), q(t))$, which lies in $S(t)$. First of all we set

$$\begin{aligned} [z, (-y(t)-a(t)-c(t)-e^0(t), q(t))] &= -[(\dot{Y}(t), -\dot{Q}(t)), (-y(t)-e^0(t), q(t)) - \gamma(t)] + \\ &+ [z, (\gamma(t) - (a(t)+c(t), q(t)))] + [z + (\dot{Y}(t), -\dot{Q}(t)), (-y(t)-e^0(t), q(t)) - \gamma(t)]. \end{aligned}$$

If we take $z = (\dot{W}(t), -\dot{Q}(t)) \in \Psi \cap (\mathcal{L}XJ - \{(\dot{Y}(t), -\dot{Q}(t))\})$, because $(\dot{W}(t), -\dot{Q}(t)) + (\dot{Y}(t), -\dot{Q}(t)) \in \mathcal{L}XJ$ and $(-y(t)-e^0(t), q(t)) - \gamma(t) \in \mathcal{V}XQ$, from the orthogonality of the two subspaces $\mathcal{L}XJ, \mathcal{V}XQ$ it follows

$$\begin{aligned} [(\dot{W}(t), -\dot{Q}(t)), (-y(t)-a(t)-c(t)-e^0(t), q(t))] &= \\ &= [(\dot{W}(t), -\dot{Q}(t)), \gamma(t) - (a(t)+c(t), q(t))] + [(\dot{Y}(t), -\dot{Q}(t)), \gamma(t) - (-y(t)-e^0(t), q(t))] \end{aligned}$$

$$\begin{aligned} & \text{On the other hand, turning to (2.11), we have for } z = (\dot{w}(t), -\dot{q}(t)) \\ & \|(\dot{w}(t), -\dot{q}(t))\|^2 \leq \frac{1}{\rho} [(\dot{Y}(t), -\dot{Q}(t)), (\gamma(t) + (y(t) + e^0(t), q(t)))] \leq \\ & \leq \frac{1}{\rho} \|(\dot{Y}(t), -\dot{Q}(t))\| \|\gamma(t) + (y(t) + e^0(t), q(t))\|, \end{aligned}$$

which point out that the mapping $t \rightarrow \|(\dot{w}(t), -\dot{q}(t))\|$ is dominated by a real valued integrable function on $[0, T]$. Finally, we have

$$(\dot{w}, -\dot{q}) \in L^1([0, T]; K) \quad (2.12)$$

If we take $(V, -Q) = (\dot{w}, -\dot{q}) + (\dot{Y}, -\dot{Q})$, then $(v, -q)$ is a proper solution of the Problem 2.1. Indeed, from condition (2.5), using the subadditivity of a subdifferential in respect with the restriction of indicator function, we obtain

$$(\dot{V}(t) - \dot{Y}(t), -\dot{Q}(t)) \in \partial \psi_{S(t) \cap \mathcal{V} \times Q}(-y(t), q(t)) + \partial \psi_{\mathcal{V} \times Q}(-y(t), q(t)) \subset \partial \psi_{S(t) \cap \mathcal{V} \times Q}(-y(t), q(t)).$$

This proves that v, y, q verifies the anisotropic hardening problem. Since $(\dot{Y}, -\dot{Q}) \in L^1([0, T]; \mathcal{L} \times J)$ and there exists (2.12), we deduce $(\dot{V}, -\dot{Q}) \in L^1([0, T]; \mathcal{L} \times J)$. We denote by $t \rightarrow v(t)$ a primitive function of $\dot{V}(t)$, such that $v(0) = v_0 \in \mathcal{L}$ and so $v \in C([0, T]; K)$.

Necessity: Let (v, y, q) be a solution of the Problem 2.1, in fact $(v(t), y(t)) \in \mathcal{L} \times \mathcal{V}$, $(v, y) \in C([0, T]; \mathcal{L})$, $\dot{Y} \in L^1([0, T]; \mathcal{V})$. By the hypotheses on the orthogonality of the two subspaces $\mathcal{L} \times J$ and $\mathcal{V} \times Q$, it is clear that

$$-(\dot{V}(t), -\dot{Q}(t)) \in \partial \psi_{\mathcal{V} \times Q}(-y(t), q(t)),$$

where we have to do a remarque: the subdifferential is computed by means of the product of K . Finally, since $\psi_{\mathcal{V} \times Q}$ and $\psi_{S(t)}$ are finite maps and $\psi_{\mathcal{V} \times Q}$ is continuous at $0 \in K$, we may apply the transversality condition of the subdifferential on the nonempty subset $S(t) \cap \mathcal{V} \times Q$ (see H. Brezis, 1972) and get

$$\begin{aligned} & -(\dot{Y}(t), -\dot{Q}(t)) \in \partial \psi_{S(t) + \alpha(t)}(-y(t) - c(t) - e^0(t), q(t)) + \partial \psi_{\mathcal{V} \times Q}(-y(t), q(t)) = \partial \\ & \psi_{S(t) + \alpha(t) + \alpha(t) + e^0(t)}(-y(t), q(t)) + \partial \psi_{\mathcal{V} \times Q}(-y(t), q(t)) = \partial \Psi_{\overline{S(t) \cap \mathcal{V} \times Q}}(-y(t), q(t)) \neq \emptyset. \end{aligned}$$

By this we mean that $(-y(t), q(t)) \in \mathcal{V} \times Q$ verifies the Problem 2.2.

Note that the anisotropic hardening problem have being reduced, by the selection of a plastic component $v \in C([0, T]; K)$ with an absolutely continuous variation, to an evolution problem, that is the generalized sweeping problem for a nonempty subset $S(t)$. Consequently, the condition 2 of the Theorem 2.1 seems to be essential for the existence of a solution of hardening problem on a Hilbert space

$$H = \mathcal{V} \times Q \quad (2.14)$$

endowed with the topology induced by K . At this stage, the restriction $S(t) \subset H$ may be considered as a time depending map on $[0, T]$ with values into H .

THE EXISTENCE OF THE SOLUTION FOR THE PROBLEM 2.2

In this section the regularized problems corresponding to the quasi-static process can be employed to derive the existence result. It is the aim of this paper to emphasize the problems associated with visco-plastic process and present the hardening process as a limit case (see also C. Ghita, 1984).

Let H be the Hilbert space defined by (2.14) and the closed convex time depending set $\bar{S}(t)$ expressed by (2.13). In order to obtain an abstract setting of this approach, we first recall some usual definitions and notations of the nonlinear functional theory. We set $\psi \nabla \varphi$ the infconvolution of two element ψ and φ of a functional space on H , namely

$$(\psi \nabla \varphi)(z) = \inf_{x \in H} \{ \psi(x) + \varphi(z-x) \} \quad (3.1)$$

If ψ and φ lies in a regular class of functionals on H (it is sufficient $\psi, \varphi \in \Gamma_0(H)$), then

$$(\psi + \varphi)^* = \psi^* \nabla \varphi^*, \quad (3.2)$$

where by ψ^* we denote the dual functional of ψ (D. Pascali & S. Sburian, 1978).

We consider now a quadratic form given by the distance at the load surface \bar{S} ,

$$F(v) = \frac{1}{2} d^2(v, \bar{S}) = \frac{1}{2} \inf_{w \in H} \|v-w\|^2 = \inf_{w \in H} \left\{ \frac{1}{2} \|v-w\|^2 + \psi \bar{S}(w) \right\}, \quad (3.3)$$

more precisely F is a convex Fréchet-differentiable functional, with derivative

$$(\text{grad} F)(v) = v - P_{\bar{S}} v \quad (3.4)$$

where $P_{\bar{S}}$ is the projection operator on \bar{S} . In other words, F consists of a regularization of the indicator functional $\psi \bar{S}$, it is easily seen that $P_{\bar{S}} v = \lim_{\lambda \rightarrow 0} J_{\lambda}(v)$, where J_{λ} is the

Yosida's regularization of the subdifferential $\Psi_{\bar{S}}$ (H. Brezis, 1972). In this way we have

$$\text{grad} F = (\partial \psi \bar{S})_{\lambda} \quad (3.5)$$

Recall that $(\partial \psi \bar{S})_{\lambda}$ is the Yosida's approximation of $\partial \psi \bar{S}$. It is well known that

$$(\partial \psi \bar{S})_{\lambda} \rightarrow \partial \psi \bar{S}, \text{ as } \lambda \rightarrow 0 \quad (3.6)$$

By the above considerations we are led to define the approach problems

$$\begin{aligned} -(\dot{y}_{\lambda}(t), \dot{q}_{\lambda}(t)) &= \frac{1}{\lambda} \text{grad} F(-y_{\lambda}(t), q_{\lambda}(t)) \\ y_{\lambda}(0) &= y_0, q_{\lambda}(0) = q_0, (-y_0, q_0) \in \bar{S}(0), \end{aligned} \quad (3.7)$$

which have unique solutions $(-y, q) \in C([0, T]; K) \cap H^1([0, T]; H)$ (see V. Barbu, 1976).

After these preparations we are ready to study the approach problems. The following lemma needs some expansions conditions of the notion of load surface and gives some informations about the boundness of the approach solutions.

Lemma 3.1 Take $\lambda = \frac{1}{n}$ and let $(-y_n, q_n)$ be the solutions of (3.7)_n. Suppose that $t \rightarrow \bar{S}(t)$ has an absolutely continuous variation $\tilde{w}(t)$, then

$$\|(-\dot{y}_n, \dot{q}_n)\| \leq \|\tilde{w}\|, \text{ in the norm of } L^2([0, T]; H) \quad (3.8)$$

Proof: Since $t \rightarrow \bar{S}(t)$ is an absolutely continuous map, with bounded variation and the solution $(-y_n, q_n)$ of $(3.7)_n$ is an absolutely continuous map on $[0, T]$, then

$$t \rightarrow d((-y_n(t), q_n(t)), \bar{S}(t)) \quad (3.9)$$

is a real-valued, absolutely continuous map. As a direct consequence we find the absolute continuity of the map

$$t \rightarrow P_{\bar{S}}((-y_n(t), q_n(t))) \quad (3.10)$$

On one hand, the functional F of (3.3) is differentiable at $t_0 \in [0, T]$ with derivative

$$\begin{aligned} \dot{F}(w) &= d(w, \bar{S}) \dot{d}(w, \bar{S}), \text{ on the other hand} \\ F(t_0, w(t_0)) &= \lim_{t \rightarrow t_0} \frac{F(t, w(t)) - F(t_0, w(t_0))}{t - t_0} = \lim_{t \rightarrow t_0} \frac{F(t, w(t)) - F(t, w(t_0))}{t - t_0} + \lim_{t \rightarrow t_0} \frac{F(t, w(t_0)) - F(t_0, w(t_0))}{t - t_0} \end{aligned} \quad (3.11)$$

However, the regularity properties of the functional $w \rightarrow F(w)$ on H assure

$$(\text{grad } F(t, w(t_0)), w(t) - w(t_0)) \leq F(t, w(t)) - F(t, w(t_0)) = (\text{grad } F(t, w(t)), w(t) - w(t_0)).$$

It is obvious that (3.4) implies the continuity of the map $t \rightarrow \text{grad } F(t, w(t))$, then the first term of the right side of (3.11) gives at limit

$$\lim_{t \rightarrow t_0} \frac{F(t, w(t)) - F(t, w(t_0))}{t - t_0} = \text{grad } F(t, w(t_0)),$$

and with the same argument applied to second term of the right side of (3.11) we obtain the following equality

$$d(w(t_0), \bar{S}(t_0)) \dot{d}(w(t_0), \bar{S}(t_0)) = (\text{grad } F(t_0, w(t_0)), w(t_0)) + d(w(t_0), \bar{S}(t_0)) \dot{w}(t_0), \text{ for all } w(t) \in H \quad (3.12)$$

In this way the smoothness requirements about w is so weakened. Hence, letting $w(t) = (-y_n(t), q_n(t))$, the solution of $(3.7)_n$, we have

$$\begin{aligned} d((-y_n(t), q_n(t)), \bar{S}(t)) &= \|(-y_n(t), q_n(t)) - P_{\bar{S}}((-y_n(t), q_n(t)))\| = \|\text{grad } F((-y_n(t), q_n(t)))\| \leq \\ &\leq \frac{1}{n} \|(-\dot{y}_n(t), \dot{q}_n(t))\| < +\infty. \end{aligned}$$

Turning now to (3.12) it follows

$$\dot{d}((-y_n(t), q_n(t)), \bar{S}(t)) + n d((-y_n(t), q_n(t)), \bar{S}(t)) \leq \dot{w}(t), \text{ a.e. } t \in [0, T] \quad (3.13)$$

It should be remarked that the initial condition $(3.7)_2$ implies $d((-y_0, q_0), \bar{S}(0)) = 0$. By an integration on $[0, T]$, from (3.12) we obtain

$$\frac{1}{n} \|(-y_n(t), q_n(t))\| + \int_0^T (-\dot{y}_n(t), \dot{q}_n(t)) dt \leq \int_0^T \dot{\tilde{w}}(t) dt,$$

particularly

$$\|(-y_n, q_n)\|_{L^1([0, T]; H)} \leq \|\dot{\tilde{w}}\|_{L^1([0, T]; H)} \quad (3.14)$$

Consequently, by (3.12) results

$$\frac{1}{2} d((-y_n(T), q_n(T)), \bar{S}(T)) + n \int_0^T d^2((-y_n(t), q_n(t))) dt \leq \int_0^T d((-y_n(t), q_n(t)), \bar{S}(t)) \dot{\tilde{w}}(t) dt.$$

Now the assertion follows applying the Gronwall's inequality (V. Barbu, 1976).

In the next we show how the approach solutions of $(3.7)_n$ uniformly converge to the solution of the Problem 2.2.

Theorem 3.2: Suppose that $t \rightarrow \tilde{w}(t)$ has a time derivative $\dot{\tilde{w}} \in L^1([0, T]; H)$. Then the sequence $\{-y_n(t), q_n(t)\}_{n \in \mathbb{N}}$ converges to the solution $(-y(t), q(t))$ of the Problem 2.2, uniformly with respect to n , a.e. $t \in [0, T]$.

Proof: Consider the approach problems (3.7) written for $\lambda = \frac{1}{n}$ and $\lambda = \frac{1}{m}$. These are employed in calculating estimates for the difference of two solutions in the H -norm, i.e.

$$\begin{aligned} \frac{d}{dt} \|(-y_n(t), q_n(t)) - (-y_m(t), q_m(t))\|^2 &= 2[(-\dot{y}_n(t), \dot{q}_n(t)) - (-\dot{y}_m(t), \dot{q}_m(t)), (-y_n(t), q_n(t)) - (-y_m(t), q_m(t))] = \\ &= +[(-y_n(t), q_n(t)) - (-y_m(t), q_m(t)), P_{\bar{S}}((-y_n(t), q_n(t))) - P_{\bar{S}}((-y_m(t), q_m(t))) - \\ &- 2[(-y_n(t), q_n(t)) - (-y_m(t), q_m(t)), \frac{1}{n}(-y_n(t), q_n(t)) - \frac{1}{m}(-y_m(t), q_m(t))] \leq \\ &\leq -2[(-y_n(t), q_n(t)) - (-y_m(t), q_m(t)), \frac{1}{n}(-y_n(t), q_n(t)) - \frac{1}{m}(-y_m(t), q_m(t))], \end{aligned}$$

where we have used the monotonicity of Yosida's approximation of the subdifferential $\partial \psi_{\bar{S}}$. Hence, by an integration on $[0, T]$ we obtain

$$\begin{aligned} 0 &\leq \frac{1}{2} \|(-y_n(T), q_n(T)) - (-y_m(T), q_m(T))\|^2 \leq \\ &\leq - \int_0^T [\frac{1}{n}(-\dot{y}_n(t), \dot{q}_n(t)) - \frac{1}{m}(-\dot{y}_m(t), \dot{q}_m(t)), (-\dot{y}_n(t), \dot{q}_n(t)) - (-\dot{y}_m(t), \dot{q}_m(t))] dt. \end{aligned}$$

therefore, we have

$$[(-\dot{y}_m, \dot{q}_m) - (-\dot{y}_n, \dot{q}_n), \frac{1}{m}(-\dot{y}_m, \dot{q}_m) - \frac{1}{n}(-\dot{y}_n, \dot{q}_n)]_{L^2([0, T]; H)} \leq 0$$

Since $\{\frac{1}{n}\}_{n \in \mathbb{N}}$ is a decreasing sequence and the sequence of the real values $\|(-y_n, q_n)\|_{L^2([0, T]; H)}$ is bounded from Lemma 3.1, it follows from an elementary property of the Hilbert spaces (see J. J. Moreau, 1974) that $\{(-y_n, q_n)\}_{n \in \mathbb{N}}$ is an increasing sequence and strongly convergent, say to $(-\tilde{y}, \tilde{q})$ in $L^2([0, T]; H)$, with $(-\dot{y}(t), \dot{q}(t)) \in H$, a.e. $t \in [0, T]$. In this case, by passing to an appropriate subsequence and using Lemma 3.1 we deduce

$$\|(-y, q)\|_{L^2([0, T]; H)} \leq \|\dot{\tilde{w}}\|_{L^2([0, T]; H)} \quad (3.15)$$

Consider now $y(t) = y_0 + \int_0^t \dot{y}(s) ds$, $q(t) = \int_0^t \dot{q}(s) ds$, hence $t \rightarrow (-y(t), q(t))$ is an absolute continuous map with a weakly derivative: $(-\dot{y}, \dot{q})$. It is not difficult to find an apriori bound which is needed to derive the convergence of the sequence $\{(-y_n, q_n)\}_{n \in \mathbb{N}}$. Indeed we have

$$\|(-y, q) - (-y_n, q_n)\|_{L^2([0, T]; H)} = \left\| \int_0^t [(-\dot{y}, \dot{q})(s) - (-\dot{y}_n, \dot{q}_n)(s)] ds \right\| \leq \sqrt{T} \|(-\dot{y}, \dot{q}) - (-\dot{y}_n, \dot{q}_n)\|_{L^2([0, T]; H)},$$

which assures the convergence of the sequence $\{(-y_n, -q_n)\}_{n \in \mathbb{N}}$ in $L^2([0, T]; H)$. Consequently

$$(-y_n(t), q_n(t)) \rightarrow (-y(t), q(t)), \text{ a.e. } t \in [0, T]. \quad (3.16)$$

It remains to show that $(-y, q)$ is a solution of the Problem 2.2. By (3.4) and (3.7)₁, using the boundness of the real sequence $\{ \|(-y_n, q_n)\| \}_{n \in \mathbb{N}}$ in the space $L^2([0, T]; \mathbb{R})$, results

$$\lim P_{\bar{S}}((-y_n, q_n)) = (-y, q), \text{ a.e. } t \in (0, T]. \quad (3.17)$$

Taking account (3.17) and the convergence of the sequence $\{(-y_n, q_n)\}_{n \in \mathbb{N}}$ and $\left\{ \begin{pmatrix} -\dot{y}_n \\ \dot{q}_n \end{pmatrix} \right\}_{n \in \mathbb{N}}$, by passing at limit in (3.7)_{1,n}, as $n \rightarrow \infty$, we obtain

$$-(\dot{y}_n(t), \dot{q}_n(t)) \rightarrow -(\dot{y}(t), \dot{q}(t)) \in \lim_{n \rightarrow \infty} (\partial \Psi_{\bar{S}(t)}(-y_n(t), q_n(t)) = \partial \Psi_{\bar{S}(t)}(-y(t), q(t)),$$

a.e. $t \in [0, T]$.

The uniqueness result is a direct consequence of the maximal monotonicity of the map $\partial \Psi_{\bar{S}}$.

We close this section with a comment about the uniqueness of the solution for the anisotropic hardening problem. It is perhaps the most difficult condition to check that the variety (2.9) can be reduced to one element of H . In this case it is superfluous to select a plastic component of deformation.

DUAL FORMULATION OF THE ANISOTROPIC HARDENING PROBLEM

Consider a mechanical system occupying a three-dimensional bounded domain Ω , whose boundary Γ is sufficiently regular. Denote by x a reference position of a material point in a deformation state. The deformation of the system may be described by the configuration $u(t) \in \mathcal{U}$, consisting in a pair (X, ε) , where X is a displacements vector and the deformation tensor. Suppose the deformation can be always achieved by acting with forces and moments $c(t) \in \mathcal{U}^* = U^* \times E = \mathcal{J}$, where U is Banach space of admissible displacements of the system, U^* the dual space of U , consisting in external forces, E the Hilbert space of admissible deformations which may be identified with the space of internal constraints. As a measure of hardening we take the work of plastic deformation $q(t) \in Q$, Q is another Hilbert space. Consider also the anisotropic factor $a(t) \in E$, which contains much more informations about directional deformation. Namely, if we define (see L. M. Kachanov, 1974)

$$a(t) = C\varepsilon(t), \text{ for some } C > 0$$

it tells us that the Bauschinger effect is everywhere satisfied in the system.

Suppose that the load surface equation is derived by the second matrix invariant $I_2(s(t))$, that is

$$S^a(t) = \{s(t) \in E / (s(t) - a(t)) \cdot (s(t) - a(t)) = \varphi(q(t))\}, \quad (4.2)$$

where φ is a positive increasing quadratic function or a positive differentiable function with positive Frechet-differential. In order to obtain an abstract formulation, define a measure of plastic deviation tensor p by generalized Prager's equations

$$\begin{aligned} p &= 0, \text{ if } [s]_{n,a} \leq 0 \\ p &= g(q) \frac{\partial I_2(s)}{\partial s} [s]_{n,a}, \text{ if } [s]_{n,a} > 0 \end{aligned} \quad (4.3)$$

where the differential form $[s]_{n,a} = \frac{\partial I_2}{\partial s} ds + \frac{\partial I_2}{\partial a} da$ preserve the continuity of the plastic deformation across the load surface, $g: E \rightarrow \mathbb{R}$ is named the hardening functional of the system. For our considerations, in accord with (4.2) we give an explicit expression of g

$$g(q) = \frac{1}{4\varphi(q) \varphi'(q)},$$

that is a decreasing function on E . It is possible to introduce $\mathcal{C} \subset Q$, a convex hardening restriction

$$\mathcal{C} = \{q(t) \in Q / q(t) \geq 0, \text{ a.e. } t \in [0, T], \dot{q}(0) = 0\} \quad (4.5)$$

It seems that a some hardening restrictions is one more general then ones previously defined and can be verified by a general class of hardening functionals g as it has seen from (4.4).

In the following we give in abstract setting the most important laws governing the mechanical system. Further, we associate W , the space of strain rates which give the system in a same configuration. If the configuration process u satisfies sufficient regularity properties, that is $u \in H^1(0, T; \mathcal{U})$, then we can identify the two spaces W and E . Consequently, W can be seen as a proper subspace of \mathcal{U} .

First, let $\mathcal{M} \subset \mathcal{U}$ a variety defined by (1.5)₁ in the Problem 1.1, in fact a configuration restriction. The most used duality between \mathcal{U} and \mathcal{U}^* corresponds to the virtual work. The space E is endowed with a scalar product defined by the internal energy of deformation

$$(\varepsilon(t), \varepsilon^*(t)) = \int_{\Omega} \varepsilon(t) A \varepsilon^*(t) d\Omega, \varepsilon(t), \varepsilon^*(t) \in E. \quad (4.6)$$

Consequently, the two subspaces \mathcal{U} and \mathcal{J} are put in duality by the dual direct product,

The usefulness and wide applicability of the static law of potential type corresponding to the restriction \mathcal{M} follows from the virtual work principle, i.e.

$$-f(t) \in \partial \psi_{\mathcal{M}}(u(t)), f(t) \in \mathcal{J}$$

We are now in the position to define the Hilbert space of dissipate hardening powers of the systems. Indeed, if the deformation work has sufficient regularity (i.e. $q \in H^1([0, T]; Q)$) we set:

$$J = \{ -\dot{q}(t) / q(t) \in Q \} \quad (4.8)$$

Consider now the mapping $B: Q \rightarrow J$, given by

$$B q(t) = -\dot{q}(t)$$

The great difficulty in applying the evolution results lies in the fact that one has to establish a dual framework, taking into account the hardening. This is by no means an easy task and great deal of this section is devoted to this precisely this question. It is at this that the choice of a subset of J , which is polar to $\mathcal{C} \subset Q$, becomes important.

Lemma 4.1 Consider $H^1([0,T] ; H)$ the space of all absolutely continuous process on $[0,T]$, endowed with scalar product

$$(q_1, q_2) = q_1(0) q_2(0) + \int_0^T q_1(t) q_2(t) dt \quad (4.10)$$

Let P be the cone of positive process, $P = \{q \in H^1([0,T] ; Q) / q \geq 0\}$, then the dual cone, denoted by P^* , is defined by

$$P^* = \{p \in H^1([0,T] ; Q) / -\dot{p} \text{ is nonincreasing, } p(0) \leq 0 \leq -\dot{p}(t)\}.$$

Proof: It is an easy consequence of an integration by parts and a choice of a particular $q_1(t) \in Q$. Indeed we have

$$(q_1, q_2) = q_1(0) q_2(0) + \int_0^T q_1(t) (-\dot{q}_2(t)) dt - q_1(t) (-\dot{q}_2(t)) \Big|_0^T$$

But the condition $(q_1, q_2) \leq 0$ with $q_1 \in P$ implies $-\dot{q}_2(t) \geq 0$, for all $t \in [0,T]$. Consequently,

$t \rightarrow -\dot{q}_2(t)$ is nonincreasing on the interval $[0,T]$. It is no difficulty to prove $q_2(0) \leq 0$.

We are now ready to state

$$\mathcal{C}^* = \{-\dot{q}(t) / q(t) \in H^1([0,T] ; Q), q(0) \leq 0 \leq -\dot{q}(t)\}, \quad (4.11)$$

and identify the both previous subsets P^* and \mathcal{C}^* .

The last submitted subset has a mechanical meaning according to the hardening condition defined by \mathcal{C} in (1.5)₁: the subset of all dissipate hardening powers which lead the system into an admissible hardening state. In view of the duality between the two spaces Q and J , given by

$$(-\dot{q}(t), p(t)) = \dot{q}(0) p(0) + \int_0^T (-\dot{q}(t)) p(t) dt \quad (4.12)$$

and the Lemma 4.1, it follows that the two subsets \mathcal{C} and \mathcal{C}^* are dual each other.

It is the aim of this section to extend some results given in Moreau (1975) by means of deformation with hardening. To stand with, we introduce some new terminology and notations. Consider now

$$S_a(t) = \{(s(t), q(t)) \in \mathcal{J} \times Q / (s(t) - a(t)) \cdot (s(t) - a(t)) = \varphi(q(t))\},$$

a closed bounded convex subset of $\mathcal{J} \times Q$. At this stage we have in mind the previous slitley mechanical identification introduced by B. Hence, by the maximal dissipate power principle and the duality between $W \times J$ and $\mathcal{J} \times Q$ we derive the evolution problem:

$$\begin{aligned} &\text{given } (s(t), q(t)) \in \mathcal{J} \times Q, \text{ find } (w(t), -\dot{q}(t)) \in W \times J \text{ such that} \\ &(w(t), -\dot{q}(t)) \in \partial \psi_{S_a \cap \mathcal{C}}(s(t), q(t)), q(0) = 0 \end{aligned} \quad (4.13)$$

Doing this, we introduce an explicit form of the nonlinear operator involving hardening property and we give an evolution problem of the same type as in K. Gröger (1977).

Everywhere in the following suppose $q \in \mathcal{C}$ and preserve the notations of the sections 1-3. Now our object is to give a criteria for existence of a Hilbert space of

admissible deformation with hardening in terms of solutions of the Cauchy problem associated with (4.13).

Lemma 4.2: Let $(u, \sigma, p, q) \in H^1([0, T]; U \times E^2 \times Q)$ be the solution of the Problem 1.1 with $B = \psi_{S_a \cap \varepsilon}$, where the time depending map $t \rightarrow S_a(t) = S(t) + a(t)$, have an absolutely continuous variation $\tilde{w}(t)$, which variation vitesse is $\dot{\tilde{w}} \in L^2([0, T]; \mathcal{F})$. Then, preserving the elastic and yielding states, there exists a Hilbert space K of admissible deformations of the system and the vector-valued functions $t \rightarrow v(t)$, $t \rightarrow y(t)$ also absolutely continuous, which satisfy the Problem 2.1.

Proof: The proof of this Lemma is technical. First, we shall find some useful dual sets. By (1.5)₁, there exists

$$\mathcal{L} = \{e \in E / e = Ku\} \quad (4.14)$$

a linear subspace of E , such that $\varepsilon(t) \in \mathcal{L} + e^0(t)$. Our interest on this particular subspace comes from geometrical restriction rewritten as a proper subspace of \mathcal{U} , that is

$$\tilde{\mathcal{L}} = \{(u, e) \in \mathcal{U} / e = Ku\}.$$

It is of particular interest because $\tilde{\mathcal{L}}$ is identified with $\tilde{\mathcal{L}} \times \{0\}$ in the product $\mathcal{U} \times J$ and a principle similar to virtual work principle in the classical mechanics ensures the existence of a dual subspace of \mathcal{L} , that is

$$\tilde{\mathcal{V}} = \{(f, \tau) \in U^* \times E / K^* \tau = f\}.$$

This can be supposed equivalent to $\tilde{\mathcal{V}} \times \{0\}$ in $\mathcal{V} \times Q$. Indeed, by virtue of geometrical restriction (1.14), there corresponds a positive admissible process of external forces

$$c(t) \in V = \{f \in U / K^* \tau = f\}, \text{ involving an equilibrium constraint } \tau.$$

Further, if $\sigma(t) \in E$ is a process of elastic constraint acting on visualized component $\varepsilon(t) \in E$, $s(t)$ the constraint process involved by the plastic component, $s(t) \in S(t) + a(t)$, mechanical consideration (Prendtl-Reuss law) suppose an equilibrium equation:

$$\sigma(t) + s(t) = 0 \quad (4.16)$$

Let $c \in H^1([0, T]; U^*)$ the process of external forces and moments acting upon the system, in the following $c(t) = (c(t), 0) \in \mathcal{V} \times Q$. We need also the notations:

$$\begin{aligned} \tilde{\varepsilon}(t) &= (u(t), \varepsilon(t)), \quad \tilde{e}^0(t) = (0, e^0(t)), \quad \tilde{s}(t) = (0, s(t)), \quad \tilde{\sigma}(t) = (0, \sigma(t)), \\ \tilde{p}(t) &= (u(t), p(t)). \end{aligned}$$

In this way, the relations (1.5 - 1.6) can be done as

$$\tilde{\varepsilon} = \tilde{e} + \tilde{p}, \quad \varepsilon(t) \in \mathcal{L} + e^0(t), \quad \tilde{c}(t) - \tilde{\sigma}(t) \in \tilde{\mathcal{V}}.$$

In order to formulate the cvasi-static equilibrium of a system, the use of a Hilbert space requires the injectivity of the operator A , which in the case of small deformation occurs. In order to obtain an abstract formulation of the dual framework, we consider $H = \text{Im}(Axi)$, endowed with the scalar product

$$[(f, \tau), (f^*, \tau^*)] = (f, i^{-1} f^*) + (\tau, A^{-1} \tau^*), \quad (4.17)$$

where $i : E \rightarrow E^*$ is an injection map.

It is to be expected that $\tilde{\mathcal{L}}$ can be identified with $(\text{Axi})(\tilde{\mathcal{L}})$ in \mathcal{J} , by this we mean that $\tilde{\mathcal{L}}$ and $\tilde{\mathcal{V}}$ are two orthogonal subspaces of H . In this way, it is an easier task to give the dual formulation of the Problem 1.1:

$$\begin{aligned} \tilde{\varepsilon}(t) - \tilde{e}^0(t) &\in \tilde{\mathcal{L}} \quad (\text{an affine relation}) \\ \tilde{c}(t) - \tilde{\sigma}(t) &\in \tilde{\mathcal{V}} \quad (\text{equilibrium equation}) \\ \tilde{\varepsilon} &= \tilde{\sigma} + \tilde{p} \\ (\dot{\tilde{p}}(t), -\dot{\tilde{q}}(t)) &\partial y_{S(t)+a(t)}(-\tilde{\sigma}(t), \tilde{q}(t)) \quad (\text{Prendtl-Reuss law}) \end{aligned} \quad (4.18)$$

with initial conditions:

$$\begin{aligned} \tilde{\sigma}(0) = \tilde{\sigma}_0 = (0, \sigma_0), \quad \tilde{p}(0) = \tilde{p}_0 = (u_0, p_0), \quad \dot{\tilde{q}}(0) = 0, \quad \text{satisfying } \sigma_0 + p_0 \in \mathcal{L} + e^0(0), \\ -\sigma_0 \in S(0) + a(0), \quad (c(0), -\sigma_0) \in \tilde{\mathcal{V}} \end{aligned} \quad (4.19)$$

where the subdifferential is understood point-wise of the duality of the two spaces $H \times Q$ and $H \times J$. In this case, having in mind the regularity conditions of $a(t)$, $c(t)$ and $S(t)$ we conclude

$$-\tilde{\sigma}(t) \in (S(t) + a(t)) \cap (\tilde{\mathcal{V}} - \tilde{c}(t)),$$

in other words:

$$(S(t) + a(t)) \cap (\tilde{\mathcal{V}} - c(t)) \neq 0 \quad (4.20)$$

This is so called admissible changes hypothesis of the hardening problem for the anisotropic behaviour of the system. Consequently, in order to use this additional hypothesis, one is led to identify the two subspaces $\tilde{\mathcal{L}}$ and $\tilde{\mathcal{V}}$ with $\mathcal{L} \times \{0\}$ and $\tilde{\mathcal{V}} \times \{0\}$ of the spaces $\mathcal{U} \times J$ and $\mathcal{J} \times Q$. Further, taking into account B from (4.9) we define

$$\tilde{B}^{-1} : Q_{\ker \tilde{B}} \rightarrow J, \quad \tilde{B} \hat{q}(t) = -\dot{\tilde{q}}(t), \quad \text{for any } q \in \hat{q} \text{ and } t \in [0, T].$$

Then, the mapping \tilde{B} is one to one from Q/R to J . Consider the inverse operator

$$\tilde{B}^{-1} : J \rightarrow Q/R, \quad \tilde{B}^{-1}(-\dot{\tilde{q}}(t)) = q(t) + R \quad (4.21)$$

Now let $(i \times A \times \tilde{B}^{-1}) : \mathcal{U} \times J \rightarrow \mathcal{J} \times Q$, be the mapping defined by

$$(i \times A \times \tilde{B}^{-1})(u, e, -\dot{\tilde{q}})(t) = (i(u(t)), Ae(t), q(t) + R) \quad (4.22)$$

which gives rise to an identification between $\mathcal{U} \times J$ and a proper subspace K of $\mathcal{J} \times Q$. As before, K can be organized as a Hilbert space, it is easily deduced from the duality between the two spaces $\mathcal{U} \times J$ and $\mathcal{J} \times Q$. Consequently, it is a linear subspace of H and the subdifferential in (4.18) may be understood in the scalar product of K .

Finally, we make a rather mild regularity hypothesis, namely $\tilde{e}^0(t) \in \tilde{\mathcal{V}}$ and $\tilde{c}(t) \in \tilde{\mathcal{L}}$ which are equivalent to $Ae^0(t) \in \ker K^*$, $c(t) = i(u(t))$, $Ku(t) \in \ker A$. But there exists a split of H ,

$$(\tilde{\varepsilon}(t) - \tilde{e}^0(t)) + (\tilde{c}(t) - \tilde{\sigma}(t)) = \tilde{p}(t) - \tilde{e}^0(t) + \tilde{c}(t) \in \tilde{\mathcal{L}} + \tilde{\mathcal{V}} = H,$$

then

$$\tilde{\varepsilon}(t) - \tilde{e}^0(t) = P_{\tilde{\mathcal{L}}}(\tilde{p}(t) + \tilde{c}(t) - \tilde{e}^0(t)), \quad \tilde{c}(t) - \tilde{\sigma}(t) = P_{\tilde{\mathcal{V}}}(\tilde{p}(t) + \tilde{c}(t) - \tilde{e}^0(t))$$

(compare with similar relations in J. J. Moreau, 1974). At this stage, a choice of the new variables

$$v(t) = P_{\tilde{\mathcal{L}}}(\tilde{p}(t)) = \tilde{\varepsilon}(t) - \tilde{e}^0(t) - \tilde{c}(t) \in \tilde{\mathcal{L}}, \quad -y(t) = P_{\tilde{\mathcal{V}}}(\tilde{p}(t)) = \tilde{\sigma}(t) - \tilde{c}(t) - \tilde{e}^0(t) \in \tilde{\mathcal{V}},$$

becomes important. Then, by virtue of the new notations, of the dual framework before defined and of the initial Hypotheses, the anisotropic hardening problem can be completed

$$v(t) \in \mathcal{L}, y(t) \in \tilde{\mathcal{V}}$$

$$(\dot{v}(t) - \dot{y}(t), -\dot{q}(t)) \in \partial \Psi_{s(t)+a(t)}(-y(t) - c(t) + e^0(t), q(t))$$

$$v(0) = v_0 = (i(u_0) - c(0), \varepsilon(0) - e^0(0))$$

$$y(0) = y_0, -y_0 \in (S(0) + a(0) + c(0) + e^0(0)) \cap \mathcal{V},$$

that is the Problem 2.1.

Remarks. 1. Note that it make no difference between the dual framework of the problem (4.18 - 4.19) and the others similar for the elastic and perfect plastic cases, studied by J.J. Moreau, 1974, 1975, B. Nayroles, 1974. Our assumption of potentiality about corresponding constitutive law (of Prandtl - Reuss type) lies in commonly evolution equation form.

2. The existence of the constitutive law (4.12)₄ involves an initial condition $-\sigma_0 \in S(0) + a(0)$, which explicitly describe initial behaviour. Thus, the plastic deformation vitesse $\dot{p}(t)$, the variation of the hardening factor $\dot{q}(t)$ and $q(t)$ itself vanishes at $t = 0$.

3. $\text{Ker } B = \{0\}$ assures the existence of the yielding state only, until the hardening factor remains invariant. In this way, the choice of the operator B makes possible to preserve the yielding state of the hardening deformation process and in point of view of analysis we make no difference between $e(t)$ and $s(t), q(t)$ and $-\dot{q}(t)$, respectively. This assumption make possible to take an adequate underlying functions space characterizing the hardening deformation of the system. Putting all of this together, we obtain an appropriate model for hardening deformation in connection with its simplest mechanical form presented by K. Gröger, 1977.

4. A uniqueness result for the unidimensional case can be found in C. Ghita, 1981.

REFERENCES

1. V.Barbu , Nonlinear Semigroups and Differential Equations in Banach Spaces , Ed. Academiei - Noordhoff Inter , Publ ., 1976 .
2. H.Brezis , Operateurs Maximaux Monotones et Semi - groupes de Contractions dans les Espaces de Hilbert , North - Holland Math . Studies , 5 , 1972 .
3. G.Duvaut & J.L.Lions , Les Inequations en Mecanique et en Physics, Dunod, 1972
4. C Ghita , Calculul componentei elastice la deformatia elasto-plastica prin tractiune, St.Cerc.Mat. , 33 , 3 (1981) , 285 - 298 .
5. C.Ghita , The quasi-static equilibrium of a system with anisotropic hardening , Rev Roum . Math . Pures et App . , 29 , 1 (1984) , 43-54 .
6. K. Gröger , Evolutions equation in the Theory of Plasticity , Proc . summer school, Verlag , Berlin , 1977 .
7. L.M.Kachanov , Fundamentales of the Theory of Plasticity , Mir . Publ . , 1974 .
8. J.L.Lions , Quelques Methodes de Resolutions des Problemes aux Limites non Lineaires, Dunod - Gauthier - Villard , Paris , 1969 .
9. J.J.Moreau , On unilateral constraints , friction and duality , "New Variational Techniques in Math . Physics " , CIME , ed . Cremonese , Roma (1974), 149 -322 .
10. J.J.Moreau , Application of convex analysis to the treatement of elasto - plastic systems, Lect . Notes Math . 503 , Springer - Verlag , (1975) , 56 -89 .
11. B.Nayroles , Point de vue algebrique , convexite et integredes convexes en mecanique des solides , "New Variational Techniques in Math . Physics , CIME , Ed . Cremonese, Roma (1974) , 323 - 404 .
12. D.Pascali & S.Sburlan , Nonlinear Mapping of Monotone Type , Ed . Academiei - Sijthoff & Noordhoff Int . Publ . , 1978 .

SOME REMARKS ON LIMIT LOADS FOR PERIODIC MATERIALS

Gelu I. Pasa

Abstract. We study the condition in which a composite material attains the limit loads, using the properties of the components. We use for this the averaging method, and a sort of limit analysis, described in [1]; averaging method is closed to homogenisation method (see [1] , [2] , [5] , [6]). The limit loads is studied using a concept of "macroscopic" domain of plasticity, introduced in [3] , [4].

1. Introduction.

We consider a composite-periodic material, contained in a domain $D \in \mathbb{R}^3$, formed by a great number of periods, each of them containing an inclusion (or fiber) with great resistance, compared with those of the enclosing matrix. To describe this periodicity, we consider that the elastic coefficients of the medium, a_{ijkh} are y periodic, y being a parallelepipedon in \mathbb{R}^3 ; in each period, fiber and matrix are separated by a surface Γ . We are interested by the case when the dimension of the periodicity cell Y is very small compared with those of the entire medium, and consider ε = ratio between the dimension of a cell and the dimension of the medium. Then is clear that a_{ijkh} are Y periodic with respect to the variable $y = x/\varepsilon$; we have the following decomposition:

$$x \in D = U(\varepsilon \cdot Y) + D^*, \quad \mu(D^*) = 1(\partial D) \varepsilon \sqrt{2}.$$

where μ = measure (area or volume). Then, we consider the medium formed by a collection of little cells, εY , and excluding a set of "negligible" measure, every $x \in D$ belong to a cell, consequently $x \in \varepsilon Y$, or $x/\varepsilon = y \in Y$. For this heterogeneous medium we have, for example, the elasticity problem:

$$\begin{aligned} \partial (a_{ijkh}(x/\varepsilon)) \partial u^\varepsilon_k / \partial x_h / \partial x_j &= f \text{ in } D; \\ u^\varepsilon / \partial D &= 0. \end{aligned}$$

Introducing a suitable topology, one can obtain "convergence" of the initial coefficients (when $\varepsilon \rightarrow 0$), thus replacing the initial problem with another one, with constant coefficients it is the aim of the homogenisation method.

Instead of homogenisation method, it is possible to use "averaging" method [1], [2], based on the concept of macroscopic and microscopic variables. We consider

Σ and E = macroscopic stress and deformation

$\sigma(y)$ and $e(y)$ = microscopic stress and deformation

Macroscopic variables are obtained as "average" of microscopic variables:

$$(1) \quad \Sigma_{ij} = \int_Y \Sigma_{ij}(y) dy / |Y| = \langle \sigma \rangle$$

$$E_{ij} = \int_Y e_{ij}(y) dy / |Y| = \langle e \rangle.$$

This definition are introduced, for example, in [1] for materials with holes; in general it is justified by the fact that the weak limit in $L_2(D)$ of $f(x/\varepsilon)$, with f Y periodic, is the average $\int_Y f(y) dy / |Y| = \langle f \rangle$, of the function f (see [5], [6]).

A difference between averaging method and homogenization method, is the fact that in averaging method, the microscopic stress and deformation are considered Y periodic- not only elastic coefficients, as in homogenization method.

Using the definition (1) we have two principal direction to study the material:

- homogenization : find the relation between Σ and E using (1), elasticity equations, and constitutive relations between microscopic stress and deformations
- localisation: find microscopic stress and deformations in terms of effective values Σ and E . For this we use the following system:

- (2) - constitutive relations between Σ and E
- elasticity equations : $\text{div} \sigma = 0$
- $\langle \sigma \rangle = \Sigma$ or $\langle e \rangle = E$.

This "localisation" procedure is used in [1] to define the limit loads of the material with holes.

2. On the boundary condition.

As it is possible to see; in (2) boundary condition are not present. Instead of boundary conditions, we use "periodicity" conditions, which must be considered of the form which ensure us the well-known relation of Hill:

$\langle \sigma : e \rangle = \langle \sigma \rangle : \langle e \rangle$, where $a:b = \sum a_{ij} b_{ij}$. In general we need some matching condition between the components in each periodicity cell, which are in general of the form: continuity of displacements and of the normal stress; but it is possible to consider condition of the slide type between fiber and matrix-studied for example in [2], [8].

We emphasize that if we have $\text{div} \sigma = 0$ and $\langle \sigma \rangle = \Sigma$ or $\langle e \rangle = E$, the solution (σ, u) it is not unique :with different boundary condition, we can obtain σ and e with given averages. In the following we describe some situation (given in [1]) of this type.

Proposition 1. $\text{div} \sigma = 0$
 $u = E y + u^*$, $u^* = y$ periodic
 $\sigma n = Y$ antiperiodic
 $[\sigma n] = 0$ on Γ

i) $\langle e \rangle = E$

ii) $\langle \sigma : e \rangle = \langle \sigma \rangle : \langle e \rangle$

Proof.

$$\text{ii) } \int_Y \sigma_{ij} e_{ij} = \int_Y \sigma_{ij} (E_{ij} + E_{ij}^*) / 2 + \int_Y \sigma_{ij} e_{ij}(u^*) = \langle \sigma_{ij} \rangle E_{ij} |Y|,$$

where we use $\text{div} \sigma = 0$ and $\sigma n = \text{antiperiodic}$.

Proposition 2.

$$\begin{aligned} \operatorname{div} \sigma &= 0 & \Rightarrow & & \text{i) } \langle e \rangle &= E \\ u_i &= E_{ij} y_j \text{ on } \partial Y & & & \text{ii) } \langle \sigma : e \rangle &= \langle \sigma \rangle : \langle e \rangle. \end{aligned}$$

Proof.

$$\begin{aligned} \text{ii) } 2 \int_Y \sigma_{ij} e_{ij} &= \int_Y \sigma_{ij} (u_i n_j + u_j n_i) - \int_Y (u_i \operatorname{div} \sigma_i + u_j \operatorname{div} \sigma_j) = E_{ik} \int_{\partial Y} \sigma_{ij} y_k n_j + E_{jp} \\ \int_{\partial Y} \sigma_{ij} y_p n_i &= E_{ik} \int_Y \sigma_{ik} + E_{jp} \int_Y \sigma_{pj}. \end{aligned}$$

Proposition 3.

$$\begin{aligned} \operatorname{div} \sigma &= 0 & \text{i) } \langle \sigma \rangle &= \Sigma \\ \sigma n &= \Sigma n \text{ on } \partial Y & \text{ii) } \langle \sigma : e \rangle &= \langle \sigma \rangle : \langle e \rangle. \end{aligned}$$

Proof.

$$\text{i) } \partial (\sigma_{ij} y_p) / \partial y_j = (\operatorname{div} \sigma)_i y_p + \sigma_{ij} \delta_{pj} = \sigma_{ip};$$

$$\text{Therefore } \int_Y \partial (\sigma_{ij} y_p) / \partial y_j = \int_{\partial Y} \sigma_{ij} y_p n_j = \int_Y \Sigma_{ij} n_j y_p = \Sigma_{ip}.$$

Remark 1. It is natural to consider the following problem : in what conditions (of periodicity type) we have $\langle \sigma \rangle = \Sigma$? In the elastic case, the answer (given although by homogenization method) is that a particular constitutive relation must be imposed between Σ and E . We consider $u = Ey + v$, v being Y periodic, as in

Proposition 1. Using $\operatorname{div} \sigma = 0$, we obtain:

$$\partial (a_{ijkh} e_{sp}(v)) / \partial y_i = - E_{kh} \partial a_{ijkh} / \partial y_i,$$

this relation being considered in sense of distributions. Then we must solve a particular equation:

$$\frac{\partial}{\partial y_j} (a_{ijsp} e_{sp}(p^{pr})) = - \partial a_{ijtu} / \partial y_j$$

and obtain (using the linearity) $v_i = E_{st} P_i^{st}$. Then we have

$$\Sigma_{ij} = \langle \sigma_{ij} \rangle = \langle a_{ijkh} e_{kh}(u) \rangle = \langle a_{ijkh} E_{kh} + a_{ijst} e_{st}(P^{kh}) E_{kh} \rangle ;$$

$$(3) \quad \Sigma_{ij} = E_{kh} \langle a_{ijkh} + a_{ijst} e_{st}(P^{kh}) \rangle = E_{kh} A_{ijkh},$$

where A_{ijkh} are so called homogenized coefficients (or effective coefficients). Then, to obtain σ with $\langle \sigma_{ij} \rangle = \Sigma_{ij}$, we must impose a macroscopical deformation E given by (3). In the plastic region, the answer is not so clear-we need a explicit expression for plastic deformation (for example using a potential).

Remark 2. In proposition 2 and 3, we not use periodicity condition, but we obtain the possibility to have microscopic deformation and stress with prescribed average. Then we can use this procedure in the case of non-periodic composites, having a so called "representative elementary volume "instead of periodicity cell Y .

3. Limit loads.

Using the localization method we can solve the following problem (considered in [1] for perforated plates):

- by an experiment we obtain relation between macroscopic stress and deformation
- solving the system (2) we can compute the local (microscopic) stress and deformation

- we can see how many components attains the plasticity limit and then give a rupture criteria for composite material :for example if 60 % of components attains plasticity limit.

It is clear that is possible to have a rough situation :

$\|\Sigma\| = \|\sigma\| \leq \ll \sigma_0 \gg$, where, for "local" domain of plasticity we can consider von Mises criterion $\|\sigma(y)\| \leq \sigma_0$, with

$\|\sigma\|^2 = \sigma_{ij}^D \sigma_{ij}^D$, $\sigma_{ij}^D = \sigma_{ij} - (\text{Tr } \sigma)I/3$. Thus, this means that the composite material can not support a effective stress greater than the average of maximum "local" suportable stress (and of course σ_0 is maximum between all " σ_0 " of the components of the material).

The more fine method is based on the definition of macroscopic domain of plasticity :

$$P(\text{macro}) = \{ \Sigma, (\exists) \sigma \text{ with } a), b), c) \}$$

a) $\sigma(y)$ " local" suportable

b) $\text{div}(\sigma) = 0$

c) $\ll \sigma \gg = \Sigma$

In [1], for perforated plates, $P(\text{macro})$ it is approximate from the "interior" and for a given direction Σ_0 of the stress.

Remark 3. The effective domain of plasticity is not possible to compute using a path in the stress field Σ - because the components can not support any stress, and we can not indicate when the macroscopic stress Σ produce a local stress greather than σ_0 ; for this, in [1] , the computation is made using a path in effective deformation E , increasing the parameter $t = \Sigma_0 : E$. The details can be founded in [1] concerning the case of perforated plates - then in fact the coefficients a_{ijkh} are constant, and the periodicity is due only to the geometrical conditions.

Remark 4. We give some details concerning the effective deformation E which must be imposed to obtain local stress σ with a given average. The constitutive relation used in [1] are :

$$\sigma = a : (e(u) - e^P(u))$$

$$\|\sigma\|^2 \leq \sigma_0^2$$

$$\dot{e}^P = \dot{l} * \sigma^D \quad \begin{cases} \dot{l} = 0 & \text{if } \|\sigma\| \leq \sigma_0 \\ \dot{l} \geq 0 & \text{if } \|\sigma\| = \sigma_0 \end{cases}$$

where e is the deformation and e^P is the plastic part of deformation. Then : $e - e^P = a^{-1} : \sigma$, $\ll e \gg - \langle e^P \rangle = a^{-1} : \ll \sigma \gg$, (in the case of perforated plates, when a_{ijkh} are constants)

imposing $\ll \sigma \gg = s \Sigma_0$ we obtain $E = a^{-1} : s \Sigma_0 + \langle e^P \rangle$.

When $t \leq t_0$, t_0 being the "moment" when plastic deformation appear, we have $e^p = 0$, then we must consider $E = (a^{-1} : \Sigma_0) \cdot c$. Condition $E : \Sigma_0 = t$ give us

$c = t / \{ (a^{-1} : \Sigma_0) : \Sigma_0 \}$, and we obtain

$$(4) \quad E = t (a^{-1} : \Sigma_0) / (a^{-1} : \Sigma_0 : \Sigma_0).$$

We consider $E = t \Sigma_0$; in the following we show that corresponding σ have an average not colinear with Σ_0 (in the isotropic case):

for $u = Ey = v$, we obtain $e(u) = t \Sigma_0 + e(v) = t \Sigma_0$,

then $\sigma(t) = \lambda (\text{Tre}(u))I = 2\mu e(u)$,

$\langle \sigma \rangle_{ij} = 1/3 \langle e_{11} \rangle \delta_{ij} = 2\mu \langle e_{ij} \rangle$ if $(\Sigma_0)_{11} \neq 0$ and $(\Sigma_0)_{ij} = 0$ for $(i,j) \neq (1,1)$.
Consequently :

$\langle \sigma_{22} \rangle$ and $\langle \sigma_{33} \rangle \neq 0$, but $(\Sigma_0)_{22} = (\Sigma_0)_{33} = 0$.

Therefore, it is possible to see, using (3) and (4), that in the case of composite materials with inclusions or fibers, instead of constant coefficients a_{ijkh} (used in [1] for perforated plates), we must need compute effective coefficients A_{ijkh} .

REFERENCES

1. J.J.Marigo, P.Mialon, J.C. Michel, P.Suquet, Plasticité et homogénéisation..., J.Mec.Theorique et Appliquee, 6(1), 1987, pp.47-75.
2. Fokrasuki, Homogénéisation et glissements dans un milieu cristallin, These 3-e cycle, Paris, 1984.
3. P.Suquet, Plasticité et homogénéisation, Thèse, Paris, 1982.
4. S.Salencon, Calcul a la rupture et analyse limite, Presses ENCP, Paris, 1983.
5. E.Sanchez-Palencia, Non-Homogeneous Media and Vibration Theory, Lect.Notes.in Physics no.127, 1980, Springer Verlag
6. J.L.Lions, A.Bensoussan, G.Papanicolau, Asymptotic Analysis for Periodic Media, 1978, North-Holland, Amsterdam.
7. H.Ene, G.Pasa, Metoda omogenizarii- Aplicatii la teoria materialelor compozite, 1987, Editura Academiei, Bucuresti. (Homogenization Method).

